GEORGIA INSTITUTE OF TECHNOLOGY OFFICE OF CONTRACT ADMINISTRATION

PROJECT ADMINISTRATION DATA SHEET

[x] ORIGINAL [ ] REVISION NO. _____

Project No. E-16-627 DATE 11/2/81

Project Director: Dr. Jechiel I. Jagoda School/Lab Aerospace Engineering

Sponsor: U. S. Environmental Protection Agency

Type Agreement: Grant No. R808953010 & Amendment 1

Award Period: From 8/26/81 To 8/25/84 (Performance) _____ (Reports)

Sponsor Amount: $153,635 (incrementally funded at $97,381 thru 8/25/83) Contracted through:

Cost Sharing: $8,087 (E-16-359) Incremental at $5,126 GTRI/~~GIT~~

Title: Soot Formation in Gaseous Diffusion Flames

ADMINISTRATIVE DATA OCA Contact Leamon R. Scott

1) Sponsor Technical Contact:

Jerry Y. C. Huang, Project Officer
Associate Science Review Administrator
Office of Research and Development
Environmental Protection Agency

202-426-2355

2) Sponsor Admin/Contractual Matters:

Diane Galvin, Grants Specialist
Grants Administration Division
Grants Operations Branch (PM-216)
Environmental Protection Agency
Washington, D. C. 20460

202-755-3490

Defense Priority Rating: None Security Classification: None

RESTRICTIONS

See Attached EPA Supplemental Information Sheet for Additional Requirements.

Travel: Foreign travel must have prior approval — Contact OCA in each case. Domestic travel requires sponsor approval where total will exceed greater of $500 or 125% of approved proposal budget category.

Equipment: Title vests with GIT, subject to accountability determination at grant expiration. Listing of all items costing $300 or more.

COMMENTS:

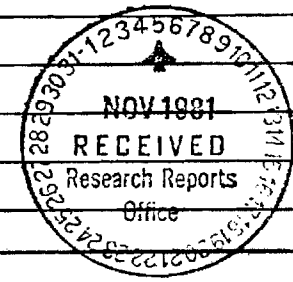

COPIES TO:

Administrative Coordinator
Research Property Management
Accounting
Procurement/EES Supply Services
Research Security Services
Reports Coordinator (OCA) ✓
Legal Services (OCA)
Library
EES Public Relations (2)
Computer Input
Project File
Other _____

FORM OCA 4:781

GEORGIA INSTITUTE OF TECHNOLOGY OFFICE OF CONTRACT ADMINISTRATION

SPONSORED PROJECT TERMINATION SHEET

Date September 22, 1983

Project Title: "Soot Formation in Gaseous Diffusion Flames"

Project No: E-16-627

Project Director: Dr. J. I. Jagoda

Sponsor: U.S. Environmental Protection Agency

Effective Termination Date: 8/25/83

Clearance of Accounting Charges: 8/25/83

Grant/Contract Closeout Actions Remaining:

- [ ] Final Invoice and Closing Documents
- [X] Final Fiscal Report SF269
- [ ] Final Report of Inventions
- [ ] Govt. Property Inventory & Related Certificate
- [ ] Classified Material Certificate
- [ ] Other _____

Assigned to: Aerospace Engineering (School/~~Laboratory~~)

COPIES TO:

Administrative Coordinator	Research Security Services	EES Public Relations (2)
Research Property Management	Reports Coordinator (OCA) ✓	Computer Input
Accounting	Legal Services (OCA)	Project File
Procurement/EES Supply Services	Library	Other _____

Soot Formation in Gaseous Diffusion Flames

1st 6 monthly progress report

submitted to the

United States Environmental Protection Agency

under Contract # R80895 3010

by

J. I. Jagoda, Principal Investigator

School of Aerospace Engineering

Georgia Institute of Technology

February 1982

DISCLAIMER:

This document has been proofed and
its original formatting has been retained.

I. Work completed to date:

A Parker-Wolfhard type burner has been constructed (Fig. 1). It consists of a sandwich of three parallel slots 2" x 3/4" whose longer sides are common. The center slot carries the fuel while the oxidizer is supplied through the outer two slots. The slots are closed at the top with sintered brass plates which ensures uniform flow. Both air flows, as well as the oxygen flow are separately controlled and monitored using needle valves and float type rotameters. The resultant double flame is wedge shaped and stabilized using a set of copper screen placed near the flame tip. The entire burner is surrounded by a jacket carrying a nitrogen flow which helps to further stabilize the flame and prevents the formation of "end flames" on the shorter sides of the fuel slot. The burner assembly can be translated in a vertical and horizontal direction such that measurements can be carried out in different parts of the flame. As described in the proposal this configuration makes it possible for the incident and transmitted beams used in the optical diagnostics to lie along a line of constant flame conditions. This leads to a long optical path for the transmitted beams resulting in accurate absorbtion measurements which require no corrections for beam passage through regions of varying flame conditions The burner performs well and has been used to produce stable flames for a variety of flow rates. Propane has been used as a fuel.

The suction probe described in the proposal has been constructed. Briefly, it consists of 3 concentric tubes as shown in Fig. 2. The soot laden flame gases are aspired through the central tube and the soot particles are collected using filters (Fig. 3). The outer two tubes carry cooling water. A small quantity of water enters the innermost tube through tiny holes near the probe tip. This water accelerates the quenching of the combustion products and prevents clogging of the probe by soot deposition. The water is removed by a system of traps which precedes the aspiring pump. The sampling rate of the pump is measured using a test meter similar to the type used to monitor domestic gas supplies. This probe system is presently ready for testing.

The simultaneous laser light scattering and absorbtion measurement facility (Fig. 4) is described in detail in the proposal and had previously been set up. During this reporting period the absorbed and scattered light detection systems were improved

using electronic filters to increase the signal to noise ratio and various actions were taken to reduce stray light detection. The optical table, which carries the scattering optics was slightly modified to accept the burner along with its translation mechanisms. The laser light scattering system was calibrated and tested using gases of known scattering cross-sections (oxygen, nitrogen and methane). The scattering measurements were found to be highly reproducable (better than 2%) and the deduced scattering cross-sections of the gases were found to be in close agreement with those found in the literature (better than 3%).

Laser light scattering and absorbtion measurements have been started for propane-air flames on the Parker-Wolfhard burner. An example of the light absorbtion results obtained are shown in Fig. 5. In this figure the soot fraction by volume F(V) is plotted against horizontal position in a single flame sheet for flames of different gas flow rates and at different heights in the flame. The soot fractions have been calculated using equation

$$F(V) = \frac{\lambda}{6\pi L} \frac{\ell n(I_{tr}/I_o)}{Im\left(\frac{m^2-1}{m^2+2}\right)}$$

where λ = 5145 nm (wavelength of laser); I_{tr} = transmitted laser intensity I_o incident laser intensity and m = complex refractive index of soot.

For the derivation of this equation see Chapter 3 of Mr. Wey's M. S. Special Problem Report which is attached.

II. Activities Planned for the next Reporting Period:

Simultaneous laser light scattering and absorbtion measurements will be carried out systematically throughout a number of different propane-air flames. This will lead to a determination of local soot agglomerate sizes and number densities throughout the flames as well as soot loading distributions by volume using the theory explained in some detail in the attached report.

The specially constructed suction probe will be tested and used to sample the flame gases throughout the propane-air diffusion flames. Soot thus collected will be weighed to establish soot loading distributions by mass. The samples will then be examined using transmission electron microscopy to establish the size distribution of the individual spherical soot spherules which combine in the flame to form agglomerates.

The optical and probe measurements described above will be carried out in flames whose adiabatic flame temperature will be reduced by the addition of nitrogen to the fuel flow. This will permit the determination of the effect of temperature on the quantities and physical properties of soot produced in diffusion flames. Similar experiments will also be carried out using fuels with molecular structures different from propane such as acetylene and benzene. Finally an ionization detection probe such as a Langmuir probe is to be designed to determine ionization levels distributions in the diffusion flames investigated. To this end contact has been made with Dr. Calcote of AeroChem Inc., who is one of the leading proponents of the ionic theory of soot formation in flames.

During the past reporting period Mr. C. Wey the graduate student supported by this project has successfully completed his M. Sc. A copy of his Special Problem Report is attached. Mr. Wey is continuing to work on this investigation as part of his Ph. D. program.

Funds used during this reporting period

Personal Services	8,303.98
Supply & Services	0
Travel	0

No funds for supplies and services were used during this reporting period as the materials used for the construction of the burner and probes were in stock prior to the commencement of the contract and no electron microscopy has, as yet, been carried out.

No travel has been undertaken in conjunction with this project during this reporting period.

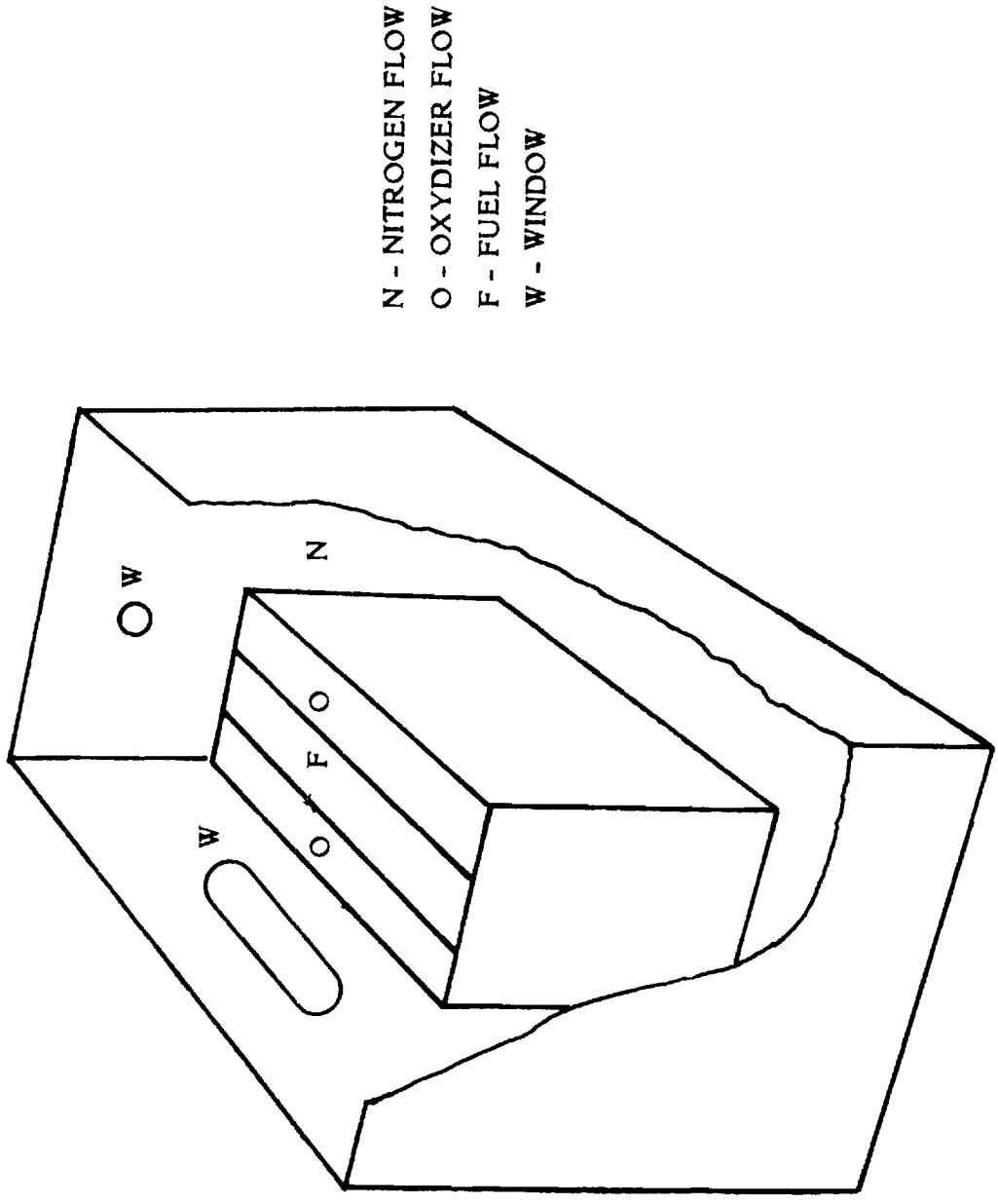

Fig. 1., Parker Wolfhard Burner

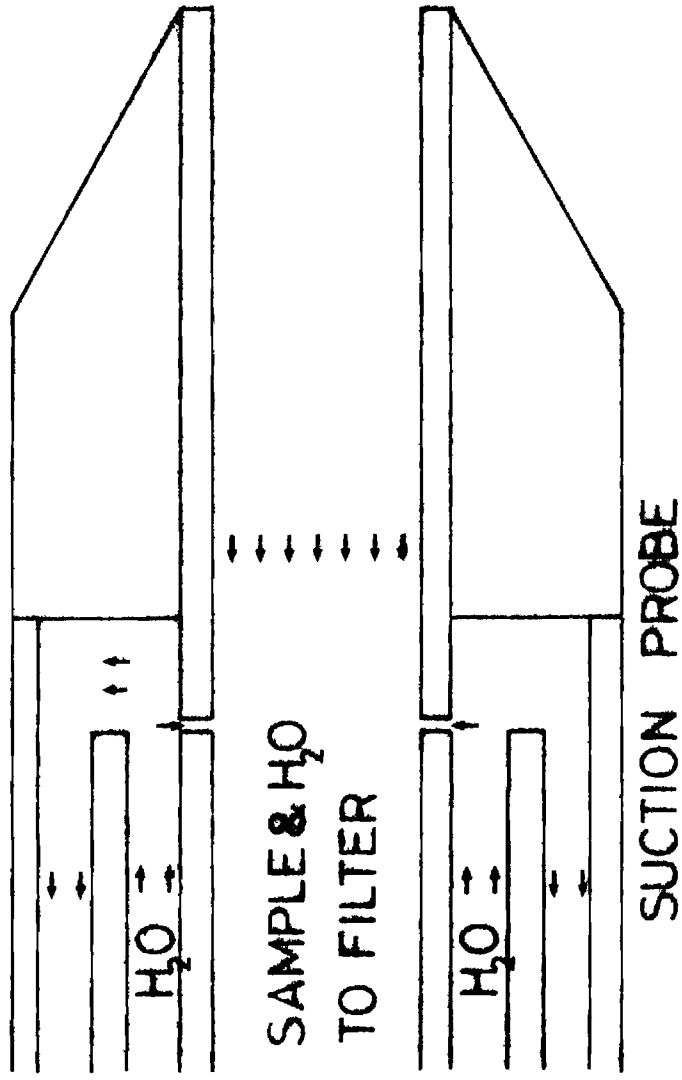

Fig. 2., Suction Probe

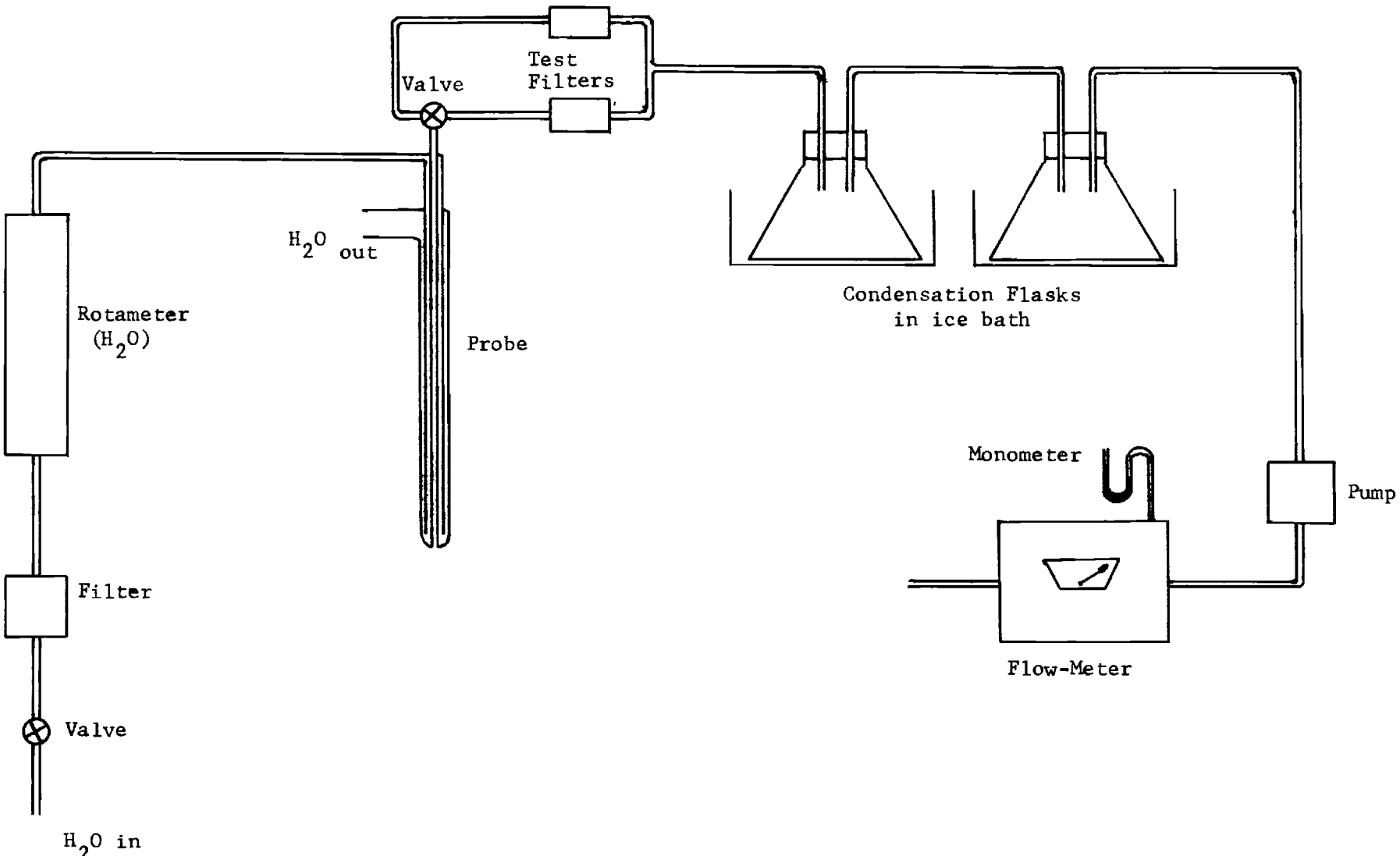

Fig. 3. Schematic of Probe Arrangement.

HT - POWER SUPPLY
L - LENS
C - CHOPPER
F - FILTER
M - MONOCHROMATOR
S - SLIT
O/S - OSCILLOSCOPE
C/R - CHART RECORDER
PM - PHOTOMULTIPLIER
O - OPTIC FIBER
PSD - PHASE SENSITIVE DETECTOR

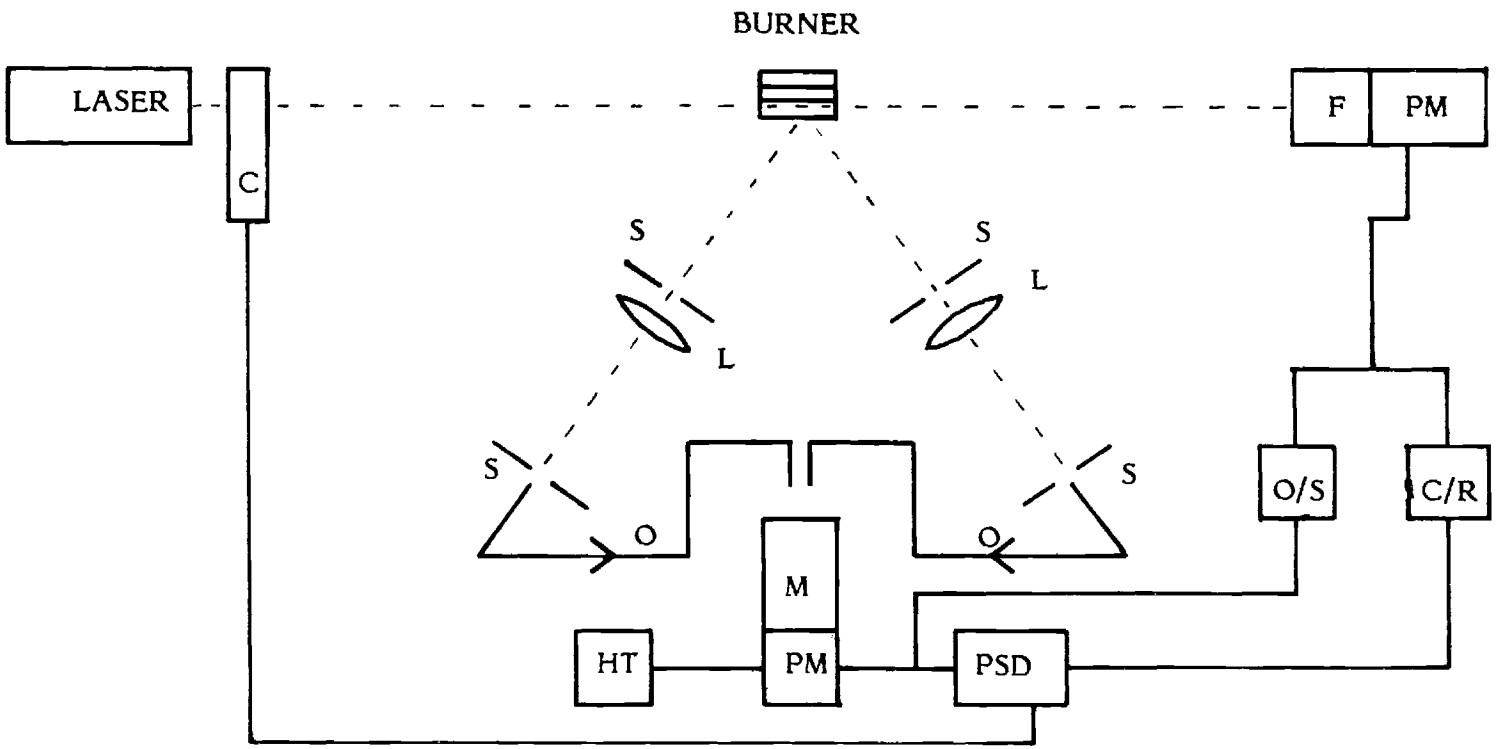

Fig. 4. Optical Set up.

	Gas flow rate (l/min) Air	Fuel	Height above burner (mm)
+	11.5	3.4	9
o	11.5	3.4	12
Δ	18.9	4.0	12

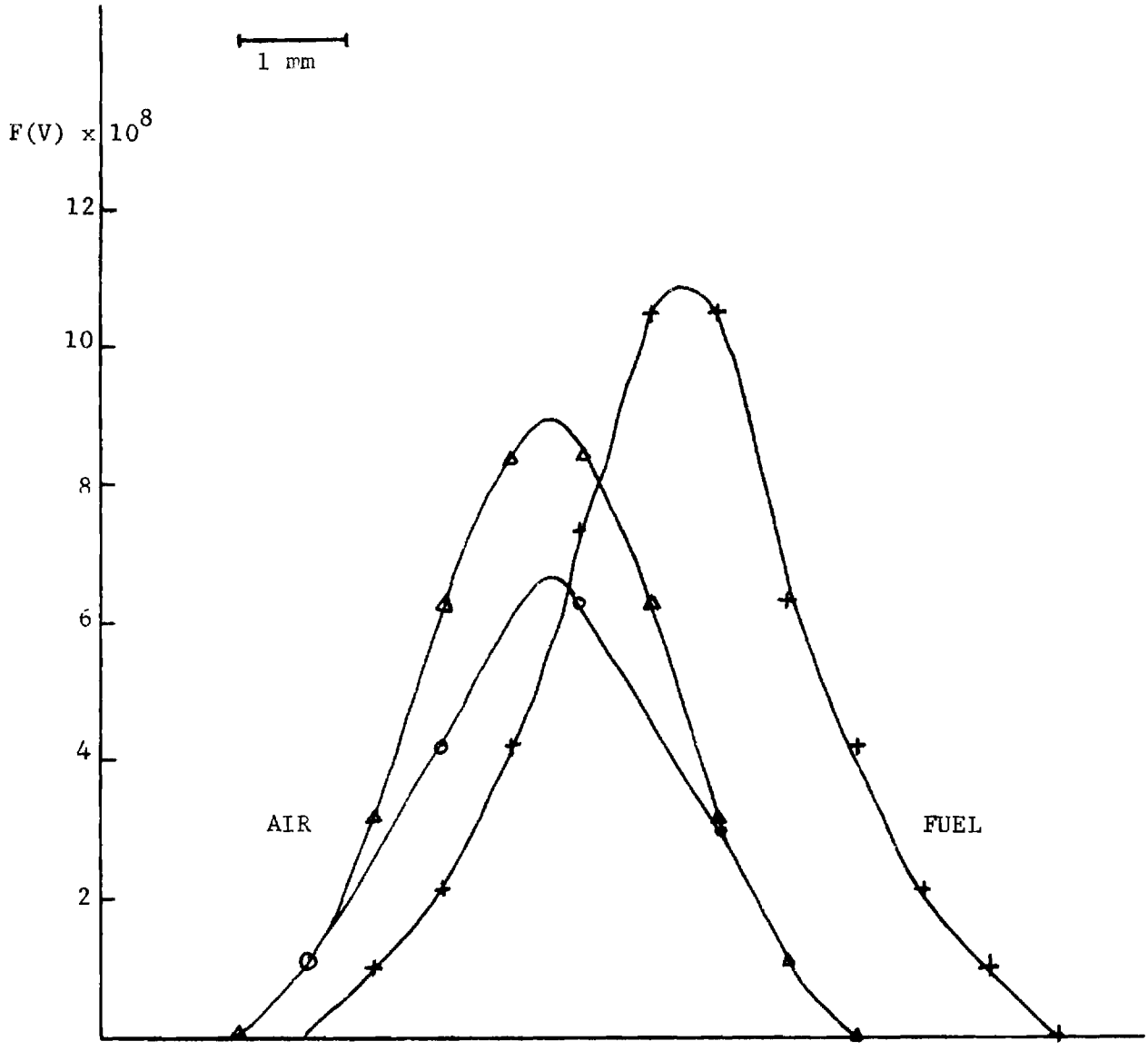

Fig. 5. Soot Concentration by Volume vs. Horizontal Distance for a Flame Sheet for Different Heights and Gas Flow Rates.

Soot Formation in Gaseous Diffusion Flames

2nd 6 monthly progress report

submitted to the

United States Environmental Protection Agency

under Contract # R80895 3010

by

J. I. Jagoda, Principal Investigator

School of Aerospace Engineering

Georgia Institute of Technology

August 1982

I. Work completed during the past reporting period.

Simultaneous laser light scattering and absorbtion measurements have been carried out in a number of different propane-air diffusion flames. From these measurements the soot fractions by volume were calculated as outlined in our first progress report. The local extinction coefficient (K_{ext}) and the Rayleight scattering coefficient (Q) were calculated from the measured values of the transmitted and scattered light intensities respectively using the following equations:

$$K_{ext} = \frac{1}{L} \ln \frac{I_{tr}}{I_o}$$

where I_{tr} = transmitted laser intensity, I_o = incident laser intensity and L = length of the optical path of the laser beam in the flame
and

$$I_{sc} = \eta_{el} \eta_{opt} Q(\Delta V)(\Delta \Omega) I_o$$

where I_{sc} = the laser intensity scattered from volume ΔV over solid angle $\Delta \Omega$ and η_{el} & η_{opt} = the efficiencies of the electronics and the optics respectively. The η's ΔV and $\Delta \Omega$ were determined by calibration using a gas of known Q such as nitrogen or methane.

The Mie theory in the Rayleigh approximation expresses both K_{ext} and Q as function of the number density of soot aggregates (N) and their mean diameter (D) in the following form

$$K_{ext} = \frac{\pi^5}{\lambda^4} \text{Im} \left| \frac{m^2 - 1}{m^2 + 2} \right| ND^3$$

$$Q = \frac{\pi^4}{4\lambda^4} \text{Re} \left| \frac{m^2 - 1}{m^2 + 2} \right| ND^6$$

where λ = wavelength of the laser light and m = the complex refractive index of soot.

The above equations are then solved simultaneously to obtain N and D. For the derivation of these equations see Chapter 3 of Mr. Wey's M. S. Special Problem Report which has been forwarded previously.

The following results were obtained during the past report period:

Fig. 1 shows the distribution of soot fraction by volume vs the distance from the burner center at different heights above the burner for a given flame. The increase in soot levels with height above burner, especially some distance downstream, indicates that the soot formation rate there exceeds the depletion rate by burn out. Fig. 2 shows that the mean size of the soot aggregates increases in the downstream direction. This increase is in part due to agglomeration of soot particles as indicated in Fig. 3 where a decrease in the number of aggregates in the downstream direction is evident. This agglomeration process is particularly pronounced in the lower part of the flame. The agglomeration is accompanied by surface growth since the increase in soot content in the flame with distance downstream noted in Fig. 1 cannot be explained by agglomeration, a process which does not affect the total amount of soot present.

Diffusion flames burn essentially under stoichiometric conditions in their flame front and, thus, their adiabatic flame temperatures are fixed for a given fuel and oxidizer. Their flame front temperatures can, therefore, only be varied by adjusting either oxidizer or fuel composition. To determine the effect of the flame temperature on soot formation, the percentage nitrogen content in the oxidizer flow was varied while keeping both fuel and oxidizer flow rates constant. Since the nitrogen acts as a heat sink an increase in nitrogen causes a decrease in flame temperature. Fig. 4 is a plot of soot fraction by volume vs. distance from the burner center at a fixed height in the flame and for different nitrogen levels. It can be seen that a

decrease in nitrogen content and, thus, an increase in the flame temperature results in a marked increase in the amount of soot formed. This is in good agreement with previous work carried out at Princeton which demonstrated the increase in sooting tendency of a diffusion flame with increase in temperaure using overall sooting height measurements. Furthermore, Fig. 5 shows that the mean soot agglomerate sizes increase with temperature. Soot was then extracted at this downstream position from the different flames and viewed under a transmission electron microscope. The diameter distribution for the spheroids which make up the agglomerates was determined for each flame temperature. The mean spheroid diameters were found to be 27, 34 & 38 nm for the temperatures plotted in Figs. 4 & 5, whereby the spheroid diameters increase with temperature, indicating that the increase of agglomerate dimension with temperature is mainly caused by the larger spheroids of which they are made up.

II. Activities planned for the next reporting Period.

The next 6 months will see the complete mapping of various propane-air diffusion flames with different nitrogen contents in their oxidizer and, thus, different flame temperatures. Measurements will be carried out using simultaneous laser light scattering and extinction measurements as will soot collection followed by transmission electron miroscopy. This will permit the determination of the physical properties of both the soot spheroids and their agglomerates throughout the flame. Flame temperatures will be measured using thermocouples while other means of temperature determination, such as spectroscopic line reversed techniques, will be investigated. Furthermore, a Langmuir probe for the determination of ionization levels in the flame is to be constructed. As they become available, all results obtained will be compared with the different models for individual steps in the process of soot formation found in the literature.

III. Funds used during this reporting period.

Personal Services:	10,297.70
Supply & Services:	1,981.81
Travel:	1,050.42

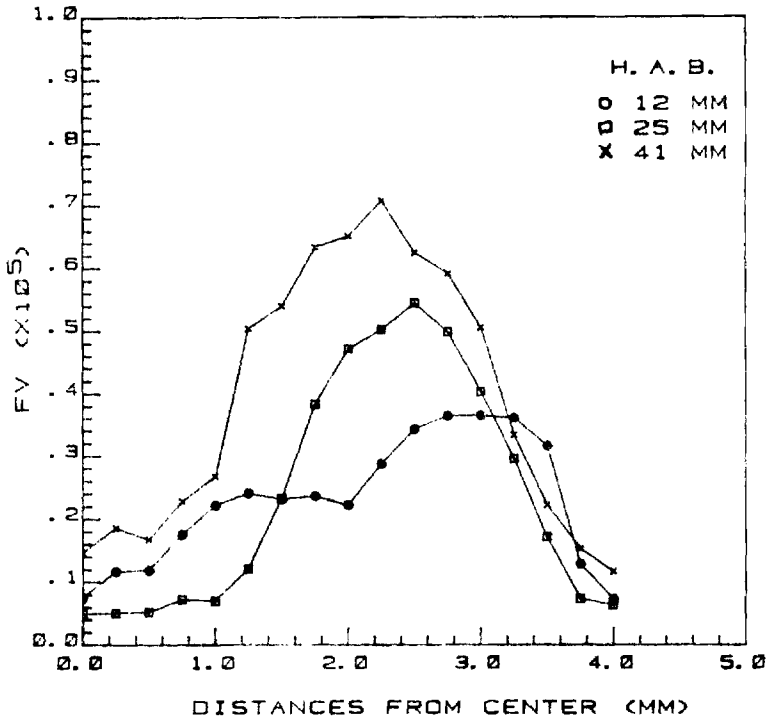

Fig. 1. Soot concentration by volume vs. distance from burner center for different heights above burner.

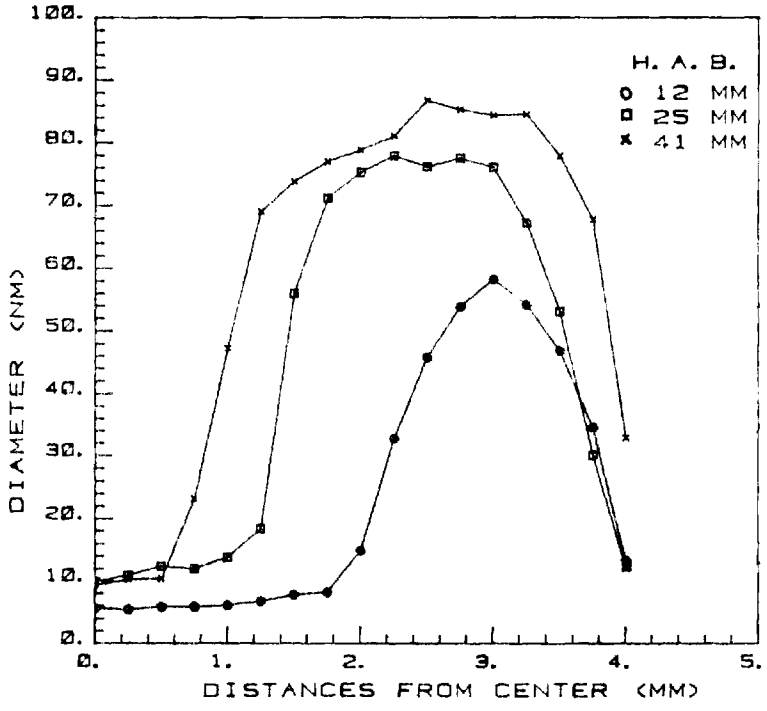

Fig. 2. Mean aggregate diameters vs. distance from burner center for different heights above burner.

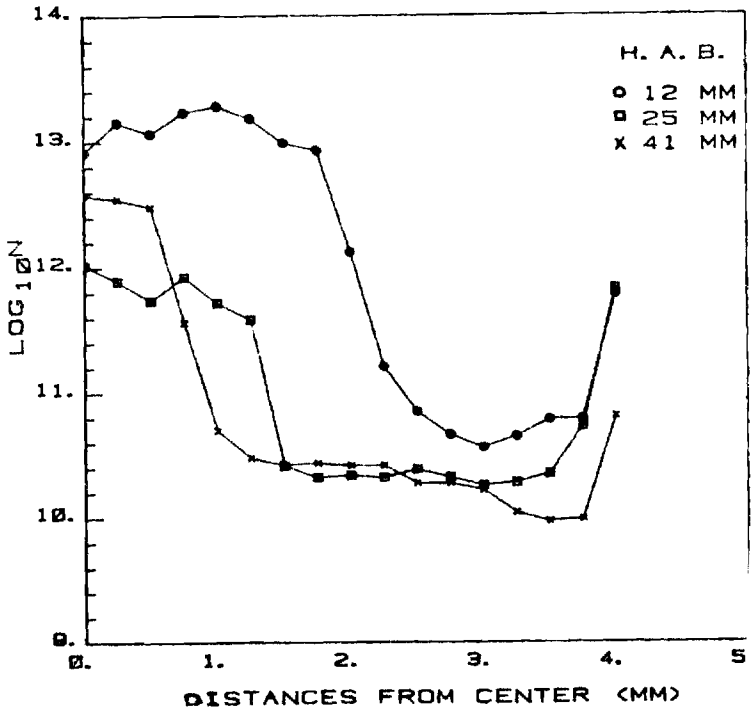

Fig. 3. Number density of aggregates vs. distance from burner center for different heights above burner.

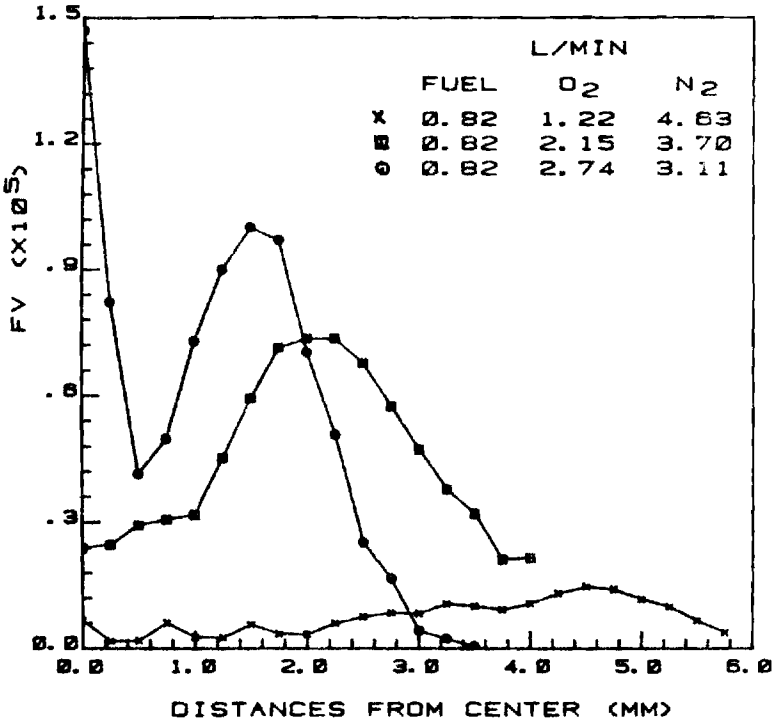

Fig. 4. Soot concentrations by volume vs. distance from burner center for different flame temperatures.

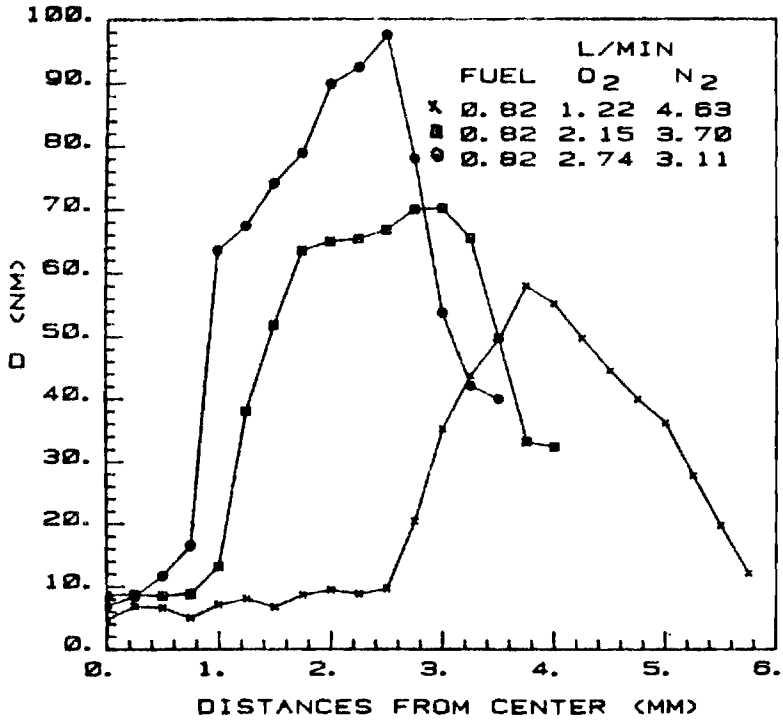

Fig. 5. Mean aggregate diameters vs. distance from burner center for different flame temperatures.

E-16-627

Soot Formation in Gaseous Diffusion Flames

3rd 6 monthly progress report

submitted to the

United States Environmental Protection Agency

under Contract # R80895 3010

by

J. I. Jagoda, Principal Investigator

School of Aerospace Engineering

Georgia Institute of Technology

February 1983

I. Work completed during the past reporting period.

During the past six months the burner was modified to include water cooling. This permitted extended run times without the danger of overheating the device. The simultaneous laser light scattering measurements were completed for propane oxygen diffusion flames at different flame temperatures. Since in diffusion flames the combustion occurs under essentially stoichiometric conditions the flame temperature had to be varied by using oxidizer flows of different nitrogen contents whereby the nitrogen acts as a diluent. The laser absorbtion measurements yielded local soot volume fractions (F_v) while simultaneous absorbtion and scattering measurement resulted in the determination of local mean diameters of soot aggregates (D) and their number densities (N). The relationships used for determining these quantities from the optical measurements were detailed both in the proposal and the second progress report.

Complete mappings of F_v, D and N are presented here for 3 different flame temperatures corresponding to oxygen indices OI = .27, .33 and .41. (The oxygen index is defined as the ratio of the number of moles of oxygen to the number of moles of nitrogen. An increase in oxygen index corresponds to an increase in temperature.) Fig. 1 shows a series of contour maps showing lines of constant local number density throughout the flames of different oxygen indices. Moving outwards from the center of the flame, which is coincident with the left vertical axis, the number density decreases at first and then increases again near the flame front. (The dotted lines in Figs. 1-3 correspond to the lines of minimum values of the quantities being mapped out) Fig. 2 shows contour maps for lines of constant soot agglomerate diameters for the three temperatures. Here the diameters increase and then decrease for all three temperatures as one moves from the burner center to the flame front. In Fig. 3 the contour maps for soot volume fractions are presented for the same flame temperatures. Again the soot volume fractions peak as one moves radially outwards from the burner center to the flame front. Closer inspection of the contour maps indicates that with an increasing temperature soot formation is observed at lower distances above the burner. This reflects the higher reaction rate for chemical processes leading for soot formation with increasing temperature and will be referred to again later.

A better understanding of the evolution of the soot properties can be obtained by plotting them as a function of radial distance from the burner center for different constant heights above the burner, as seen in Figs. 4,5 & 7. Fig. 4 shows the distribution of soot volume fraction as a function of radial distance for different heights, measured in mm, above the burner, for the three temperatures. At all temperatures the soot present in the flames clearly increases with height above the burner. The soot formation rate thus far exceeds soot removal by, for example, burn-out even for the higher temperatures. Furthermore, the amount of soot present at any height above the burner increases with increased temperature. Thus the increase of

reaction rate with temperature in the lower region of the flame prior to soot formation which reduces the height of first soot appearance for increasing flame temperature persists into the sooting region of the flame. Also any reactions that may lead to soot removal seem to be less influenced by the increase in temperature than steps leading to soot formation.

In Fig. 5 the soot aggregate diameters are plotted against distance from the burner center for different constant heights above the burner surface for the three different temperatures. Clearly the mean soot aggregate diameters always increase with increasing height in the flame. This could be due to an increase in agglomeration or particle surface growth or both. In any case the increase in soot concentration with height above the burner seems at least partially due to an increase in soot aggregate size for all flame temperatures investigated. Furthermore, the increase in temperature has the effect of increasing the soot agglomerates found at given heights above the burner. As described in the last progress report the soot agglomerates consist of spherical elementary particles . While agglomerate properties are determined using the simultaneous scattering and absorbtion measurements, the spheroid dimensions are obtained from electronmicroscopy. Soot samples were extracted from the flame at locations at which laser diagnostic measurements had been carried out. These soot samples were viewed under a transmission electron microscope and the mean diameters (d) of the particles which make up the agglomerates were measured. Some of these results are plotted in Fig. 6. Clearly there is an increase in fundamental particle diameter with height above burner for a given oxygen index or temperature. This increase is particularly pronounced in the lower parts of the flame where agglomeration is not yet too extensive. A similar increase in spheroid diameter can be obtained by raising the flame temperature as effected by increasing the oxygen index. The increase in soot agglomerate diameters both with height above the burner and with temperature can, therefore, at least partially be explained by an increase in the diameter of the fundamental soot spheroids which make up the agglomerates. This is especially true in the lower part of the flame.

In Fig. 7 the agglomerate number densities are plotted against distance from the burner center for various heights above the burner at the three temperatures. It should be noted that the values of N are less accurate than those of the aggregate diameters and the soot volume fractions. This is due to the fact that the scattered intensity is proportioned to ND^6 while the amount of light absorbed varies as ND^3. Small errors in D, therefore, translate into large uncertainties in N. This is particularly problematic near the center of the flame up to approximately 1.4 mm from the burner center where the possible existance of small flamelets and the presence of large molecules or soot precursors may drive up the recorded values of N. A careful inspection of the three plots in Figure 7 shows that there is a trend of decrease in N with increasing height above the burner which is consistant with an aggregation process of soot in the flame. This aggregation seems particularly pronounced in the lower part of the flame. This is the trend for

all three flame temperatures reported here, as for the effect of temperature on the aggregate number density it seems to be far less pronounced than the influence of temperature on either the soot volume fraction or the mean aggregate diameters.

In summary, it has, thus, been observed that soot increases with both height above burner and with temperature. The number of soot agglomerates only changes significantly in the early part of the flame, where it is reduced due to agglomeration. In this region the agglomerate diameters are further increased by a rapid increase in the size of the spherical soot particles which make up the agglomerates. The increase in the amount of soot produced may thus be due to both new particle inception and surface growth. Higher up in the flame the basic spheroid diameters grow at a reduced rate while agglomerate number densities are essentially constant. Agglomeration is, thus, relatively small in that region unless it is compensated by new particle inception. It is felt that this is not very likely since lots of new particles would reduce the mean agglomerate diameters, which has not been observed. The effect of an increase in flame temperature is most clearly seen in large spheriod diameters, which leads to larger agglomerate diameter and soot volume fractions. There may also be some increase in agglomeration but the total number of agglomerates seems relatively insensitive to flame temperature.

In order to try to quantize the effects of both the height above the burner and the flame temperature, selected soot properties were plotted against height above the burner for the three temperatures. Since the reactions leading to soot formation may be expected to be accelerated by an increase in temperature, we have attempted to account for this. If the reactions responsible for continued soot formation in the flame are affected by temperature in a similar fashion as the reactions leading to the initial soot formation all heights above the burner at the different temperatures must be normalized by the distance above the burner where soot is first observed for that temperature. (i.e., measured height above burner divided by first sooting height for that temperature). The soot properties selected for these plots are the total soot volume fraction at different heights above the burner (= areas under the curves) and corresponding maximum aggregate diameters. These quantities were plotted against height above burner and normalized height above burner for all three temperatures.

Fig. 8 shows the total soot volume faction across the flames as a function of height above burner (HAB) and normalized HAB for all threetemperatures. The total soot increases for all three flames in the downstream direction. However, when plotted against normalized HAB the values for total soot at all temperatures fall much closer to a common line. When the lowest point for the middle temperature is neglected (it lies in a region where small particles are agglomerating; these may be susceptible to increased burn out at the high temperature) the slopes, or rates of soot formation with time, are almost equal for all three temperatures. When maximum soot agglomerate diameters are plotted against HAB and

normalized HAB the rate of diameter increase with HAB can be seen to be essentially the same for all three temperatures which is not the case for the normalized HAB. (The differences in the absolute values of the agglomerate diameters for different temperatures is at least partially due to the increase in spheroid sizes with temperature.) There is, thus, a difference in the behaviour between the soot formation and agglomerate growth processess. Since HAB is essentially a time scale, soot generation is proportional to time normalized by the reaction rate in the presooting region while particle growth rate is just a function of time. In all the above, boyancy effects due to the different flame temperatures and the influence of the different densities of fuel and oxidizer have been neglected. These effects are currently being investigated by introducing the temperature and density differences into a Burke-Schuman type model of the diffusion flame. This may reduce some of the scatter in the data although the correlation coefficients between the measured data and the least squares straight lines in Figs. 8 and 9 are better than .95, in some cases better than .99. Various models are also being considered to attempt to predict the soot agglomeration rates and these will be compared with measured data. Adiabatic flame temperatures have been determined using a simplified model neglecting dissociation and equilibrium shift due to temperature. These results which are expected to be high are summarized as follows:

OI	predicted max. temperature
.27	2394 ^{o}K
.33	2670 ^{o}K
.41	2930 ^{o}K

These predictions are currently being improved by incorporating a NASA code into our model which allows the effect of dissociation and chemical equilibrium to be fully accounted for. The predicted temperatures will then be compared with those currently being measured in the flame using an improved thermocouple technique and sodium line reversal.

II. Activities planned for the next reporting period.

In the next reporting period we are proposing to complete the determination of the effect of density and temperature variations on the data obtained during the past six months. Furthermore, the diameters measured in the flames will be compared with those predicted from different agglomeration models and improved temperature predictions will be carried out by making use of the above mentioned NASA code. In a more general vain, we shall further compare our findings with soot formation models found in the literature. This coincides well with an invitation to write a review paper on soot formation which has been extended by the editor of "Progress in Energy and Combustion Science" to the principal investigator of this study.

On the experimental side we shall complete our mapping of temperatures in the flames investigated. Traces of oxygen will be premixed into the fuel side of the diffusion flame and soot properties measured in order to note its effect on the chemical reaction rates which have been shown to strongly influence the soot volume fractions generated. Lastly preparations will be made to introduce aromatic fuels into the fuel flow. Since even simple aromatic fuels such as toluene are liquid at room temperature air atomizing and evaporizing systems will be designed and incorporated in the fuel line. The effect of aromatic molecules on the process of soot formation will then be studied.

III.Funds used during this reporting period:

Personal Services	16,959.00
Supply & Services	1,352.93
Travel	656.27

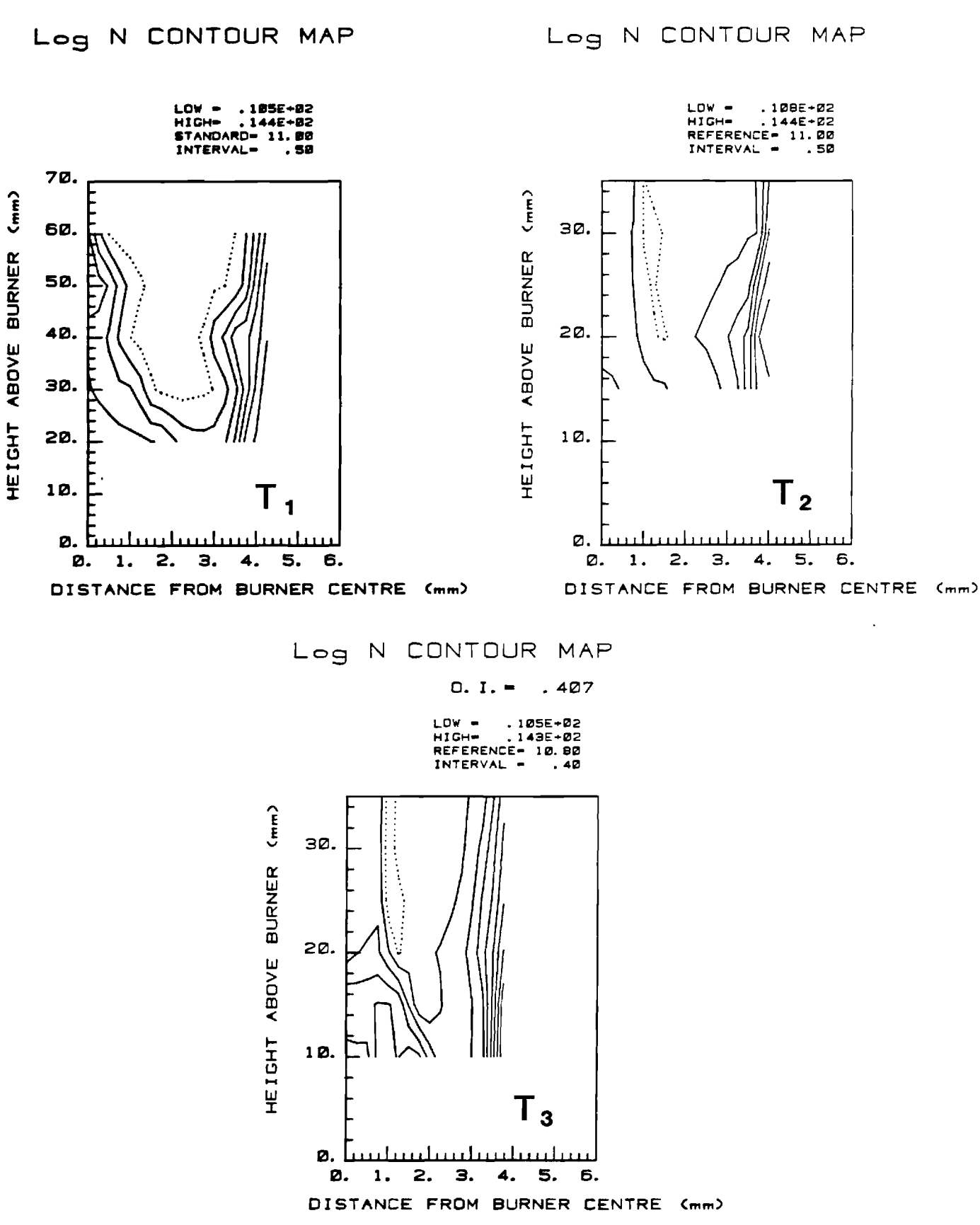

FIG. 1., MAPS OF SOOT AGGREGATE NUMBER DENSITIES FOR THREE TEMPERATURES ($T_1 < T_2 < T_3$)

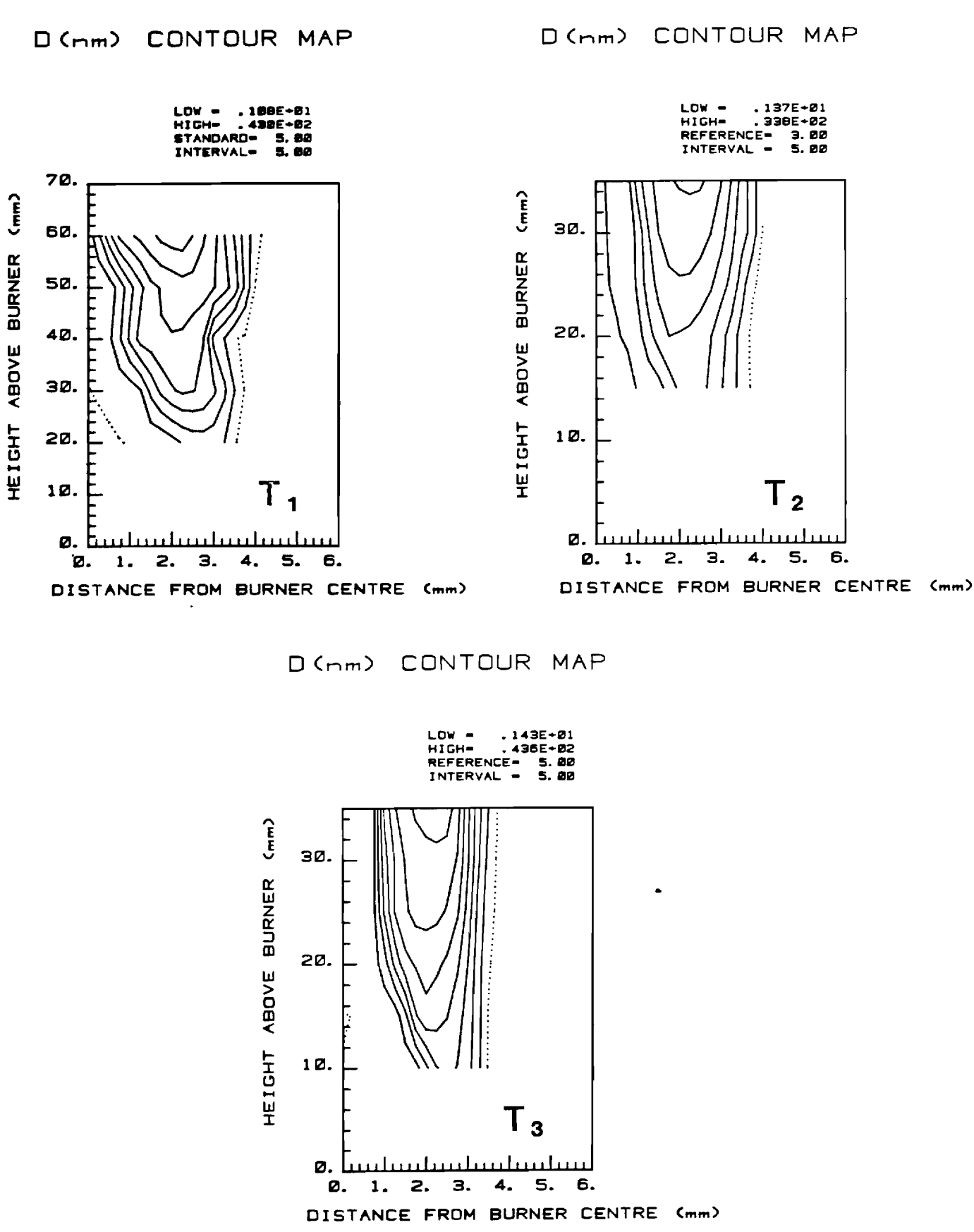

FIG. 2, MAPS OF SOOT AGGREGATE DIAMETERS FOR THREE FLAME TEMPERATURES ($T_1 < T_2 < T_3$)

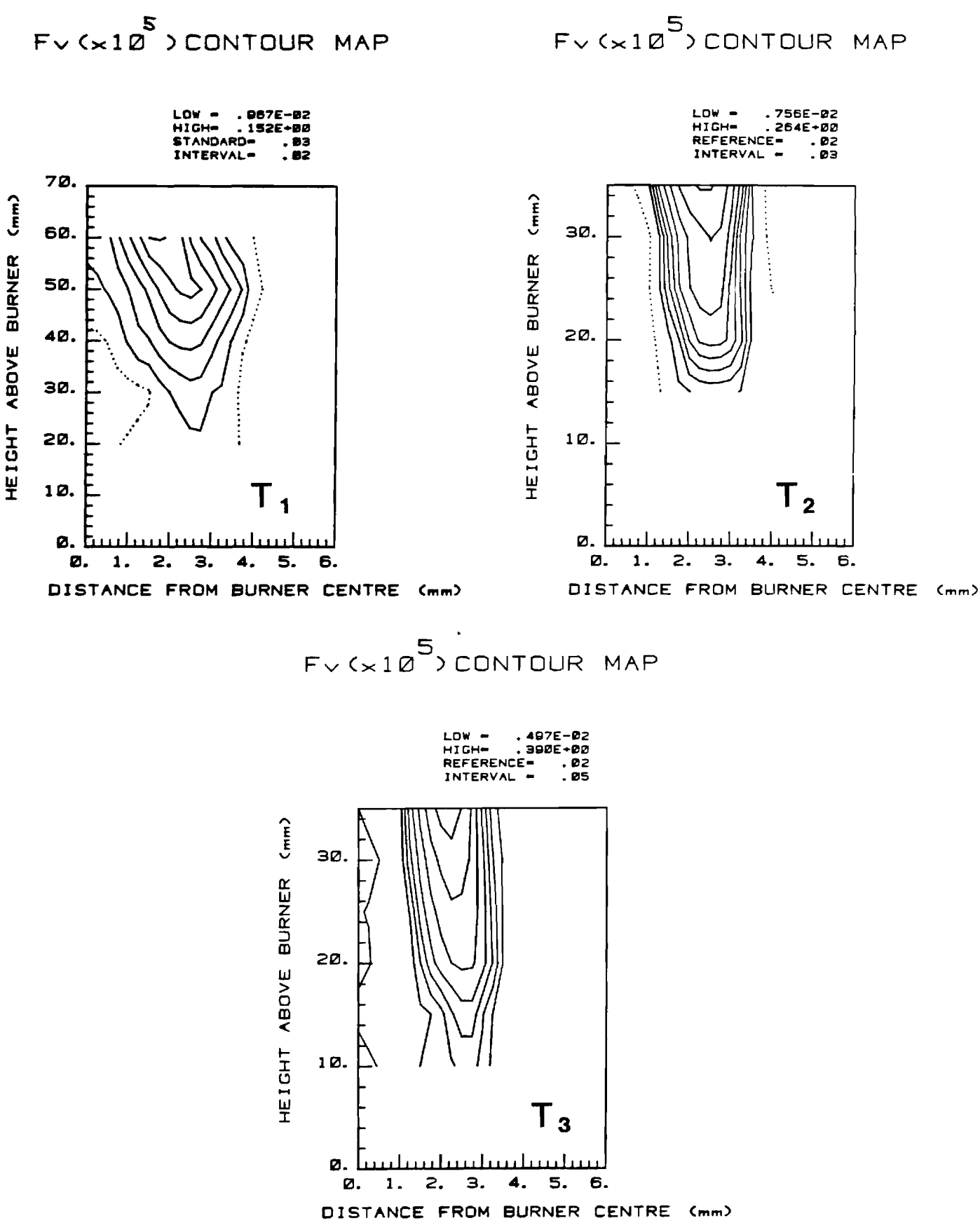

FIG. 3, MAPS OF SOOT VOLUME FRACTION FOR THREE FLAME TEMPERATURES ($T_1 < T_2 < T_3$)

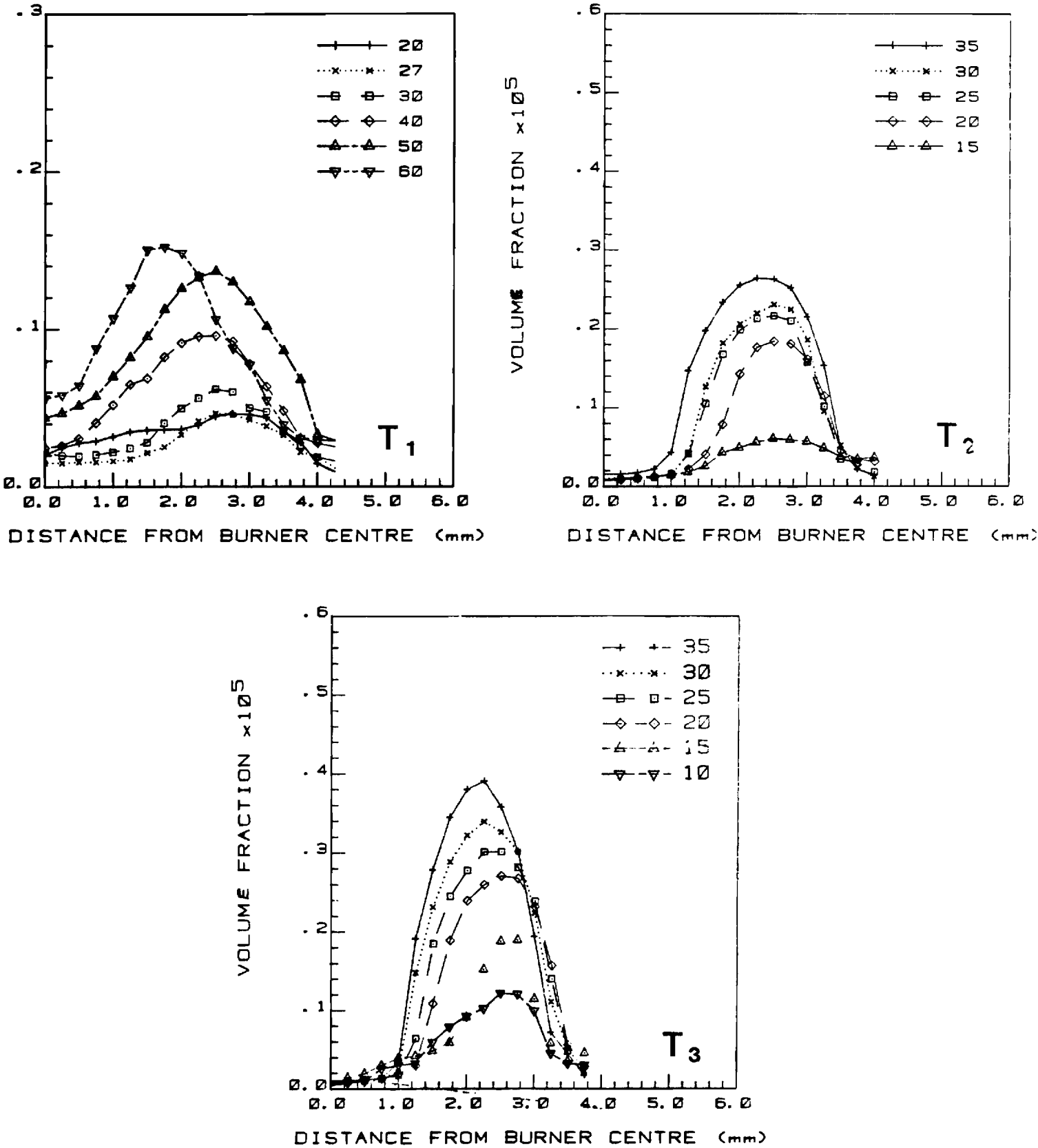

FIG. 4, SOOT VOLUME FRACTIONS VS DISTANCE FROM BURNER CENTRE FOR THREE FLAME TEMPERATURES ($T_1 < T_2 < T_3$)

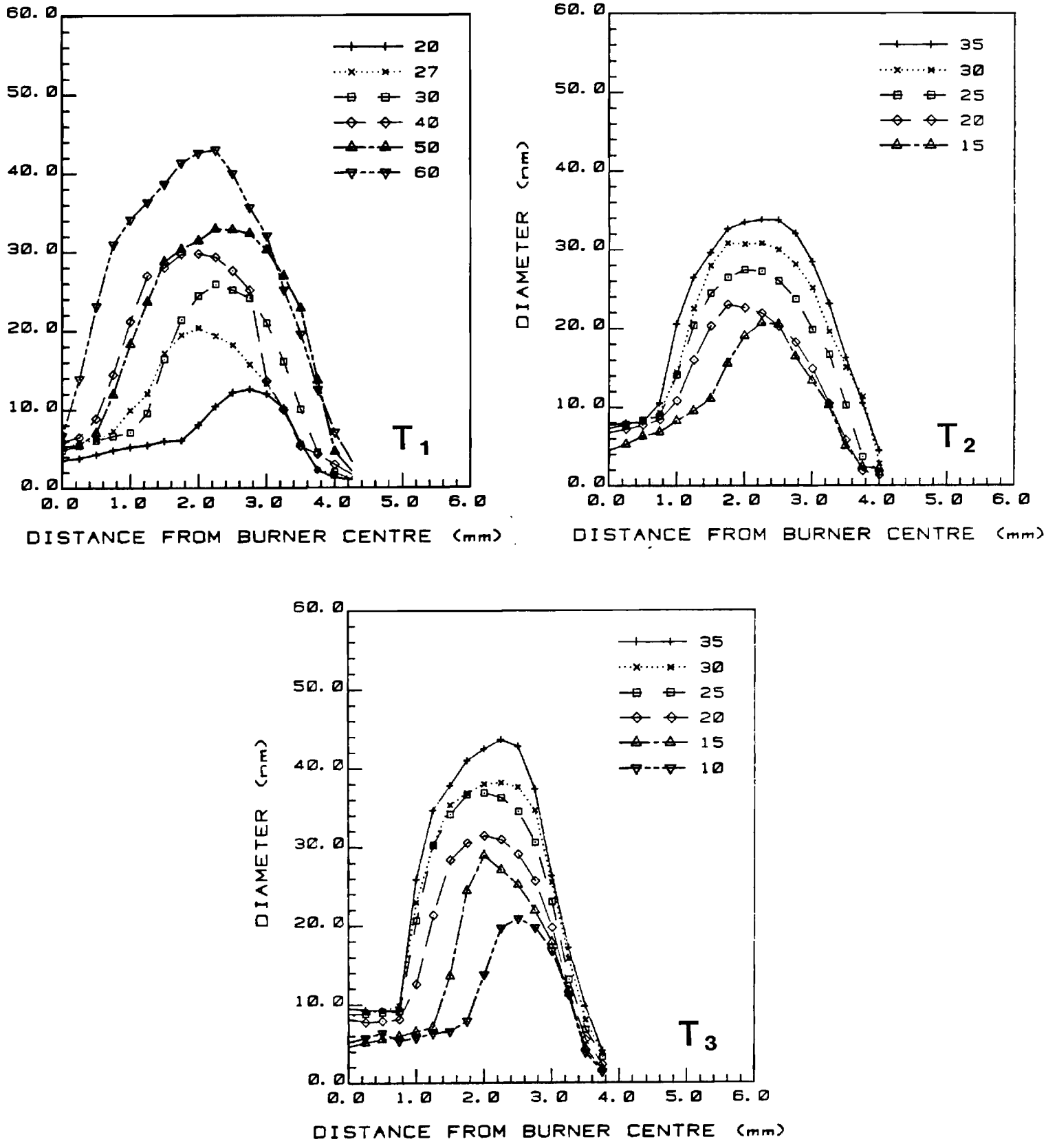

FIG. 5, SOOT AGGREGATE DIAMETERS VS. DISTANCE FROM BURNER CENTRE FOR THREE FLAME TEMPERATURES ($T_1 < T_2 < T_3$)

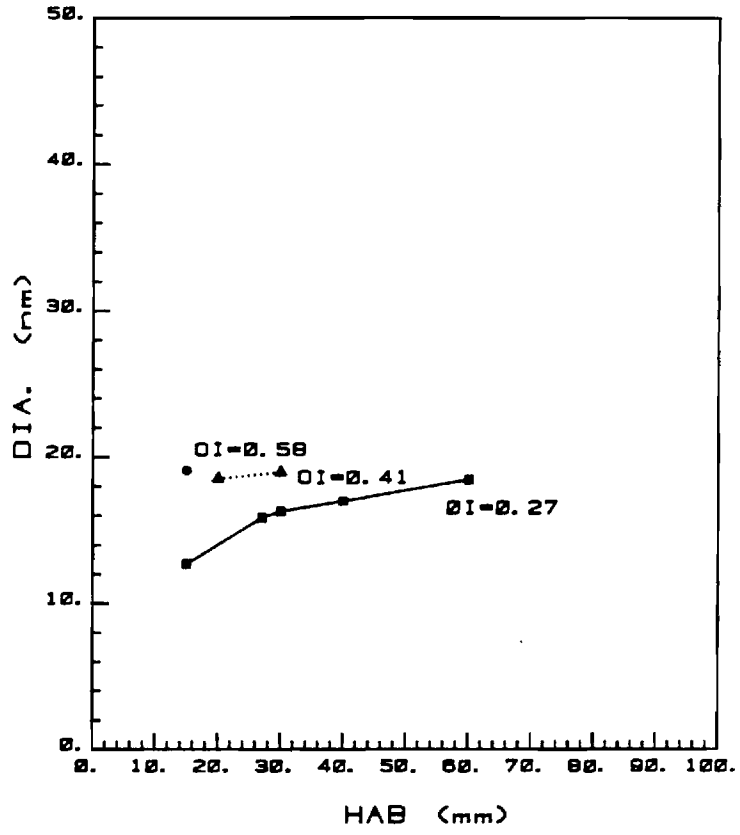

FIG. 6, SOOT SPHEROID DIAMETERS VS HEIGHT ABOVE BURNER

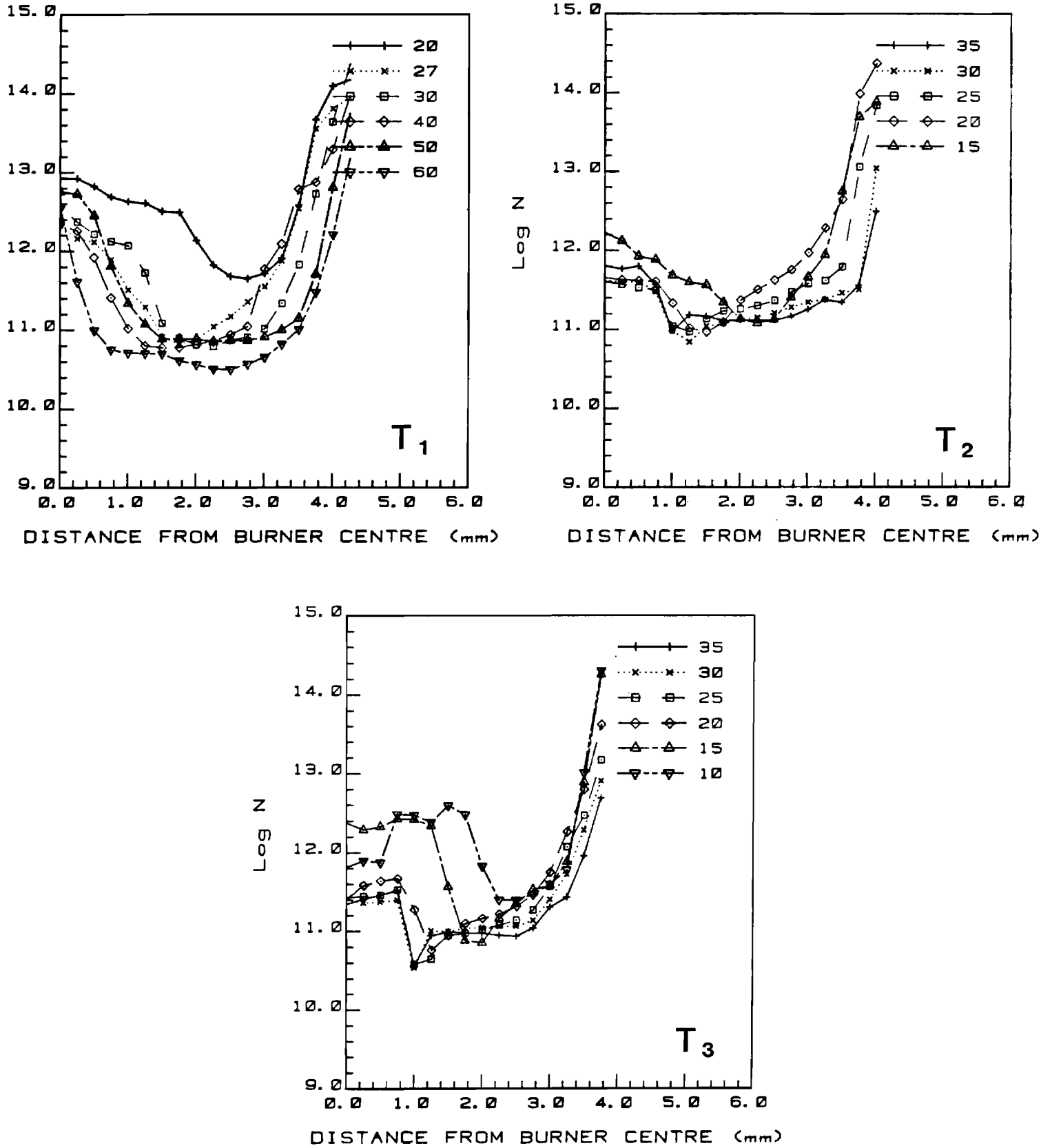

FIG. 7, SOOT AGGREGATE NUMBER DENSITIES VS DISTANCE FROM BURNER CENTRE FOR THREE FLAME TEMPERATURES ($T_1 < T_2 < T_3$)

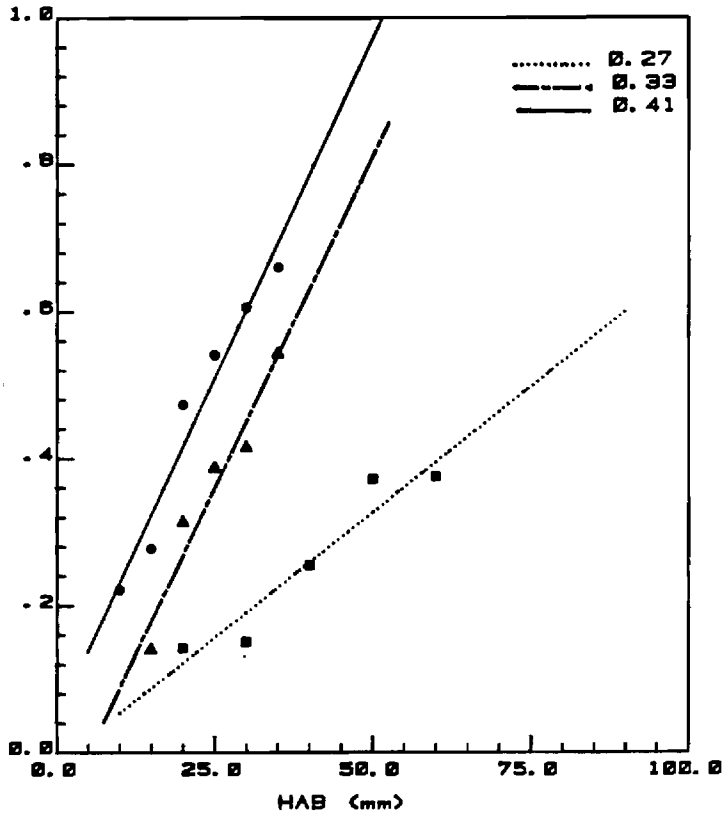

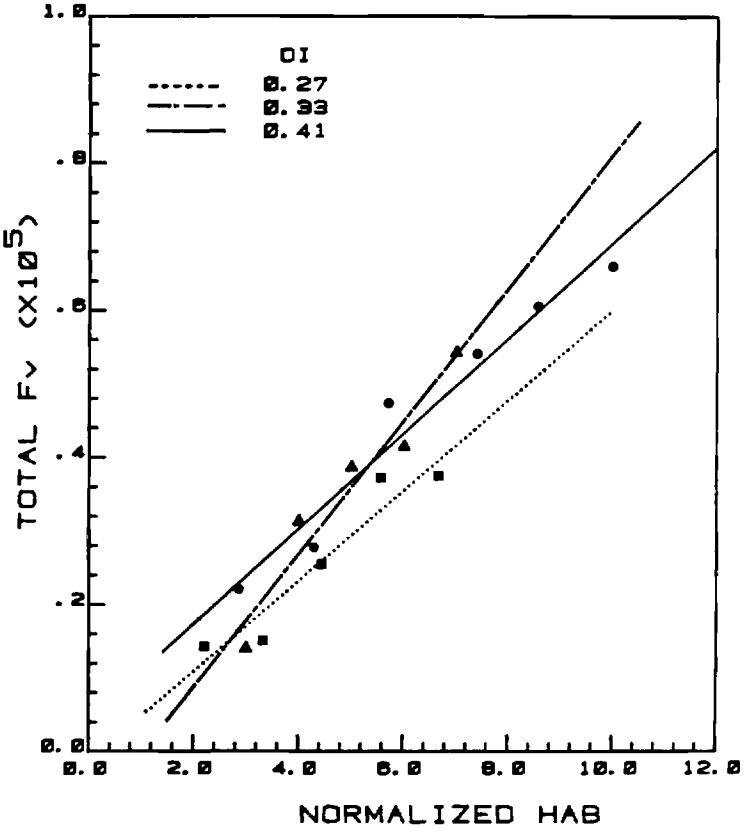

FIG. 8, TOTAL SOOT VOLUME FRACTION VS HEIGHT ABOVE BURNER AND NORMALIZED HEIGHT ABOVE BURNER

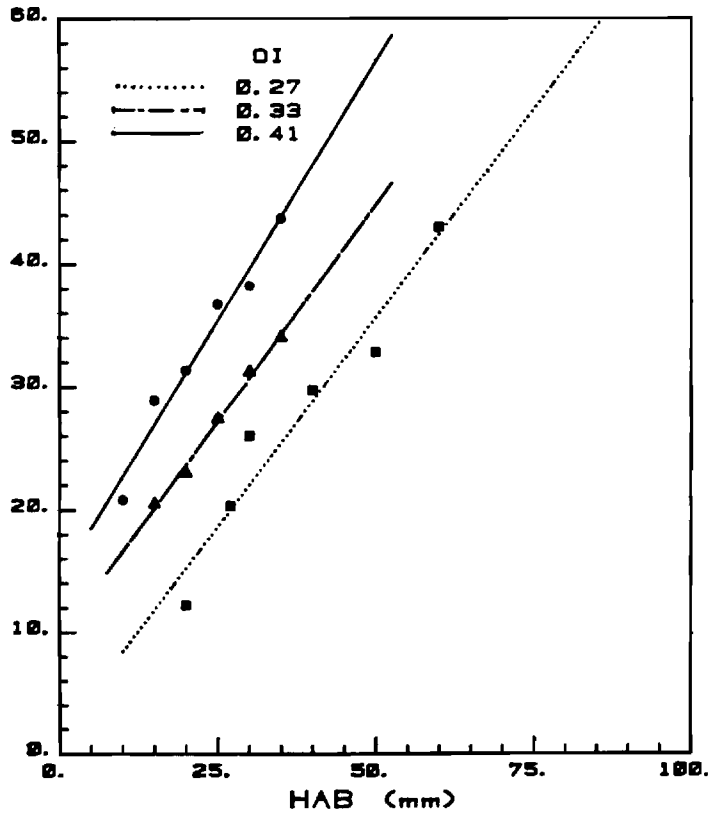

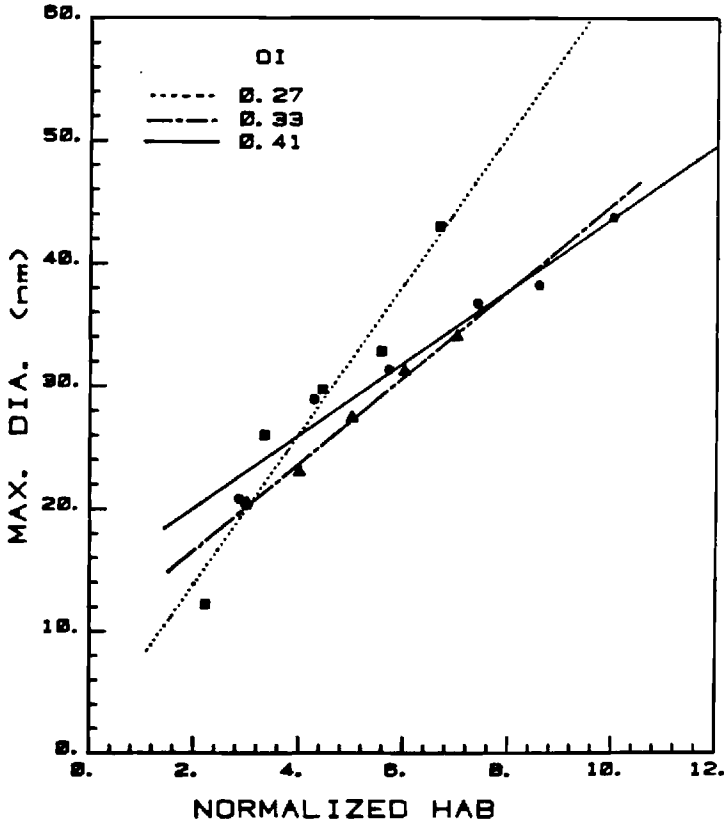

FIG. 9, MAXIMUM AGGREGATE DIAMETER VS HEIGHT ABOVE BURNER AND NORMALIZED HEIGHT ABOVE BURNER

Soot Formation in Gaseous Diffusion Flames

4th 6-Monthly Progress Report

Submitted to the

United States Environmental Protection Agency

Under Contract # R 80895 3010

by

J. I. Jagoda, Principal Investigator

School of Aerospace Engineering

Georgia Institute of Technology

August 1983

I. Work completed during the past reporting period.

Part of the work carried out during the past six months has been described in the progress-section of the renewal proposal which was submitted to EPA at the end of May 1983. Much of the remainder of the activities of the present budget period are included in a manuscript which has recently been submitted for publication to Combustion Science and Technology, a copy of which is attached. The most important results obtained during the past six months are summarized here to differentiate them from work carried out earlier under this contract.

Adiabatic flame temperatures for the three flames investigated in detail have been theoretically determined using NASA code SP-273. This model takes into account the equilibrium concentration of species in the flame. The results are tabulated below and compared with the simple enthalpy balance predictions reported in the last six monthly progress report.

Flame	Predicted Adiab. Flame Temperature Simple Enthalpy Balance	Predicted Adiab. Flame Temperature Including Equilibrium Considerations
T_1	2394°K	2279°K
T_2	2670°K	2417°K
T_3	2930°K	2540°K

Fig. 1 shows the temperature distribution for the propane-pure air diffusion flames (i.e., T_1) as determined using a Pt - Pt 13% Rhodium thermocouples. The flame front, which lies in the region of maximum temperature, exhibits a temperature which is quite constant with height above the burner. As one moves horizontally away from the flame front, the temperature drops both in the direction towards the fuel and towards the oxidizer. Nearer the center of the flame the temperature increases somewhat with height. Heat losses by radiative heat transfer from the soot particles are, thus, more than compensated by heat addition through convection from the flame front to the center of the pyrolysis zone for this part of the flame.

Comparison of Fig. 1 with the graphs of soot distribution in flame T_1 in the last six-monthly report shows that all soot appears to be present inside the fuel rich side of the flame front.

The temperatures in the flame fronts for the flames with higher oxygen to nitrogen ratios (i.e., "T_2" and "T_3") were found to be above the melting point of platinum, causing the thermocouples to break. In order to obtain an indication of the relative temperature changes between the three flames, a shielded Pt-Pt 13% Rh thermocouple was used at selected positions in all three flames. This probe resulted in lower readings because of the heat loss due to the shield and no melting occurred. It was noted that the ratios between measured "shielded" temperatures in the flame front and calculated adiabatic flame temperatures were the same for all three flames within 1%. Flame temperatures for flames "T_2" and "T_3" were, therefore, extraplated by multiplying the ratio between the unshielded measured

temperature of flame "T_1" and its calculated adiabatic flame temperature by the calculated adiabatic flame temperatures for flames "T_2" and "T_3". Values for the flame front temperatures of 1973^{o}K for flame "T_1", 2063^{o}K for flame "T_2" and 2195^{o}K for flame "T_3" were, thus, obtained. The shapes of the isotherm lines for the three flames are assumed to be similar.

In order to quantify the effect of the flame temperature on the global reaction rate of the soot formation reaction, the total soot volume fractions at different heights above the burner (i.e., area under soot volume fraction plots) and the corresponding maximum aggregate diameters were plotted versus height above burner and normalized heights above burner in the last six-monthly report. For a more meaningful presentation, however, the height above burner needs to be converted into residence time. Residence time is defined as the time required for a pocket of gas to travel from the burner to a given height. Since no velocity measurements were carried out in this flame, the residence time in the flame had to be related to the height above the burner using theoretical considerations. Kent and Wagner (1982), who carried out velocity measurements in a similar diffusion flame, have established that buoyancy forces cause considerable acceleration of the vertical velocities in this type of flame. The relationship between the time required to reach a given vertical position and its height above the burner is, therefore, not linear.

A simple, one-dimensional model of two parallel streams of gases of differing densities based on the work by Powell and Browne (1956) was, therefore, developed, which takes into account both the difference in

density of fuel and oxidizer and the difference in temperature of the combustion products and the surrounding oxidizer flow.

The fuel at temperature T_f and oxidizer at temperature T_o are assumed to leave the burner in parallel streams with velocity u_i at height y = 0. The cross-sectional area of the oxidizer and fuel streams at y = 0 are A_{o_i} and A_{f_i} respectively (Fig. 2). The streams are bounded on the outside by parallel walls, but the position of the interface between the two streams (which corresponds to the reaction zone) is free to vary with height such that the cross-sectional areas of the two streams also vary with height with $A_f + A_o = A$ = constant. Frictional effects at the walls and the interface are neglected, and at each height the pressures in the two streams are equal. It is also assumed that T_o and T_f do not vary with height.

Applying Bernoulli's equation to each stream separately between stations o and y and using $p_f = p_o$ yields:

$$(u_o/u_i)^2 - (\rho_f/\rho_o)(u_f/u_i)^2 = \left[\frac{Y}{(u_i^2/2g)} - 1 \right] \left[(\rho_f/\rho_o) - 1\right] \qquad (1)$$

Conservation of mass for the two streams gives:

$$u_o/u_i = \frac{(u_f/u_i)}{(1+T)(u_f/u_i)-r} \qquad (2)$$

where the area ratio $r = A_{f_i}/A_{o_i}$. The density ratio ρ_f/ρ_o is given by

$$\rho_f/\rho_o = (m_f/m_o)(T_o/T_f) \qquad (3)$$

where m_f and m_o are the molecular weights of the fuel and oxidizer and the temperatures are absolute.

Equations (1) and (2) must be solved simultaneously in order to obtain the fuel and oxidizer velocities, u_f and u_o, as functions of height above the burner, y. The parameters that must be specified are the fuel/oxidizer area ratio r, the initial velocity u_i, and the fuel and oxidizer temperatures T_f and T_o. These latter values must be obtained from temperature measurements in the flame, and are needed to obtain the density ratio ρ_f/ρ_o. In solving these equations, it is convenient to use the dimensionless variables $U_f = u_f/u_i$, $U_o = u_o/u_i$ and $Y = y/(u_i^2/2g)$. A computer code was developed to solve equations (1) and (2) numerically by an iterative technique.

In order to evaluate the model, velocities were calculated for the ethylene/air flames investigated by Kent, et al(1981). For their burner r = 0.05 and u_i = 7 cm/sec. The temperatures T_o and T_f were estimated from the measured temperature profiles they presented for various heights (Fig. 3). Thus T_f was taken to be 1300°K. The oxidizer temperature was more difficult to estimate so two cases were considered: (1) T_o = 300°K (room temperature) and (2) T_o = 800°K (mean between room temperature and T_f). The model predicts excessive vertical fuel velocities for T_o = 300°K (ρ_f/ρ_o = 0.615). A curve fit was also obtained by matching the experimental data at 90 mm by choosing ρ_f/ρ_o = 0.368. This gives excellent agreement with the experimental data down to 30 mm (Fig. 3). The small deviations of the experimental data from the theoretical curve for heights below 30 mm are most likely caused by vertical temperature gradients in the flame. This

model was used to calculate the vertical velocity distribution in the flame which, in turn, was used to convert "heights above the burner" to time elapsed from the instant a pocket of gas leaves the burner mouth. These calculations showed that while the gas velocity in the flame is strongly affected by buoyancy (6 cm/sec at the burner mouth to 85 cm/sec at 5 cm above the burner for flame "T_1") the difference in residence time to reach a given height for the three flames is small (e.g., 83.6 msec in flame "a", 78.5 msec in flame "T_2" and 74.8 msec in flame "T_3" to reach a height of 30 mm above the burner). The increase of soot content and soot aggregate diameter with increasing temperature is, thus, valid even when considering the data as a function of "time elapsed" rather than "height above burner".

Figure 4a shows the variation of total soot volume fraction at given heights with residence time in the flame for all three flame temperatures. The increase in soot mass loading with temperature is clearly seen, while there is a pronounced increase in soot formation rate (slope) in going from flame "T_1" to flames "T_2" and "T_3". If the increase in reaction rate in the pre-sooting zone leading to earlier soot formation in the flames of higher temperature is similar to the reaction rate increase leading to heavier soot loading, the residence times for every height above the burner in each flame may be normalized by dividing it by its residence time to first sooting. When total soot volume fractions are plotted against these normalized residence times, the points do, indeed, fall close to a single line as shown in Figure 4b.

A plot of maximum agglomerate diameters versus residence time (Figure 4c) shows that the rate of agglomerate growth (slope) is almost

independent of temperature. The increase of absolute aggregate diameters with temperatures is due partially to increased spherule diameters and partially, to increased agglomeration. When plotting these maximum diameters against normalized residence time the points move closer to a common line but the correlation is not as good as that for the case of total volume fraction (Figure 4d).

The effect of the adiabatic flame temperature or the process of soot formation as observed in our measurements was discussed in the last six-monthly report and in the progress section of the continuation proposal and summarized in the publication which is attached. Only the most central features are, therefore, summarized below.

The general features of soot distribution are similar for the three flames at different temperatures which were investigated. In the region of high temperature nearest the flame front on the fuel side where nucleation is postulated to occur, the aggregate number density is highest while their diameter and soot volume fractions are low. The soot particles then move towards the center of the flame by convection and thermophoresis. The mean aggregate diameters increase due to agglomeration which, in turn, reduces the number densities. At the same time, the soot content increases due to surface growth and, possibly, some new soot inception For all flame temperatures considered the soot loadings and aggregate diameters increase with height indicating that the rate of soot formation exceeds that of soot depletion.

As the flame temperature is increased soot is beginning to be formed earlier in the flame due to an increase in the rate of pyrolysis reactions in

the pre-sooting region. This increased pyrolysis also leads to an increase in soot loading at given heights above the burner with increasing adiabatic flame temperature. This more extensive sooting at higher temperature was found to be due to larger soot agglomerates which, in turn, are formed partially by an increase in the size of the spherules and partially by an increase in the degree of agglomeration. The agglomerate number densities are largely insensitive to the change in the flame temperature. When plotting the total soot volume fractions at different heights above the burner against normalized residence time, the values for the flames at all three temperatures were found to lie along one single straight line. The rates of growth of the maximum soot agglomerate diameters, as determined from the slopes of the curves of these diameters plotted against non-normalized residence time, appear independent of temperature.

In a recently published report by Glassman (1979) it was pointed out that the sooting tendency of a diffusion flame can be increased by introducing traces of oxidizer into the fuel streams. This can be explained in terms of the homogeneous catalytic effect of small amounts of oxidizer on pyrolysis reactions leading to an increase in large hydrocarbons available for soot formation. The above quoted report is based on overall sooting tendency measurements and has caused us to investigate the effect of the oxidizer traces on the individual steps of the soot formation process.

For this purpose 5% oxygen has been added to the fuel side of the diffusion flame with pure air as oxidizer. Optical determinations of soot volume fraction and the soot agglomerate properties have been carried out for the flames both with and without oxygen trace for fuel and air for cold

burner exit velocities of 2 cm/sec. This reduced velocity results in a shorter flame which permits the measurements to be extended all the way to the flame tip. Incidentally, a comparison between flames of pure fuel and pure oxidizer at different cold gas velocities will permit the effect of reactant flow rates on soot formation to be determined.

Figs. 5, 6 and 7 show the variation of soot volume fraction aggregate diameters and number densities respectively vs distance from the burner center for different heights above the burner. Each of these figures shows plots for the flames with and without oxygen trace for easy comparison. The trends observed for the propane-air diffusion flame with 6 cm/sec reactant velocity (i.e., T_1) are still found in this smaller flame. Nearer the flame tip (above 30 mm for this flame), however, the increase in soot loading begin to diminish as does the increase in soot diameter. The soot aggregate number densities are still highest in the vicinity of the flame front and decrease towards the burner center. Some decrease in number density is observed in this flame with increasing height above the burner due to agglomeration, especially in the lower region of the flame. Nearer the flame tip the soot particle number density remains essentially constant.

The addition of 5% oxygen to the fuel side of this flame seems to have only produced minor effects. Essentially the flame has become narrower by the addition of oxygen to the fuel and has somewhat decreased in height. This is indicated by the absence of a minimum in the soot volume faction at the heighest measurement level (40 mm above the burner) for the flame with oxygen. This suggests that at 40 mm downstream the oxygeneated flame is closer to its tip than the flame with pure fuel.

Furthermore, the diameters near the tip begin to diminish, this effect, again, being more pronounced in the flame with oxygen in the fuel. Similarly, the effect of the oxygen on the aggregate number density is small except that at 20 mm the extensive aggregation continues in the pure fuel flame while the number density has already reached close to its final value for the oxygenated flame.

In general it would appear that the addition of oxygen causes an increase in soot loading, aggregate diameter and agglomeration in the early part of the flame but also tends to reduce the flame height. This is consistent with a "speeding up" of the combustion process by the presence of oxygen traces in the fuel.

Finally the equipment necessary for carrying out temperature measurements in the flames whose adiabatic flame temperature is too high for the use of thermocouples has been assembled and tested. The sodium line reversal technique will be used as will optical pyrometry.

II. Activities planned for the next reporting period:

During the next reporting period we are proposing to complete the determination of the effect of oxygen in the fuel stream on the soot formation process in diffusion flames. The effect of different amounts of trace oxygen will be investigated. Furthermore the effect of adding toluene or butadiene to the fuel will be investigated, in order to shed some light on the effect of polycyclic aromatic hydrocarbon and conjugated molecules on the process of soot formation. Optical and sampling techniques will, again,

be applied in order to fully characterize the soot properties. Temperature distributions will be measured for all the above described flames using thermocouples and optical techniques. The bouyancy model will then be applied to all flames to convert height above the burner to residence time. Selected flames will be investigated using thermocouples, sodium line reversal and optical pyrometry and the results compared.

On the theoretical side, the buoyancy model will be improved to better take account of temperature gradients observed both in the downstream direction and across the flame. The first approach will be to develop a one-dimensional two-stream model which allows the temperature (and density) to vary with height above the burner, but requires constant properties over the cross-sectional area of each stream. The temperature variation with height will be obtained from measurements in the flame, so that the energy equation will not need to be. Applying conservation of mass and momentum to the two streams with $P_o = P_f$ is expected to yield simultaneous ordinary differential equations to be solved for the vertical velocities u_o and u_f as a function of height. The second approach will be a three stream method in which the middle stream will correspond to reaction products and will have a temperature T_p which is obtained from measurements in the reaction zone. In this case a coupled set of differential equations will be obtained which must be solved numerically for u_o,u_p and u_f as a function of height. In both of these models the effects of friction will be neglected. It is anticipated, that this will permit a more accurate determination of the history of soot development with time as the particles move through the flame.

III. References:

Glassman, I. (1979). Phenomenological Models of Soot Formation in Combustion Systems, Princeton University Mech. and Aero Eng. Rep. No. 1450.

Kent, J. H., Jander, H. and Wagner, H. G. (1981). Soot Formation in a Laminar Diffusion Flame. 18th Symposium (International) on Combustion, Waterloo, pp. 1117-1126.

Kent, J. H. and Wagner, H. G. (1982). Soot Measurements in Laminar Ethylene Diffusion Flames. Comb. Flame, Vol. 47, pp. 53-65.

Powell, H. N. and Browne, W. G. (1956). Some Fluid Dynamic Aspects of Laminar Diffusion Flames. 6th Symposium (International) on Combustion, New Haven, CT, pp. 918-922.

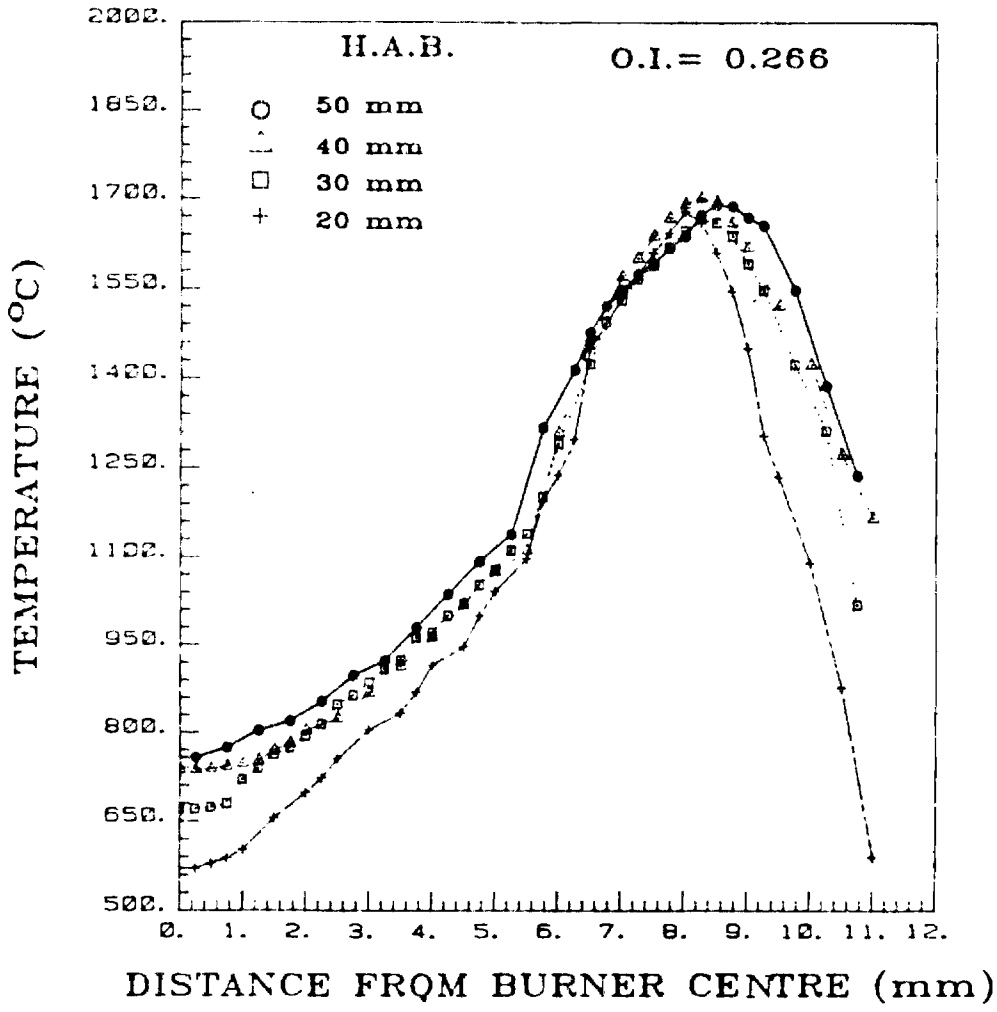

Fig. 1. Temperature Distribution for Propane/Pure Air Diffusion Flame (6 cm/sec Cold Flow Velocity)

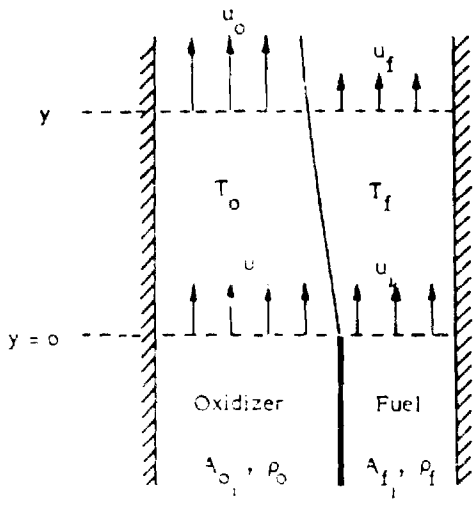

Fig. 2. Schematic Diagram for Buoyancy Model.

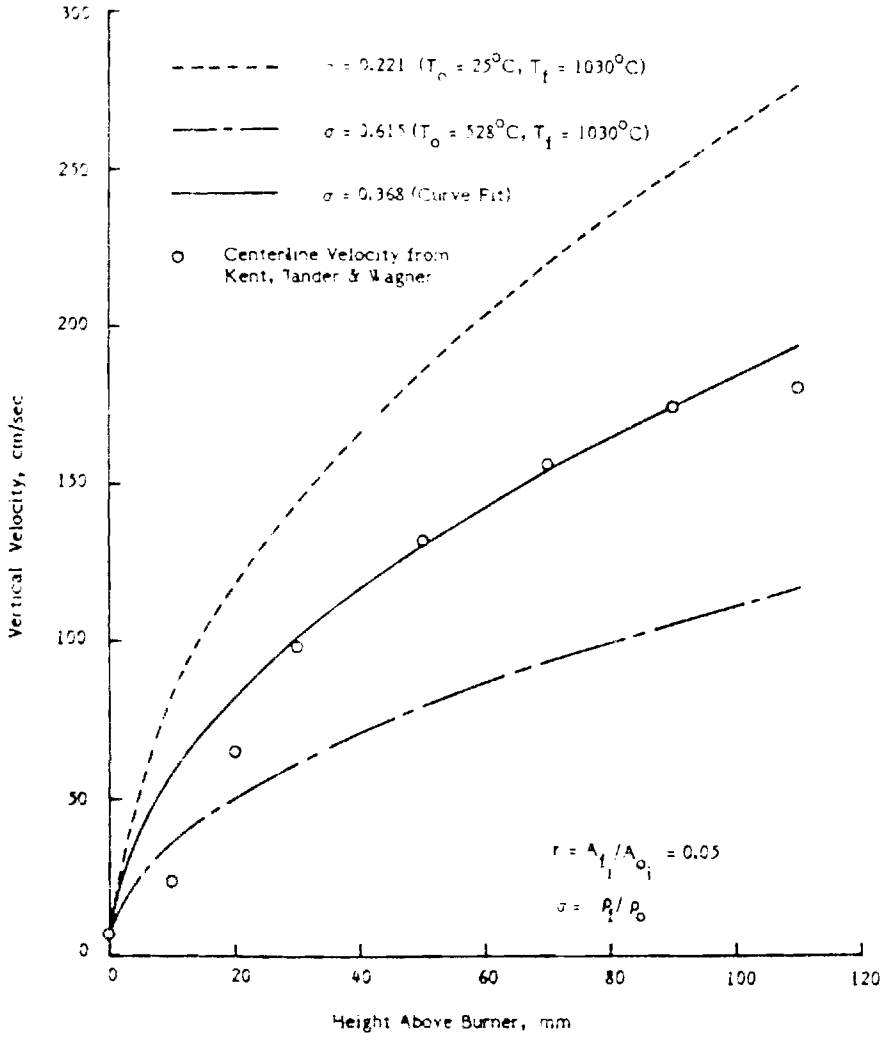

Fig. 3. Vertical Velocity Predictions for Ethylene/Air Flame and Comparison with Experimental Data.

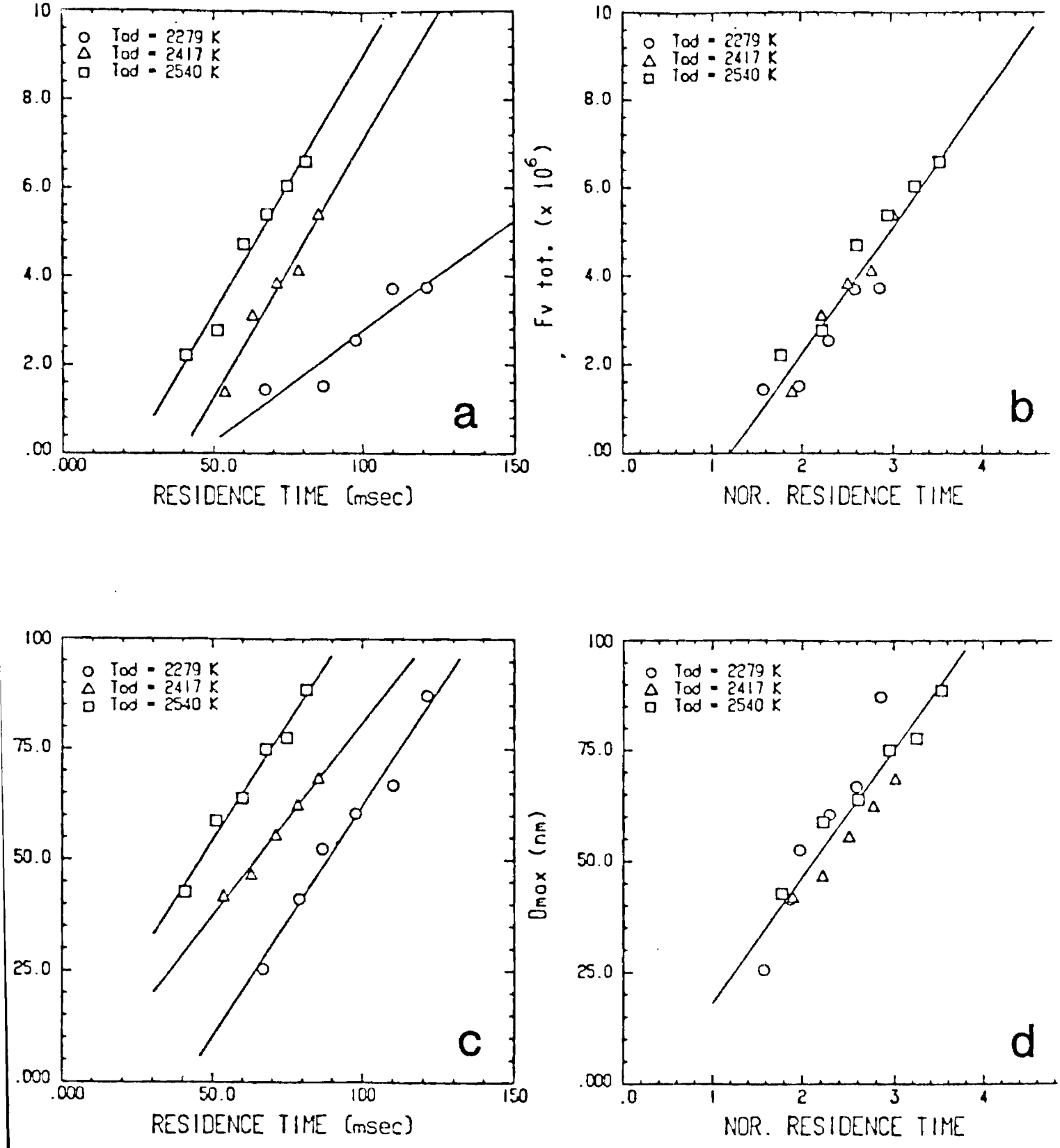

Fig. 4. Total Soot Volume Fractions at Different Heights above Burner versus Residence Time (a), and Normalized Residence Time; Maximum Soot Agglomerate Diameters at Different Heights above Burner versus Residence Time (c), and Normalized Residence Time (d).

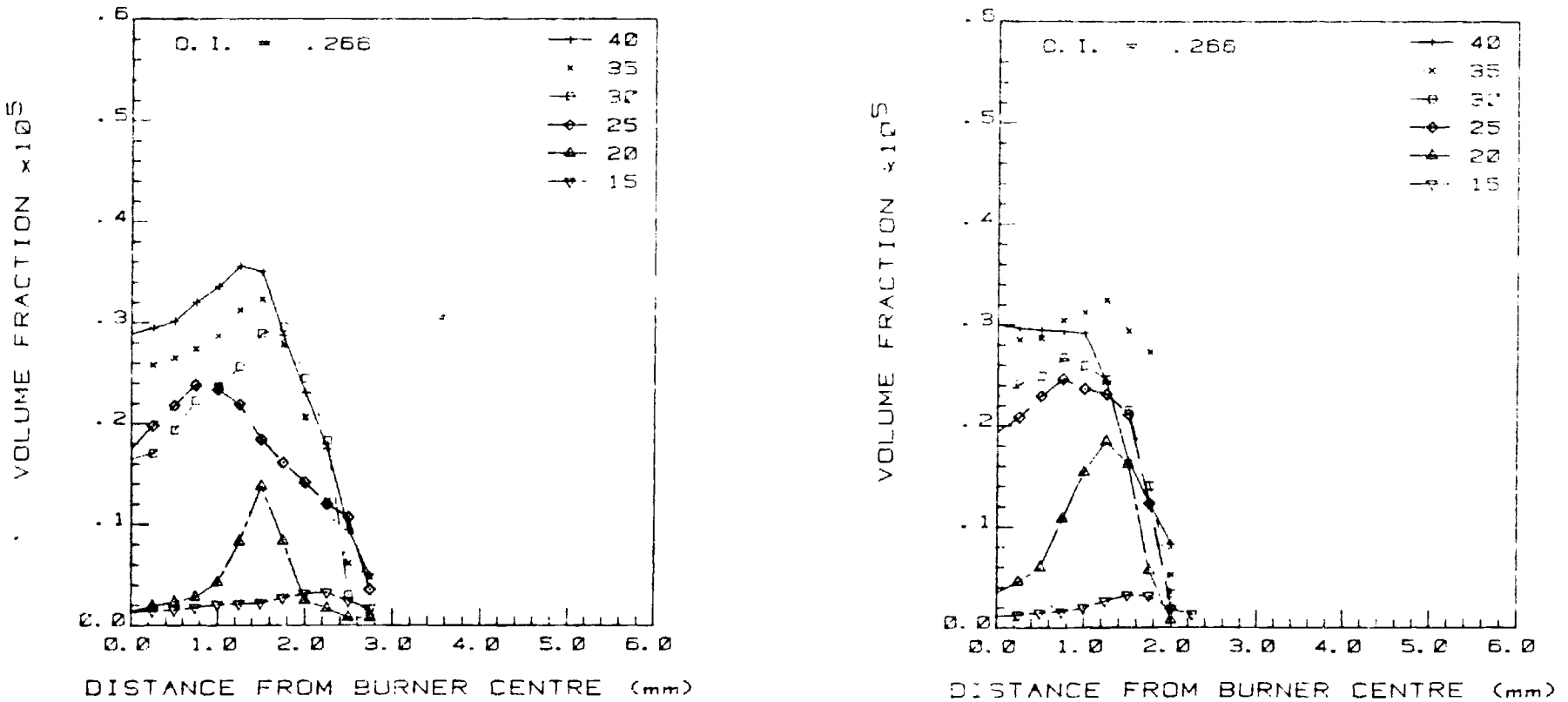

Fig. 5. Soot Volume Fraction vs. Distance from Burner Centre for Flames with Pure Fuel (LHS) and Fuel + 5% Oxygen (RHS)

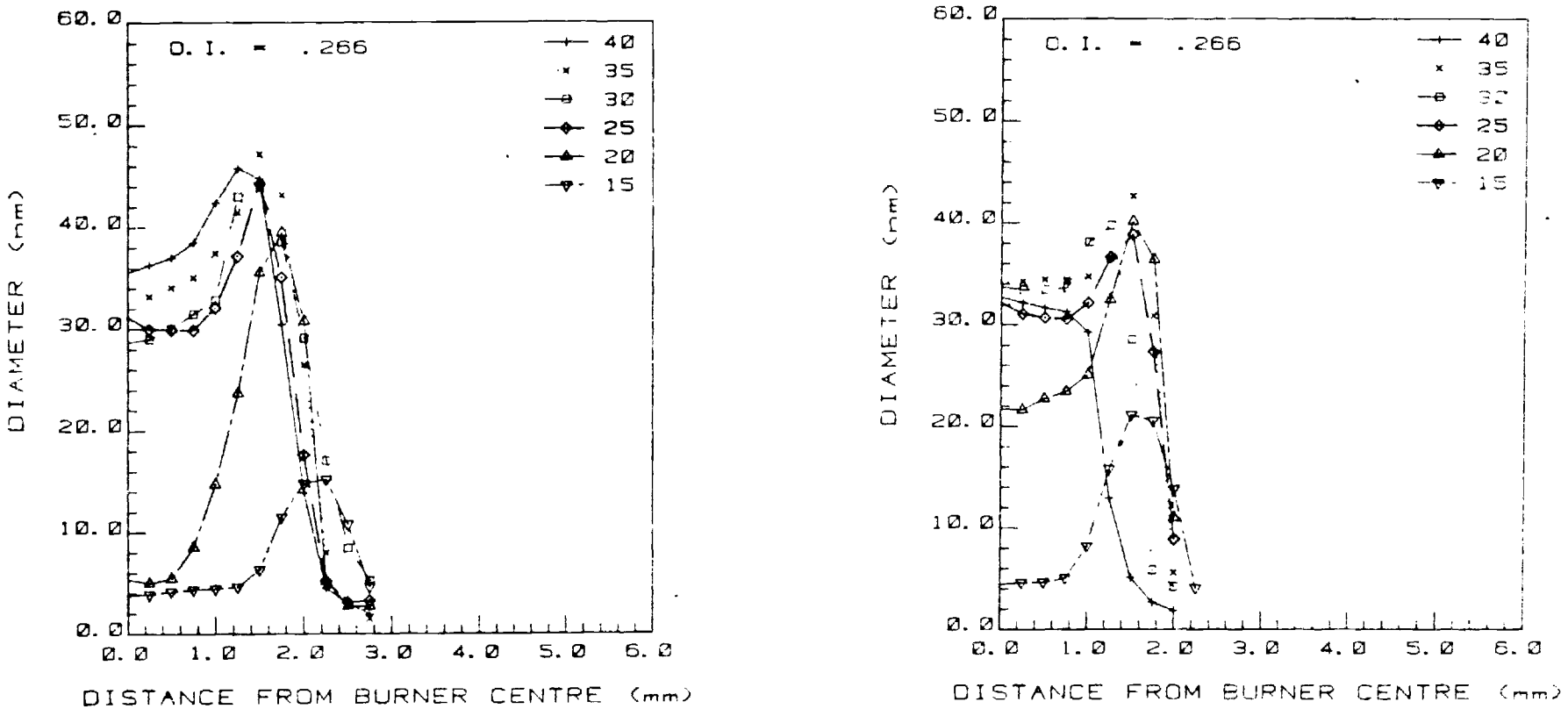

Fig. 6. Soot Agglomerate Diameters vs. Distance from Burner Centre for Flames with Pure Fuel (LHS) and Fuel + 5% Oxygen (RHS).

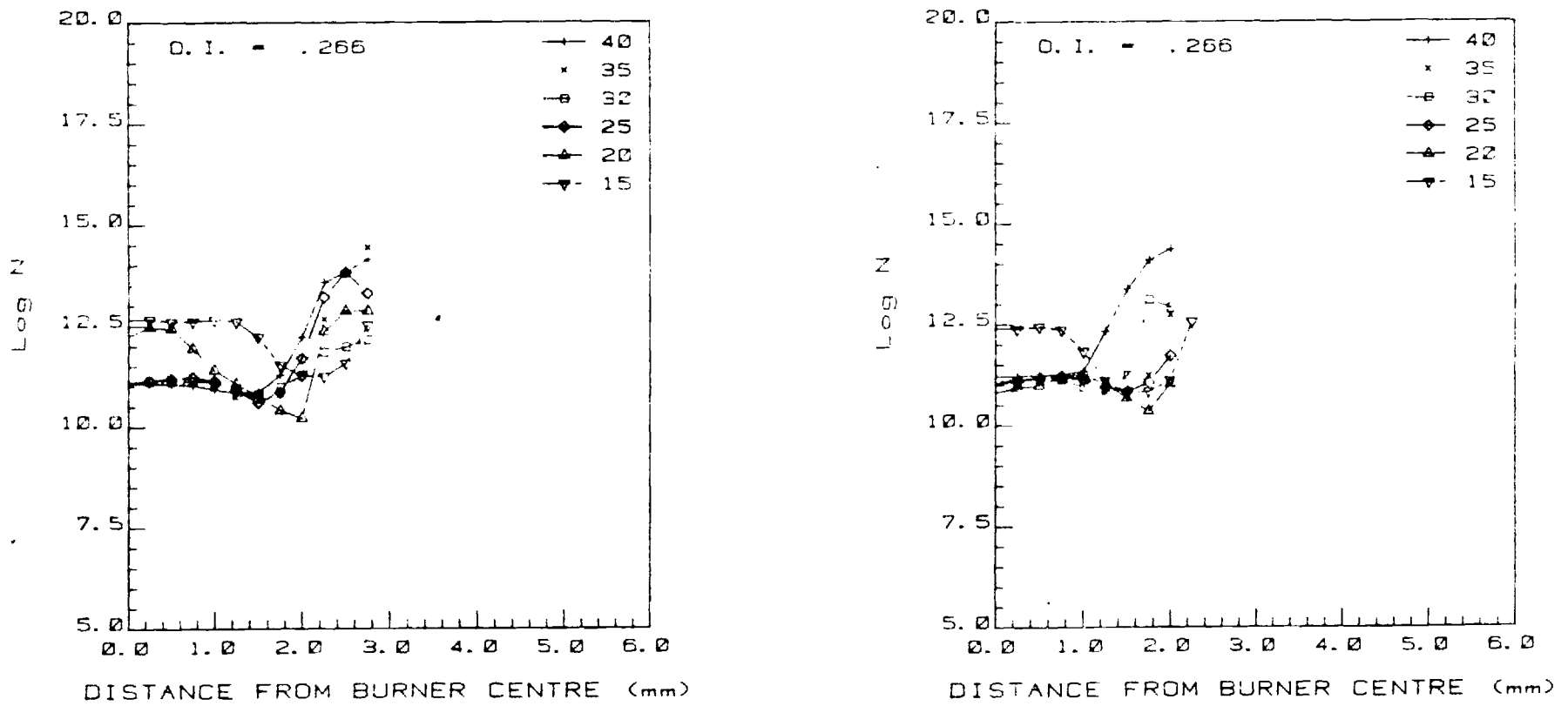

Fig. 7. Soot Agglomerate Number Densities vs. Distance from Burner Centre for Flames with Pure Fuel (LHS) and Fuel + 5% Oxygen (RHS)

THE EFFECT OF TEMPERATURE ON THE SOOTING BEHAVIOR OF LAMINAR DIFFUSION FLAMES

by

C. Wey

E. A. Powell

J. I. Jagoda*

School of Aerospace Engineering

Georgia Institute of Technology

Atlanta, GA 30332

submitted to

Combustion Science and Technology

* Author to whom correspondence should be addressed.

ABSTRACT

The effect of temperature on soot formation in a laminar propane diffusion flame was investigated. The temperature of the flame on a Parker Wolfhard burner was varied by adjusting the inert nitrogen content in the oxidizer flow. Soot aggregate properties, such as aggregate diameters and their number densities as well as soot volume fraction were determined using simultaneous laser light scattering and extinction methods, while spherule diameters were obtained using sample extraction and transmission electron microscopy. Soot volume fractions and aggregate diameters were seen to increase with height above the burner, while the opposite trend was noted for aggregate number densities for the three flame temperatures investigated. Spherule diameters were seen to increase with height particularly in the early part of the flame. An increase in temperature resulted in a considerable increase in local soot volume fractions and aggregate diameters. Spherule size and degree of agglomeration also varied somewhat with temperature. Heights above the burner were converted to residence times in the flame allowing for buoyancy. The mean rate of growth of soot aggregates was found to be essentially independent of flame temperature, although the absolute soot particle diameters were larger in the hotter flames. When the residence times were normalized with respect to residence time to first appearance of soot in each flame, the amount of soot generated for given normalized times was the same for all flame temperatures investigated.

I. INTRODUCTION

The formation of soot during the combustion of hydrocarbons has become a matter of increasing concern over the last decade. Smoke has been recognized as the major cause of fatalities in building fires [see Neville (1972)] and as a source of atmospheric pollution generated by many practical combustion devices. Furthermore, the increased wall heating due to radiative heat transfer from the solid soot particles results in materials design problems in many combustors. With this in mind a great number of studies have been undertaken to further the understanding of the mechanisms responsible for the formation of soot under a variety of different combustion conditions. A number of excellent review papers have recently been published covering many aspects of the soot formation problem including Wagner (1981), Haynes and Wagner (1981), Lahaye and Prado (1978), Palmer and Cullis (1965), Homan (1967) Howard and Kausch (1980) and Calcote (1981). Since all building fires and many controlled combustion processes occur, at least partially, in the form of diffusion flames, it was decided to further study the effect of various parameters on the formation of soot in laminar diffusion flames.

Glassman (1979), in a review of phenomenological models of soot formation, addressed the differences in the dependence of sooting behavior on temperature between premixed and diffusion flames. He reported that while for premixed flames an increase in flame temperature will result in a decrease in sooting tendency, a similar rise in temperature in diffusion flames will tend to increase the likelihood of soot being formed. These results were obtained using the concept of sooting height [see also Glassman and Yaccarino (1981)]. Similar observations in laminar diffusion flames were made by Dearden and Long (1968) who report an increased amount of soot collected with increasing flame temperature. This also sheds new light on results reported by Powell et al. (1979) on the effect of temperature on the sooting history of flames on wood and PVC. Here, post flame soot loadings and particle diameters were seen to increase with temperature when determined optically in the flue above their test chamber.

Glassman (1979) explained the differences in sooting trends with temperature in premixed and diffusion flames in terms of competing pyrolysis and oxidation reactions in the pre-sooting zones. In premixed flames, the rate of oxidation of soot precursors is accelerated more strongly by an increase in temperature than their formation via the pyrolysis reaction, leading to a reduction in soot. In diffusion flames, on the other hand, no oxidation takes place during preheating leaving only the pyrolysis reactions, which leads to an increase in sooting with temperature. Indeed, traces of oxygen which may diffuse into the pyrolysis zone of a diffusion flame tend to act as a homogeneous catalyst during pyrolysis and increase the sooting rate as was shown by Glassman and Yaccarino (1980) and Schug et al. (1980).

All the above observations were made in terms of global measurements such as sooting heights, amount of soot collected, etc. It would be interesting to extend these measurements to determine the effect of temperature on the properties of the soot particles as they are formed inside both premixed and diffusion flames. Soot consists of essentially spherical particles, or spherules, which agglomerate to form the soot agglomerates commonly observed in most flames. The local soot parameters in the flame, which would be of interest, are soot loadings, agglomerate number densities, agglomerate diameters, spherule diameters and, thus, degrees of agglomeration.

Prado et al. (1981) have investigated the effect of temperature on the process of soot formation in a propane-air premixed flame [see also Prado and Lahaye (1981)]. They found that for a given fuel air ratio the local soot volume fraction decreases throughout the flame with increasing temperature. At the same time the soot agglomerate diameter decreases with increasing temperature as do the spherule diameters. This is in accordance with the reduction of the sooting tendency of premixed flames with increasing temperature reported by Glassman (1979).

On the other end of the spectrum, earlier work by Lahaye and Prado (1978) and Prado and Lahaye (1981) on the oxygen-free pyrolysis of methane and benzene indicates

that in such a system the amount of soot formed increases with temperature. Spherule diameters decreased slightly with increasing temperature, and agglomerate dimensions were not measured. An increase with temperature in the sooting tendency of benzene during pyrolysis was also observed by Vaughn et al. (1981) during shock tube studies up to a temperature of about 2000^{o}K.

A diffusion flame may be considered to consist of an essentially oxygen-free pyrolysis region surrounded by a flame front. It is the purpose of this study to determine the local soot concentrations and soot particle properties within such a flame.

II. EXPERIMENTAL APPARATUS AND PROCEDURE

Burner

A Parker Wolfhard burner which supports two vertical flat flame sheets was chosen for this study in order to avoid the need for a deconvolution of the absorption signal necessary in flames of cylindrical geometry see Jagoda et al. (1980) and Santoro et al (1983) . The burner, which is similar to the one used by Kent et al. (1981) and Haynes and Wagner (1980), consists of three parallel slots 51 mm in length. The outer slots, which carry the oxidizer, have a width of 16 mm each, while the inner fuel slot is 5 mm wide. For equal fuel and oxidizer burner exit velocities this results in a stable, somewhat under-ventilated flame. The burner is surrounded by a nitrogen carrying jacket to exclude drafts and to prevent end-flamelets from forming across the width of the fuel slot. Further flame stabilization is assured by the use of screens near the tip of the flame. In order to permit steady operation over extended periods of time, the burner housing is water cooled. The burner can be displaced in the vertical and horizontal directions to enable measurements to be carried out in different parts of the flame without disturbing the optical system.

Diagnostics

A simultaneous laser light scattering and absorption system similar to the one pioneered by D'Alessio et al. (1975) and described in detail by Jagoda et al. (1980) has been set up. The beam from a 4 watt argon ion laser operating at 514.5 nm is focused into the test section in the flame using a 50 cm focal length lens and passes along the flat flame sheet onto a photomultiplier which measures the intensity of the transmitted light. A second photomultiplier is used to monitor the intensity of the beam scattered at 90^{o} to the incident beam. A system of lenses and apertures limits the solid angle over which scattered light is collected and eliminates radiation from any part of the laser beam other than the 60 x 60 x 100 micron test volume under consideration. Direct radiation from the flame to the photomultiplier is reduced using a monochromator and a narrow band width interference filter. The remaining stray light is eliminated by placing a chopper in the incident beam and passing the output from the photomultiplier through a phase sensitive detector which amplifies only the signal in constant phase with the chopper, i. e., radiation originating from the laser beam. The absorption and scattering signals are observed on an oscilloscope and registered on a chart recorder.

The Mie theory in the Rayleigh approximation as detailed by Kerker (1969) is used to obtain the local soot volume fractions and the mean diameters and number densities of the soot agglomerates from the absorption and scattering measurements. From the treatment in Kerker (1969), $\dot{Q}_{vv}$ is defined as

$$\dot{Q}_{VV} = NC_{sca} = (2/3)(\lambda^2/\pi)\ \alpha^6 NX \qquad (1)$$

where $\alpha = \pi D/\lambda$ and $X = \left| \frac{m^2-1}{m^2+2} \right|^2$

where N is the number density of scatterers, C_{sca} their total Rayleigh cross-section (over 4 steradians), λ the wavelength of the laser line used, D the mean diameter and m the

complex refractive index of soot as measured by Dalzell and Sarofim (1969).* Furthermore, the extinction coefficient K_{ext} may be shown to be given as

$$K_{ext} = NC_{ext} = (\lambda^2/4)\ \alpha^3\ N\ Y \tag{2}$$

where

$$Y = -\ Im\ \left(\frac{m^2 - 1}{m^2 + 2}\right)$$

Here C_{ext} is the extinction cross-section of the soot aggregates. Solving equations (1) and (2) simultaneously and from the definition of the soot volume fraction F_v one obtains the following expressions for the soot agglomerate diameters, their number densities and the soot volume fraction:

$$D = (\lambda/\pi)\ \left[(3/2)(Y/X)(\dot{Q}_{VV}/K_{ext})\right]^{1/3} \tag{3}$$

$$N = (2/3)(\pi/\lambda^2)(X/Y^2)(K_{ext}{}^2/\dot{Q}_{VV}) \tag{4}$$

and

$$F_V = (\pi/6)\ D^3N = (\lambda/6\pi)(K_{ext}/Y) \tag{5}$$

The above treatment assumes a monodisperse distribution of spherical soot particles. When comparing the results presented in the next section with those obtained by Santoro et al. (1983), who assumed self-preserving or log normal distributions, the D above corresponds to their $D_{6,3}$ while the above N must be multiplied by 2. Since in Santoro's treatment the soot volume fraction is given by $ND^3_{3,0}$ and the ratio $(D_{6,3}/D_{3,0})^3 = 2$, the

---

*) The above expression differs by a factor of $8\pi/3$ from the expression used by other workers, e.g., Haynes & Wagner (1980). This discrepancy is due to the fact that while some workers use the differential Rayleigh cross-section, C_{sca} in the above expression is integrated over the entire sphere. Care must be taken to use a scattering cross-section for the calibration gas compatible with its definition for particulate scatterers [see equation (8)].

soot volume fraction is unchanged.

The quantities D, N and F_v in equations (3), (4) and (5) are related to the measured quantities I_o, the incident laser intensity, I_{tr}, the transmitted intensity, and I_{sca}, the scattered intensity, by Lambert's law

$$K_{ext} = (1/L)\ \ell n\ (I_{tr}/I_o) \tag{6}$$

where L is the optical path length of the laser beam in the absorbing medium, and

$$I_{sca} = \eta_{opt}\ \eta_{el}(\Delta\Omega)(\Delta V)\dot{Q}_{VV}\ I_o \tag{7}$$

where η_{opt} and η_{el} are the optical and electronic efficiencies, $\Delta\Omega$ the solid angle over which the scattered light is collected and ΔV the size of the test volume. It is interesting to note that the determination of K_{ext} is less precise than that of $\dot{Q}_{VV}$ since the absorption measurements integrate over the entire length of the flame and are, therefore, dependent on its two-dimensionality. Small deviations from perfect flame flatness and the possible existance of small end-flames reduce the accuracy in the determination of K_{ext}. Inspection of equations (3) and (4) , therefore, indicates that the values of N, which are proportional to the square of K_{ext} may be expected to be less accurate than those of D which only varies as the inverse of the cube root of K_{ext}.

Rather than determine the η's, $\Delta\Omega$ and ΔV , the scattering system was calibrated using gases whose scattering cross sections were calculated, namely methane and nitrogen. As a matter of fact, this calibration was carried out daily to check the optical alignment.

The following expressions taken from Penney (1969) and Müller-Dethlefs (1979) were used to determine the scattering cross section of the calibration gases:

$$C_{sca}(gas) = (8\pi/3)\ \sigma_o\ (1 + 2\rho_V) \tag{8}$$

where ρ_v, the depolarization ratio was assumed to be $<< 1$ and σ_o the differential scattering cross section is given by

$$\sigma_o = \frac{4\pi^2(\mu_o - 1)^2}{N_o^2 \lambda^4} \frac{3}{3 - 4\rho_v} \qquad (9)$$

with μ_o being the refractive index of the gas at the wavelength of the incident light λ and N_o Avogadro's number per unit volume at the temperature at which the calibration is carried out. The calculated scattering cross sections of the calibration gases compared very well with those quoted by D'Alessio et al (1975) and Rudder and Bach (1968) for the respective wavelengths. (Please note these authors quote σ_o, not C_{sca}.)

The Mie theory of scattering in the Rayleigh approximation assumes spherical scatterers whose $D << \lambda$. This latter criterion is not strictly observed, but it can be shown that for particles of 100 nm diameter the error introduced is only of the order of 10%. Furthermore, the soot aggregates are not spherical and only "equivalent diameters" could, therefore, be established.

Both scattering and extinction measurements had to be averaged over excursions of the order of 5% in most parts of the flame. In areas of steep soot concentration gradients, these fluctuations due to small movements of the flame were somewhat bigger, but the results were, nevertheless, reproducible.

The optical measurements described above are a function of the properties of the agglomerates. The spherules which make up the agglomerates cannot be detected in this way. Soot was, therefore, extracted from various locations in the flame to determine the spherule diameter distributions using transmission electron microscopy. Local degrees of agglomeration could, thus, be obtained. When viewing the electron micrographs, extensive agglomeration can be observed. This, however, is due mostly to agglomeration during sample collection and treatment, and is not representative of the degree of agglomeration in the flame. It is, therefore, important to realize that the scattering and microscopy techniques are truly complimentary.

The temperature distribution in the flame was measured using uncoated Pt, Pt - 13% Rh thermocouples with a 125 micron diameter junction. Conductive losses were minimized by introducing the leads parallel to the flame sheet. Since relative temperatures rather than their absolute values are of interest here, the thermocouple results were not corrected for radiative losses.

Flame Temperature Variation in a Diffusion Flame

In this study the effect of temperature on the sooting process in a propane-air diffusion flame has been investigated. In the flame front of a diffusion flame the combustion proceeds, essentially, under stoichiometric conditions. For given fuel and oxidant compositions the adiabatic flame temperature is, therefore, essentially fixed. In order to be able to introduce a variation in adiabatic flame temperature for the diffusion flames, the inert nitrogen content of the oxidizer, which acts as a diluent, was varied. A decrease in nitrogen content, thus, corresponds to an increase in flame temperature, and vice versa. Results for flames of oxygen to nitrogen ratios, by mole, in the oxidizer flow of .27, .33 and .41 will be reported here. These flames will be referred to as "a", "b" and "c". Adiabatic flame temperatures, T_{ad}, were calculated for these three cases taking into account the equilibrium concentration within the flame as computed using the NASA code developed by Gordon and McBride (1971).

III. RESULTS AND DISCUSSION

Soot volume fractions, soot aggregate diameters and their number densities for flames of three adiabatic flame temperatures are reported here. They correspond to oxygen to nitrogen ratios of .27, .33 and .41 with calculated adiabatic flame temperatures of 2279° K, 2417° K and 2540° K. The fuel was pure propane, and the cold gas velocity of fuel and oxidizer was maintained at 6 cm/sec for all cases.

Propane-Air Flame

Flame "a" corresponds to a propane-air diffusion flame. Its soot volume fractions, mean agglomerate diameters and number densities are plotted versus distance from the burner center for different heights above the burner in Figures 1a, 2a and 3a respectively. Figure 4 shows the temperature distribution in the vertical plane normal to the burner slots for this flame. It is observed that the flame front temperature remains constant with height in the part of the flame investigated. As one moves horizontally away from the flame front the temperature drops both in the direction towards the fuel and the oxidizer. In the pyrolysis zone, near the center, the temperature increases somewhat with height.

Comparison of Figures 1a and 4 shows that the entire sooting region lies well within the fuel side of the flame. The soot loading increases with height above the burner indicating that in this part of the flame the soot formation rate far exceeds any possible soot depletion rate due to particle burn out. Figure 2a indicates that the regions of maximum soot loading also correspond to those in which soot agglomerates of largest diameters are found. Furthermore, the agglomerate diameters increase with height above the burner.

The aggregate number density distributions shown in Figure 3a, on the other hand, show a different trend. The maximum number of particles exists closest to the flame front with their number density decreasing towards the region of maximum diameter and soot concentration. As mentioned in the previous section, the values of number densities are less reliable than those obtained for mean diameters and soot volume fraction because of their strong dependance on K_{ext}. Since the absorption near the burner center was relatively small and was influenced by the possible existence of end-flames and large polycylic aromatic hydrocarbons in the fuel rich part of the flame, number densities are only plotted up to 1 1/2 mm from the burner center. For similar reasons the soot volume fractions and diameters near the burner center plotted in Figures 1a and 2a may be somewhat high. Careful inspection of Figure 3a indicates that there is a detectable decrease in the number density of soot particles with height above the burner suggesting

an agglomeration in excess of the possible creation of new particles.

In order to determine the degree of agglomeration of the spherical soot particles (or spherules) into agglomerates, soot samples were extracted at heights above the burner at which the aggregate properties had been determined. Unfortunately, the spatial resolution for sampling is not as good as that for the optical measurements, and only an average sample per height could be obtained. These samples were viewed under a transmission electron microscope and the diameter distribution of the soot spheroids were recorded. The mean spherule diameters are plotted versus height above the burner in Figure 5. Clearly, the diameter of these elementary soot particles increases with height in the flame due to surface growth. This growth is particularly pronounced in the early part of the flame. Since the agglomerates, unlike the spherules, are not spherical, their measured diameters correspond to "equivalent diameters". Their degree of agglomeration was estimated by comparing the mean volume of the spherules with that calculated using the equivalent diameter of the agglomerates as determined by the light scattering method. These degrees of agglomeration were determined using the largest mean agglomerate diameters observed at the different heights. Table I indicates that the degree of agglomeration increases with distance in the flame.

Table I. Mean Degree of Agglomeration for Flames "a", "b" and "c".

Ht. ab. Burner/Adiab. Fl. Temp(^{o}K): (mm)	2279	2417	2540
10	-	-	7.3
15	-	12.9	-
20	5.6	-	14.7
25	-	22.3	-
30	27.1	-	22.6
35	-	38.6	-
40	26.1	-	-
50	33.4	-	-

The optical results described above are in good agreement with measurements carried out in flames using different fuel by Kent et al. (1980) and by Haynes and Wagner (1980), as well those by Santoro et al. (1983) using a cylindrical burner. Sampling to obtain spherule dimensions and degrees of agglomeration were not carried out by these workers. Similarly to Haynes and Wagner (1980), we conclude that soot particles are created in the high temperature region near the flame front where the particle number density is high, but their diameters small. These particles then move upward by convection and the effect of buoyancy of the combustion products, as well as away from the flame front towards the burner center by convection and thermophoresis. As the particles move away from their position of inception into a region of lower temperature they grow by agglomeration as witnessed by the increase in degree of agglomeration with height above the burner. Agglomeration by itself, however, does not lead to an increase in soot volume fraction. This increase of soot loading must, therefore, be ascribed to surface growth as indicated by the increase in spherule diameter in the downstream direction. Some particles may also be formed as one moves towards the region of high soot concentration, but this generation rate must be small since the particle number decreases and the mean diameter increases in this direction indicating that aggregation predominates. This aggregation process is most pronounced in the vicinity of particle inception, i.e., the number of particles decreases most sharply near the flame front. This may be due to the higher number densities leading to more frequent collisions in these regions but also indicates a greater tendency of the small, reactive "young" soot particles to stick together because of the presence of free radicals adsorbed on their surface. The smaller particles observed near the center of the flame may have been formed in the early part of the flame and have spent less time in the region of growth as suggested by Haynes and Wagner (1980).

Effect of Flame Temperature

In order to visualize the effect of flame temperature on the soot volume fraction, soot agglomerate diameters and their number densities the distributions of these quantities for the three flames are plotted in Figures 1, 2, and 3 respectively. Turning

first to the soot volume fractions presented in Figure 1 it can be seen that the soot present in the flames clearly increases with height above the burner for all flame temperatures investigated. The soot formation rate, thus, far exceeds its removal rate by, for example, burn out even for the higher temperatures. Comparison between Figures 1a, b & c shows that the increase in temperature leads to soot being formed earlier in the flame. Furthermore, the amount of soot present at any given height above the burner increases with increase in flame temperature. Thus, the increase in the reaction rate with temperature, which accelerates the production of soot precursors in the lower region of the flame prior to soot formation and leads to the reduced height at which soot first appears, persists in the sooting region of the flame. There the increase in temperature results in an increase in the pyrolysis rate which appears to be more temperature dependent than soot burn out in this part of the flame as postulated by Glassman et al. (1981). This leads to the increase in sooting tendency with temperature which they observed for diffusion flames.

In Figure 2 the mean soot aggregate diameters are plotted against distance from the burner center for different constant heights above the burner surface for the three flames. Clearly the mean soot aggregate diameters increase with increasing height in the flame for all temperatures investigated. Furthermore, the increase in temperature has the effect of increasing the soot agglomerate sizes found at given heights above the burner. This may be due to either an increase in the diameters of the fundamental spheroids which make up the agglomerates or to more extensive agglomeration. Samples extracted from the flames at different temperatures indicate that there, indeed, is some increase in spheroid diameters with adiabatic flame temperature, particularly in the early part of the flame (Fig. 5) and between flames "b" and "c". The mean degree of agglomeration seems to increase from flame "a" to flame "b" and decrease somewhat from flame "b" to flame "c" within the experimental accuracy.

The effect of temperature on the number density of soot aggregates is shown in Fig. 3. Bearing in mind the reduced accuracy in the number density determination, the

changes in this parameter are far less pronounced than those discussed so far. Nevertheless, it is apparent that the number density decreases somewhat with increasing heights in the flame for all temperatures investigated. This is indicative of agglomeration taking place. Furthermore, there appears to be little change in number density with increasing temperature.

The temperatures in the flame fronts for the flames with higher oxygen to nitrogen ratios (i.e. "b" and "c") were found to be above the melting point of platinum, causing the thermocouples to break. In order to obtain an indication of the relative temperature changes between the three flames, a shielded Pt-Pt 13% Rh thermocouple was used at selected positions in all three flames. This probe resulted in lower readings because of the heat loss due to the shield and no melting occurred. It was noted that the ratios between measured "shielded" temperatures in the flame front and calculated adiabatic flame temperatures were the same for all three flames within 1%. Flame temperatures for flames "b" and "c" were, therefore, extrapolated by multiplying the ratio between the unshielded measured temperature of flame "a" and its calculated adiabatic flame temperature by the calculated adiabatic flame temperatures for flames "b" and "c". Values for the flame front temperatures of 1973^{o}K for flame "a", 2063^{o}K for flame "b" and 2195^{o}K for flame "c" were, thus, obtained. The shapes of the isotherm lines for the three flames are assumed to be similar.

In order to quantify the effect of the flame temperature on the global reaction rate of the soot formation reaction, the total soot volume fraction at different heights above the burner (i.e., area under soot volume fraction plots) and the corresponding maximum aggregate diameters were plotted versus residence time. The residence time is defined as the time required for a pocket of gas to travel from the burner to a given height. Since no velocity measurements were carried out in this flame, the residence time in the flame had to be related to the height above the burner using theoretical considerations. Kent and Wagner (1980), who carried out velocity measurements in a similar diffusion flame, have established that buoyancy forces cause considerable acceleration of the vertical velocities

in this type of flame. The relationship between the time required to reach a given vertical position and its height above the burner is, therefore, not linear.

A simple, one dimensional model of two parallel streams of gases of differing densities based on the work by Powell and Browne (1956) was, therefore, developed, which takes into account both the difference in density of fuel and oxidizer and the difference in temperature of the combustion products and the surrounding oxidizer flow. The details of this model are presented in the Appendix. Using the fuel and flame temperatures reported by Kent and Wagner (1980), their measured fuel velocities could be predicted with good accuracy, particularly by fitting the density ratio mentioned in the Appendix using the velocity measured at one point 90 mm above the burner. This model was applied to the flames presented here and their vertical velocities were predicted from the temperature distribution measured. These vertical velocity distributions were used to convert the "height above the burner" into a time axis.

Figure 6a shows the variation of total soot volume fraction at given heights with residence time in the flame for all three flame temperatures. The increase in soot mass loading with temperature is clearly seen, while there is a pronounced increase in soot formation rate (slope) in going from flame "a" to flames "b" and "c". If the increase in reaction rate in the pre-sooting zone leading to earlier soot formation in the flames of higher temperature is similar to the reaction rate increase leading to heavier soot loading, the residence times for every height above the burner in each flame may be normalized by dividing it by its residence time to first sooting. When total soot volume fractions are plotted against these normalized residence times, the points do, indeed, fall close to a single line as shown in Figure 6b.

A plot of maximum agglomerate diameters versus residence time (Figure 6c) shows that the rate of agglomerate growth (slope) is almost independent of temperature. The increase of absolute aggregate diameters with temperatures is due partially to increased spherule diameters and partially, to increased agglomeration. When plotting these maximum diameters against normalized residence time the points move closer to a

common line but the correlation is not as good as that for the case of total volume fraction.

IV. CONCLUSIONS

The in situ soot parameters including soot loading, soot aggregate diameters and number densities, as well as spherule diameters, have been determined for propane diffusion flames at three different flame temperatures. The general features of soot distribution are similar for all three cases. In the region of high temperature nearest the flame front on the fuel side where nucleation is postulated to occur, the aggregate number density is highest while their diameter and soot volume fractions are low. Towards the center of the flame the mean aggregate diameters increase due to agglomeration which, in turn, reduces the number densities. At the same time, the soot content increases due to surface growth and, possibly, some new soot inception. For all flame temperatures considered the soot loadings and aggregate diameters increase with height indicating that the rate of soot formation exceeds that of soot depletion.

As the temperature is increased soot is beginning to be formed earlier in the flame due to an increase in the rate of pyrolysis reactions in the pre-sooting region. This increased pyrolysis also leads to an increase in soot loading at given heights above the burner with increasing adiabatic flame temperature. This more extensive sooting at higher temperature was found to be due to larger soot agglomerates which, in turn, are formed partially by an increase in the size of the spherules and partially by an increase in the degree of agglomeration. The agglomerate number densities are largely insensitive to the change in the flame temperature. Even though buoyancy causes considerable acceleration of the flame gases in the vertical direction, the difference in temperatures between the three flames is sufficiently small to affect the gas residence times in the flames by only a small amount ($< 7\%$). All observations detailed above are, thus, still valid even when considering soot loading and particle diameters as a function of residence time in the flame rather than heights above the burner. When plotting the total soot volume fractions at different heights above the burner against normalized residence time, the

values for the flames at all three temperatures were found to lie along one single straight line. The rates of growth of the maximum soot agglomerate diameters, as determined from the slopes of the curves of these diameters plotted against non-normalized residence time, appear independent of temperature. In conclusion, it is felt that the findings reported here help to shed new light on the global observation by Glassman (1979) and others, which have reported an increase of sooting tendency with temperature for diffusion flames.

ACKNOWLEDGEMENT

We thank the Environmental Protection Agency for supporting this work under Grant # R808953. We also thank Don Carey for serving as project monitor.

V. APPENDIX: CORRECTION FOR BUOYANCY

The model used to correct the velocity field in the flame for the effect of buoyancy is based on an analysis by Powell and Browne (1956) which deals with the investigation of the effect of the differing densities of cold fuel and oxidizer streams upon the fluid dynamic characteristics of diffusion flames. This model was expanded to take into account the effect of the differing temperatures of the combustion gases and the oxidizer stream upon their densities. The fuel at temperature T_f and oxidizer at temperature T_o are assumed to leave the burner in parallel streams with velocity u_i at height $y = 0$. The cross-sectional area of the oxidizer and fuel streams at $y = 0$ are A_{o_i} and A_{f_i} respectively. The streams are bounded on the outside by parallel walls, but the position of the interface between the two streams (which corresponds to the reaction zone) is free to vary with height such that the cross-sectional areas of the two streams also vary with height with $A_f + A_o = A$ = constant. Frictional effects at the walls and the interface are neglected, and at each height the pressures in the two streams are equal. It is also assumed that T_o and T_f do not vary with height.

Applying Bernoulli's equation to each stream separately between stations o and y

and using $p_f = p_o$ yields:

$$(u_o/u_i)^2 - (\rho_f/\rho_o)(u_f/u_i)^2 = \left[\frac{Y}{(u_i^2/2g)} - 1\right]\left[(\rho_f/\rho_o)-1\right] \quad (A1)$$

Conservation of mass for the two streams gives:

$$u_o/u_i = \frac{(u_f/u_i)}{(1+T)(u_f/u_i)-r} \quad (A2)$$

where the area ratio $r = A_{f_i}/A_{o_i}$. The density ratio ρ_f/ρ_o is given by

$$\rho_f/\rho_o = (m_f/m_o)(T_o/T_f) \quad (A3)$$

where m_f and m_o are the molecular weights of the fuel and oxidizer and the temperatures are absolute.

Equations (A1) and (A2) must be solved simultaneously in order to obtain the fuel and oxidizer velocities, u_f and u_o, as functions of height above the burner, y. The parameters that must be specified are the fuel/oxidizer area ratio r, the initial velocity u_i, and the fuel and oxidizer temperatures T_f and T_o. These latter values must be obtained from temperature measurements in the flame, and are needed to obtain the density ratio ρ_f/ρ_o. In solving these equations, it is convenient to use the dimensionless variables $U_f = u_f/u_i$, $U_o = u_o/u_i$ and $Y = y/(u_i^2/2g)$. A computer code was developed to solve equations (A1) and (A2) numerically by an iterative technique.

In order to evaluate the model, velocities were calculated for the ethylene/air flames investigated by Kent, et al (1981). For their burner r = 0.05 and u_i = 7 cm/sec. The temperatures T_o and T_f were estimated from the measured temperature profiles they presented for various heights. Thus T_f was taken to be 1300°K. The oxidizer temperature was more difficult to estimate so two cases were considered: (1) T_o = 300°K (room temperature) and (2) T_o = 800°K (mean between room temperature and T_f). The model predicts excessive vertical fuel velocities for T_o = 300°K (ρ_f/ρ_o = 0.221) and deficient fuel velocities for T_o = 800°K (ρ_f/ρ_o = 0.615). A curve fit was also obtained by matching the experimental data at 90 mm by choosing ρ_f/ρ_o = 0.368. This gives excellent agreement with the experimental data down to 30 mm. The small deviations of the

experimental data from the theoretical curve for heights below 30 mm are most likely caused by vertical temperature gradients in the flame. This model was used to calculate the vertical velocity distribution in the flame which, in turn, was used to convert "heights above the burner" to time elapsed from the instant a pocket of gas leaves the burner mouth. These calculations showed that while the gas velocity in the flame is strongly affected by buoyancy (6 cm/sec at the burner mouth to 85 cm/sec at 5 cm above the burner for flame "a") the difference in residence time to reach a given height for the 3 flames is small (e.g., 83.6 msec in flame "a", 78.5 msec in flame "b" and 74.8 msec in flame "c" to reach a height of 30 mm above the burner).The increase of soot content and soot aggregate diameter with increasing temperature is, thus, valid even when considering the data as a function of "time elapsed" rather than "height above burner".

VI. REFERENCES

Calcote, H. F. (1981). Mechanism of Soot Nucleation in Flames - A Critical Review. Comb. Flame, Vol 42, pp 215-242.

D'Alessio, A., DiLorenzo, A., Micera, G. and Beretta, F. (1975) Laser Light Scattering Measurements in the Soot Nucleation Zone of Rich Methane-Oxygen Flames. 2° Simposio di Dinamica delle Reazioni Chimiche, Padova pp 147-156.

Dalzell, W. H. and Sarofim A. F. (1969). Optical Constants of Soot and their Application to Heat Flux Calculations. Trans. ASME, J. Heat Transf. Vol 91, pp 100-104.

Dearden P. and Long, R. (1968). Soot Formation in Ethylene and Propane Diffusion Flames. J. Appl. Chem., Vol 18, pp 243-251.

Glassman, I. (1979). Phenomenological Models of Soot Formation in Combustion Systems, Princeton University Mech. and Aero Eng. Rep. No. 1450.

Glassman, I. and Yaccarino. P. (1980). The Effect of Oxygen Concentration on Sooting Diffusion Flames. Comb. Sci. and Tech., Vol 24, pp 107-114.

Glassman, I. and Yaccarino, P. (1981). The Temperature Effect in Sooting Diffusion Flames. 18th Symposium (International) on Combustion, Waterloo, pp 1175-1183.

Haynes, B. S. and Wagner, H. G. (1980). Sooting Structure in a Laminar Diffusion Flame. Ber. Bunsenges. Phys. Chem., Vol 84, pp 499-506.

Haynes, B. S. and Wagner, H. G. (1981). Soot Formation. Prog. Energy Combust. Sci., Vol 7, pp 229-273.

Holve, F. J. (1974). Diffusion Controlled Combustion of Polymers. Ph.D. Thesis, Department of Mechanical Engineering, University of California, Berkley, Report ME-74-4, Chap. 4.6.2, pp 68-76.

Homan, K. H. (1967). Soot formation in Premixed Flames. Comb. Flame, Vol II, pp 265-287.

Howard, J. B. and Kausch Jr., W. J. (1980). Soot Control by Fuel Additives. Prog. Energy Combust. Sci., Vol 6, pp 263-276.

Jagoda, I. J., Prado, G. and Lahaye, J. (1980). An Experimental Investigation into Soot Formation and Distribution in Polymer Diffusion Flames. Comb. Flame. Vol 37, pp 261-274.

Kent, J. H. (1970). A Noncatalytic Coating for Platinum - Rhodium Thermocouples. Comb. Flame, Vol 14, pp 279-282.

Kent, J. H., Jander, H. and Wagner, H. G. (1981). Soot Formation in a Laminar Diffusion Flame. 18th Symposium (International) on Combustion, Waterloo, pp 1117-1126.

Kent, J. H. and Wagner, H. G. (1982). Soot Measurements in Laminar Ethylene Diffusion Flames. Comb. Flame, Vol 47, pp 53-65.

Kerker, M. (1969). The Scattering of Light and other Electromagnetic Radiation. Academic Press, New York and London, Chap. 3.2 pp 31-39.

Lahaye, J. and Prado, G. (1978). Mechanisms of Carbon Black Formation. In Walker P. L. and Thrower P. A. (Eds.), Chemistry and Physics of Carbon, Marcell Dekker, New York, Vol 14, pp 168-294.

Muller-Dethlefs, K. (1979). Optical Studies of Soot Formation and the Addition of Organic Peroxides to Flames. Ph.D Thesis, Imperial College, University of London, Chap. 3, pp 23-38.

Neville, A. E. (1972). America Burning. Report of the National Commission on Fire Prevention and Control. Chap. 9, pp 61-69.

Palmer, H. B. and Cullis, C. F. (1965). The Formation of Carbon from Gases. In Walker P.L. (Ed.) Chemistry and Physics of Carbon, Marcell Dekker, New York, Vol 1, pp 265-325.

Penney, C. M. (1969). Light Scattering in Terms of Oscillator Strengths and Refractive Indices. J. Opt. Soc. Am., Vol 59, pp 34-38.

Powell, E. A., Bankston, C. P., Cassanova, R. A. and Zinn, B. T. (1979). The Effect of Environmental Temperature upon the Physical Characteristics of the Smoke Produced by Burning Wood and PVC Samples. Fire and Materials, Vol 3, No. 1, pp 15-22.

Powell, H. N. and Browne, W. G. (1956). Some Fluid Dynamic Aspects of Laminar Diffusion Flames. 6th Symposium (International) on Combustion, New Haven CT, pp 918-922.

Prado, G. and Lahaye, J. (1981). Physical Aspects of Nucleation and Growth of Soot Particles. In Siegla, D. C. and Smith, G. W. (Eds.), Particulate Carbon Formation During Combustion, Plenum Press, New York-London, pp 143-176.

Prado, G., Jagoda, J., Neoh, K. and Lahaye, J. (1981). A Study of Soot Formation in Premixed Propane/Oxygen Flames by In-Situ Optical Techniques and Sampling Probes. 18th Symposium (International) on Combustion, Waterloo, pp 1127-1136.

Rudder, R. R. and Bach, D. R. (1968). Rayleigh Scattering of Ruby-Laser Light by Neutral Gases. J. Opt. Soc. Am., Vol 58, No 9, pp 1260-1266.

Schug, K. P., Manheimer-Timnat, Y., Yaccarino, P. and Glassman, I. (1980). Sooting Behavior of Gaseous Hydrocarbon Diffusion Flames and the Influence of Additives. Comb. Sci. and Tech., Vol 22, pp 235-250.

Vaughn, S. N., Lester, T. W. and Merklin, J. F. (1981). A Single Pulse Shock Tube Study of Soot Formation from Benzene Pyrolysis. In Treanor, C. E. and Hall, J. G. (Eds.), Shock Tubes and Waves, Proc. 13th Symposium on Shock Tubes and Waves, Niagara Falls, State University of New York Press, Albany, NY, pp 860-868.

Wagner, H. G. (1981). Soot Formation in Combustion, 18th Symposium (International) on Combustion, Waterloo, pp 3-19, (Plenary Lecture).

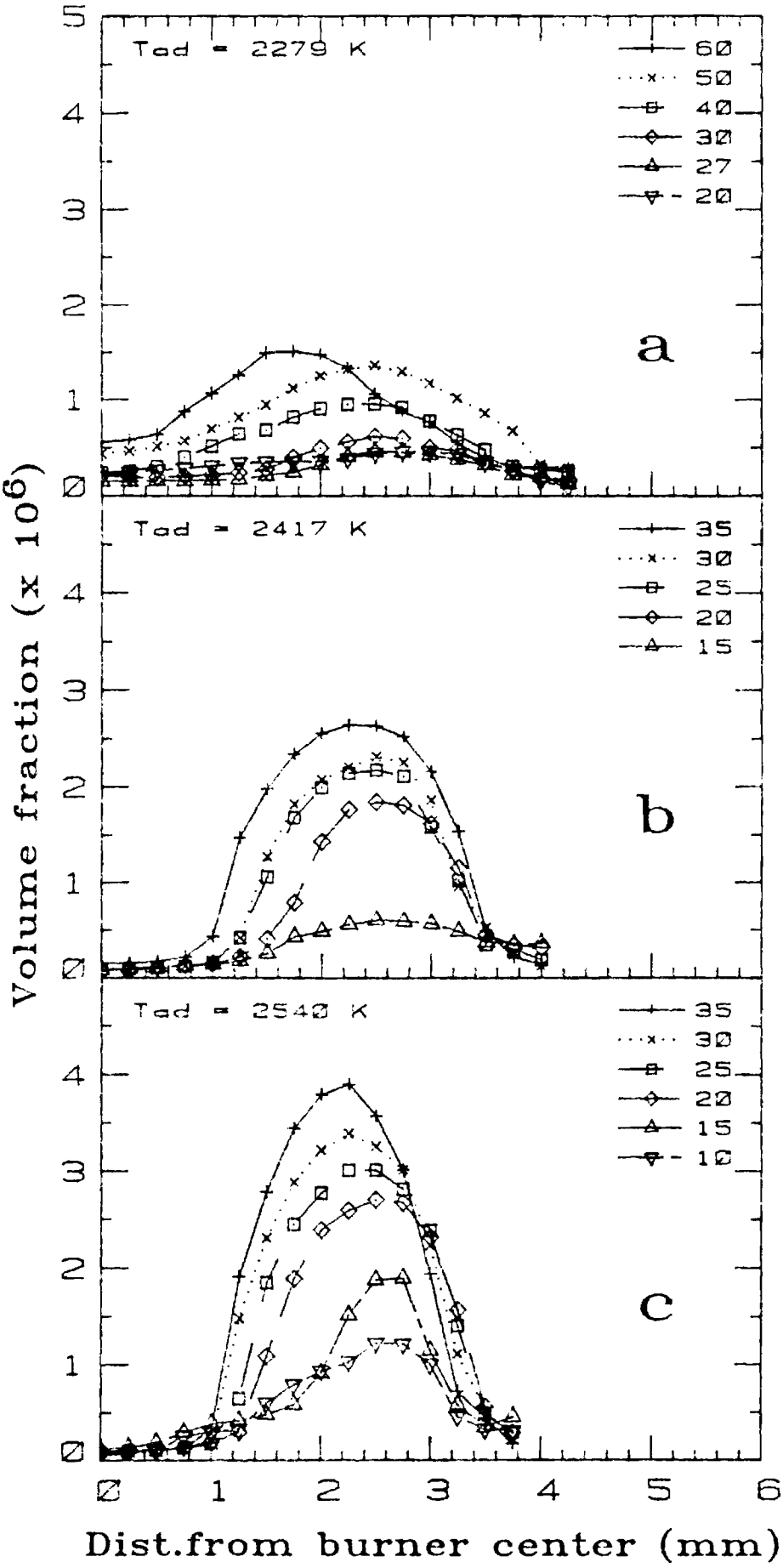
Tad = 2279 K
60
50
40
30
27
20
a
Tad = 2417 K
35
30
25
20
15
b
Tad = 2540 K
35
30
25
20
15
10
c
Volume fraction (x 10^6)
Dist.from burner center (mm)
0
1
2
3
4
5
6

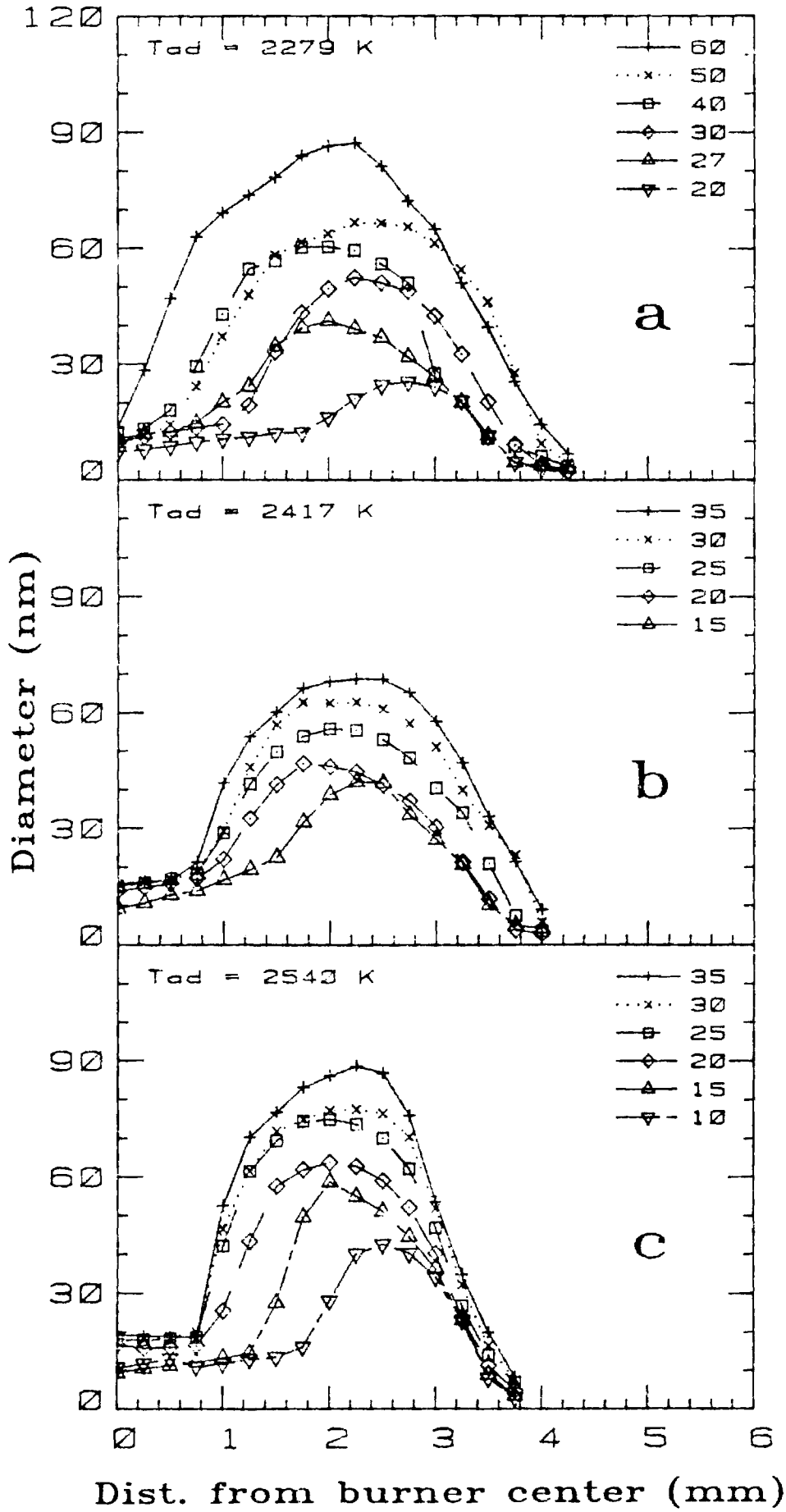
Tad = 2279 K
60
50
40
30
27
20
a
Tad = 2417 K
35
30
25
20
15
b
Tad = 2543 K
35
30
25
20
15
10
c
Diameter (nm)
Dist. from burner center (mm)
0
30
60
90
120
1
2
3
4
5
6

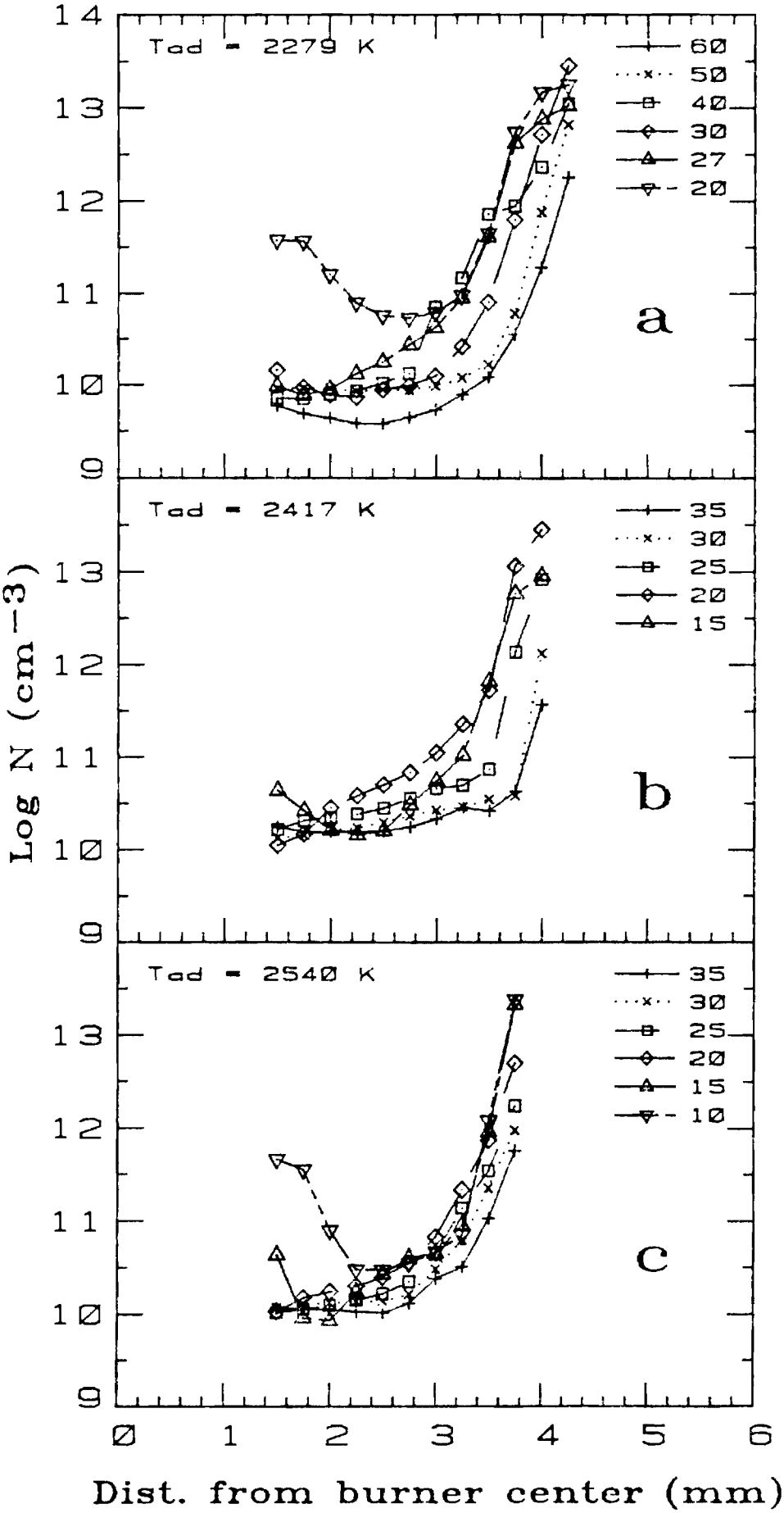
Tad = 2279 K
60
50
40
30
27
20
a
Tad = 2417 K
35
30
25
20
15
b
Tad = 2540 K
35
30
25
20
15
10
c
14
13
12
11
10
9
0
1
2
3
4
5
6
Log N (cm^{-3})
Dist. from burner center (mm)

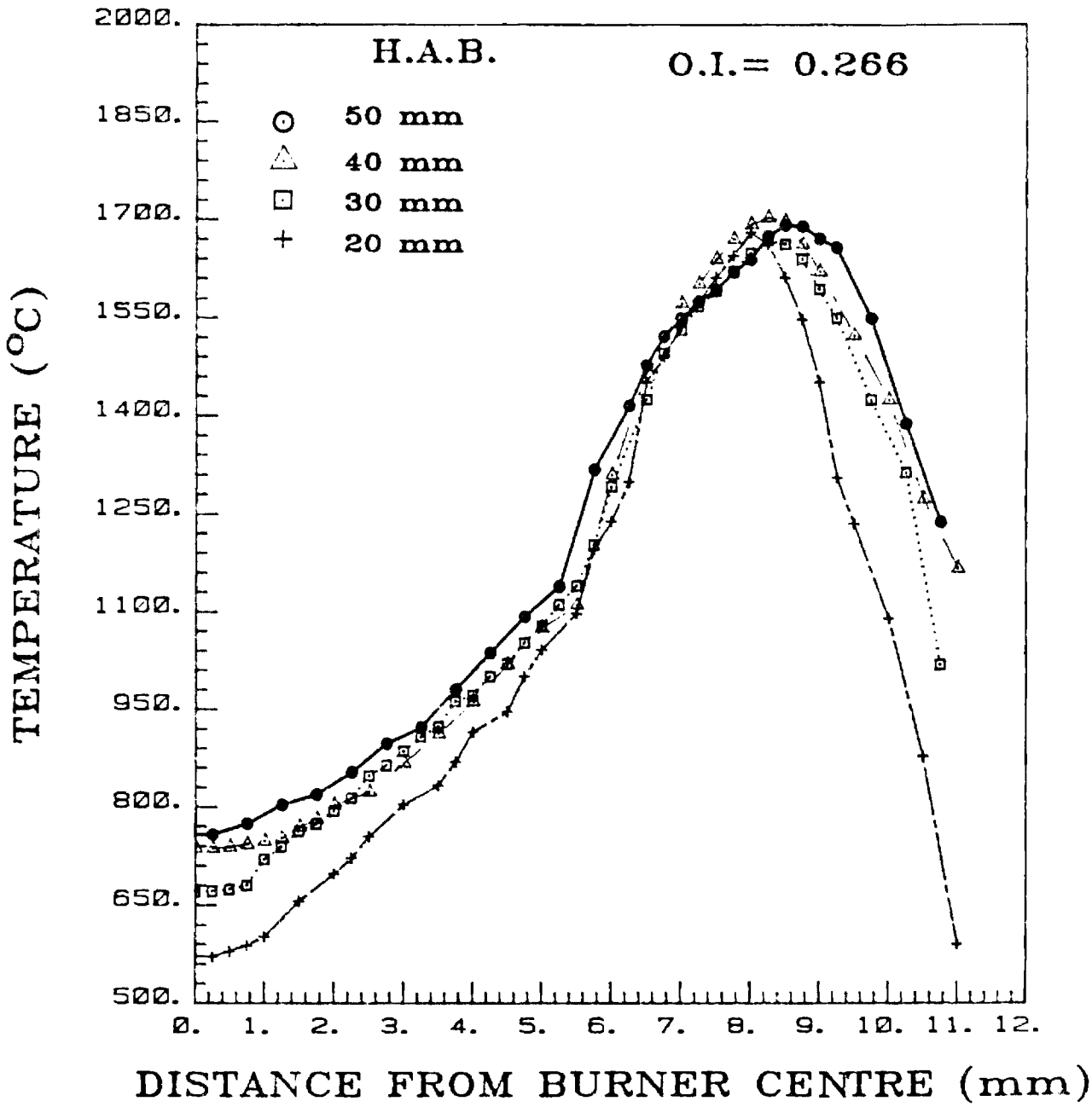
H.A.B.
O.I.= 0.266
50 mm
40 mm
30 mm
20 mm
TEMPERATURE (°C)
2000.
1850.
1700.
1550.
1400.
1250.
1100.
950.
800.
650.
500.
0. 1. 2. 3. 4. 5. 6. 7. 8. 9. 10. 11. 12.
DISTANCE FROM BURNER CENTRE (mm)

Fig 4

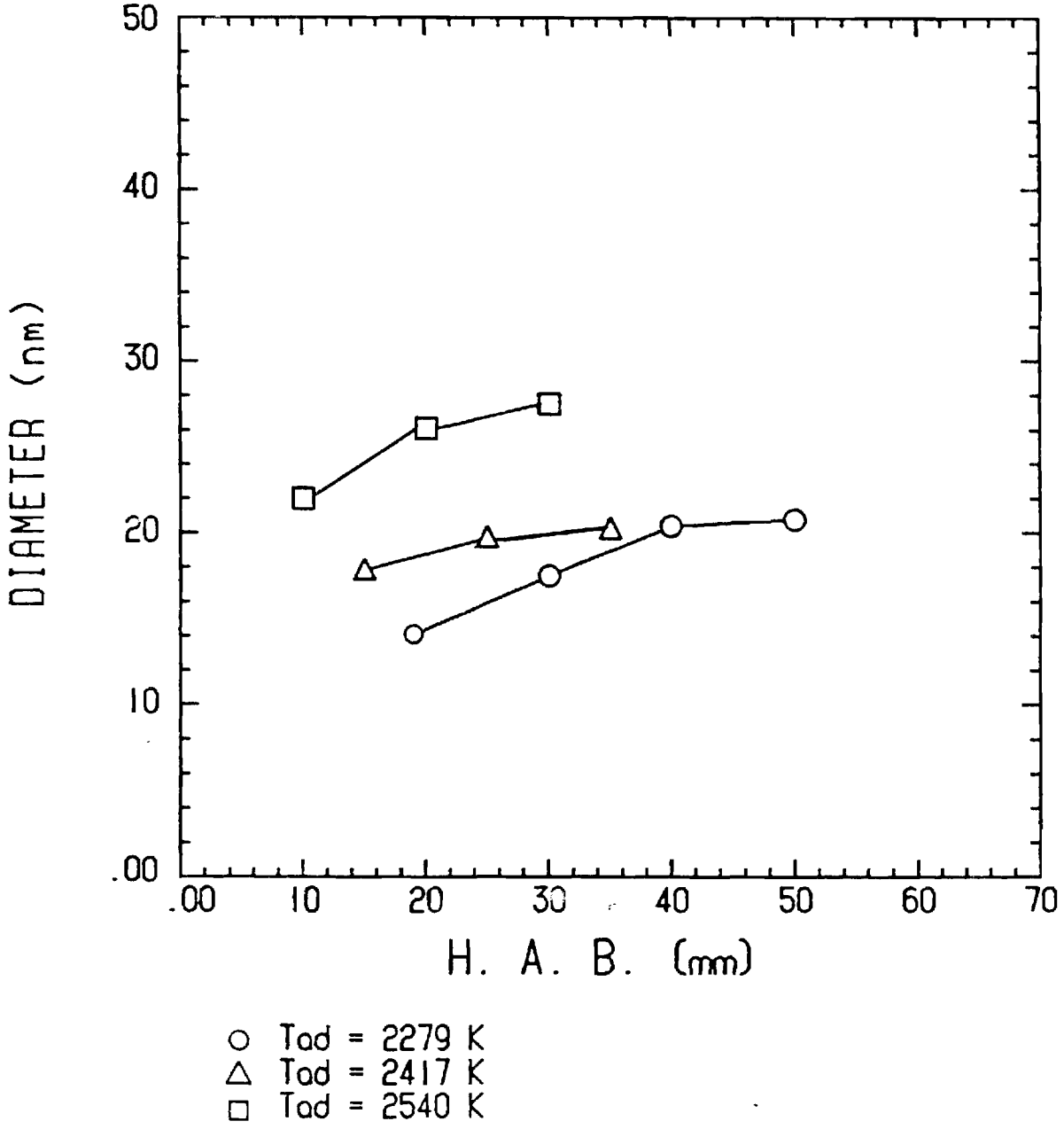
50
40
30
20
10
.00
DIAMETER (nm)
.00
10
20
30
40
50
60
70
H. A. B. (mm)
○ Tad = 2279 K
△ Tad = 2417 K
□ Tad = 2540 K

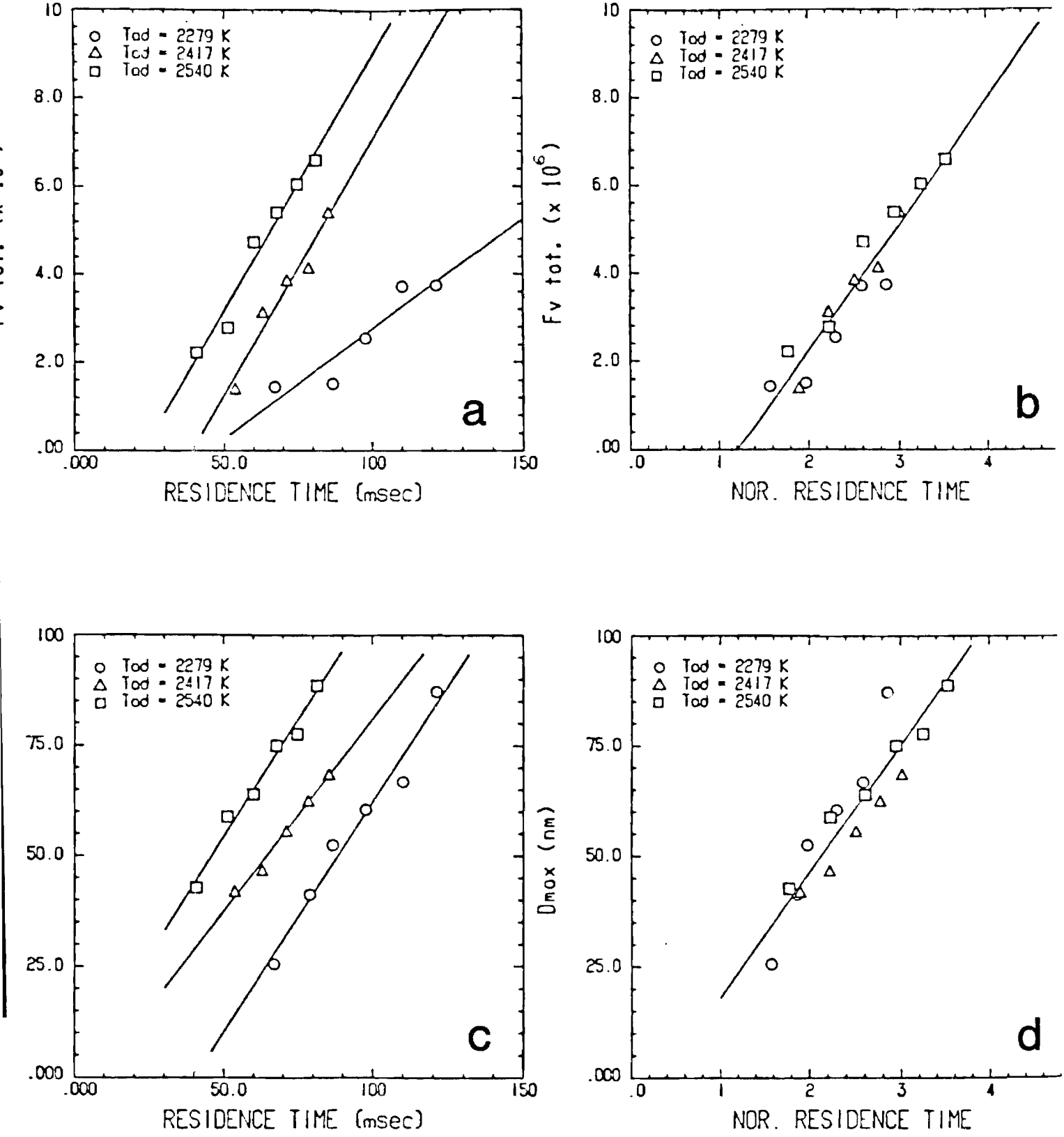
Tad = 2279 K
Tad = 2417 K
Tad = 2540 K
a
b
c
d
Fv tot. (x 10^6)
RESIDENCE TIME (msec)
NOR. RESIDENCE TIME
Dmax (nm)
10
8.0
6.0
4.0
2.0
.00
100
75.0
50.0
25.0
.000
.0
1
2
3
4
50.0
100
150

FIGURE CAPTIONS

FIGURE 1. Soot volume fractions versus distance from burner center at different heights above the burner for three adiabatic flame temperatures.

FIGURE 2. Soot agglomerate diameters versus distance from burner center at different heights above the burner for three adiabatic flame temperatures.

FIGURE 3. Soot agglomerate number densities versus distance from burner center at different heights above the burner for three adiabatic flame temperatures.

FIGURE 4. Temperatures versus distance from burner center at different heights above the burner for the flame with $T_{ad} = 2279^{o}K$.

FIGURE 5. Mean spherule diameters versus height above burner for three adiabatic flame temperatures.

FIGURE 6. Total soot volume fractions at different heights above burner versus residence time (a), and normalized residence time (b); maximum soot agglomerate diameters at different heights above burner versus residence time (c), and normalized residence time (d).

optical and probe techniques must be used to complement each other. Once the diameters of the soot spherules and their aggregates are known the degree of aggregation can be estimated.

Progress during Current Budget Period

Experimetal Techniques

A Parker Wolfhard type burner (Ref. 1) was selected for this study since it provides two parallel vertical flat diffusion flame sheets which lend themselves to more accurate absorbtion measurements without the need for deconvolution techniques to obtain local extinction coefficients as is necessary for cylindrically symmetric flames. The burner (Fig. 1) consists of three parallel slots of 2" length. The outer slots, which carry the oxidizer have a width of .63" each, while the inner, fuel slot is .2" wide. For equal fuel and oxidizer burner exit velocities this results in an extremely stable, slightly under-ventilated flame (Ref. 2). The burner is surrounded by a nitrogen carrying jacket to prevent drafts in the laboratory from disturbing the flame. Further flame stability is assured by the use of stabilizing screens near the tip of the flame. The burner can be displaced in a vertical and horizontal direction to enable measurements to be carried out in different parts of the flame without disturbing the optical system. After preliminary testing it was decided to add water cooling to the burner to ensure a consistent flame over extended running periods without overheating the facility.

Pages 1 and 2 Missing from report

A special suction probe was designed and built which permits the local sampling of soot from the flame. Flame gases are quenched to prevent further reaction in the probe while keeping the disturbance of the flame to a minimum. Details of the probe set up were discussed in Ref. 3 and in the original proposal. Briefly, it consists of three concentric tubes, the outer two carrying cooling water while the sampled gas is aspired through the central duct. Small holes in this duct near the probe tip permit small amounts of water to enter the flame gas steam in order to ensure rapid quenching and to eliminate soot deposit on the inner tube walls which could result in blockage of the probe (Fig. 2). The central duct of the probe is connected to a filter system which collects the soot and then, via a liquid nitrogen trap which removes the water, to a vacuum pump (Fig. 3). The suction rate is controlled using a precision needle valve and monitored with a dry gas meter. The cooling water flow rate is measured with a rotameter. Soot collected on the filters is weighed and observed under a transmission electron microscope.

A simultaneous laser light scattering and absorbtion test rig similar to the one described in Ref. 4 has been set up (Fig. 4). The beam from a 4 watt argon ion laser is focused into the test section in the flame and passes along the flat flame sheet onto a photomultiplier which measures the intensity of the transmitted light. A second photomultiplier is used to monitor the intensity of the beam scattered at a chosen angle to the incident beam. A system of lenses and apertures limits the solid angle over which scattered light is collected and eliminates radiation from any part of the laser other than the 60 micron cubed test section under consideration.

Direct radiation from the flame to the photomultipliers is reduced using a monocromator and a narrow band width interference filter. The remaining stray light is eliminated by placing a chopper in the incident beam and passing the output from the photomultipliers through a phase sensitive detector which only amplifies the part of the signal in constant phase with the chopper, i.e. radiation originating from the laser beam. The absorbtion and scattering signals are observed on an oscilloscope and registered on a chart recorder. The Mie theory in the Rayleigh approximation is used to obtain the local soot volume fractions and the mean diameters and number density concentrations of the soot agglomerates. The theory of the scattering of electromagnetic radiation is developed in Refs. 5 & 6. Only the actual formulae used in the analysis of the optical data will be quoted here. The soot volume fractions are being calculated using equation:

$$F_v = \frac{\lambda}{6\pi L} \frac{\ell n(I_{tr}/I_o)}{I_m\left|\frac{m^2 - 1}{m^2 + 2}\right|} \qquad (1)$$

where $\lambda = 514.5$ nm (wavelength of the laser light), I_{tr} = transmitted intensity, I_o incident laser intensity and m = 1.57 - .56i (complex refractive index of soot Ref. 7). The local extinction coefficient (K_{ext}) and the Raleigh scattering coefficient (Q) are being calculated from the measured values of the transmitted and scattered light intensities respectively using the following equations:

$$K_{ext} = \frac{1}{L} \ell n \frac{I_{tr}}{I_o} \qquad (2)$$

where L = length of the optical path of the laser beam in the flame as determined using a traveling microscope, and

$$I_{sc} = \eta_{el}\ \eta_{opt}\ Q(\Delta V)(\Delta\Omega)I_o \qquad (3)$$

where I_{sc} = laser intensity scattered from volume ΔV over solid angle and η_{el} & η_{opt} = the efficiencies of the electronics and the optics respectively. In order to avoid having to determine the efficiencies and the scattering volume and solid angle, the system is calibrated using gases of known scattering cross-section, usually nitrogen and methane. These calibrations are repeated daily, and also serve as a means of checking the optical alignment of the facility. All soot particles observed so far have been observed to fall within the Rayleigh regime. A small error is, however, introduced by the non-sphericity of the soot particles.

Accurate temperature measurements in sooting flames are notoriously difficult. To date all temperature measurements have been carried out using thin Pt, Pt-13% Rh thermocouples. A special system of translation stages has been assembled which permits the thermocouple to be traversed throughout the flame. Since soot deposited on the wires in the sooty part of the flame does affect the heat transfer to the junction and, thus, the recorded temperature, all horizontal flame traverses are originated in the soot free, high temperature region on the oxidizer side of the flame. As the probe enters the sooting region of the flame and carbon is deposited on the wires the thermocouple is moved back into the non-sooty part of the flame to burn off the deposit before advancing it to the next measuring position. A system for measuring flame temperatures using the sodium

line reversal technique will be set up. Here radiation from a tungsten strip lamp is passed through the flame seeded with sodium chloride and analyzed using a spectrograph (Ref. 9). The intensity of the calibrated lamp is varied until the intensity of the lamp at the sodium line frequency is exactly matched by that emitted by the sodium in the flame. From the calibration of the tungsten lamp the temperature of the flame can be determined. Again some error is introduced in the regions of high soot concentrations due to absorbtion of radiation by the carbon particles. The temperature measurements obtained by thermocouple and sodium line reversal will be compared with those determined using the Kurlbaum method. In this technique the natural radiation emitted by the soot particles is measured using an optical pyrometer. Clearly this is only possible in regions of the flame in which soot is present. The combination of the three techniques may be expected to result in the required temperature field to an accuracy exceeding the requirements for our comparison purposes.

Results

As a first step soot volume concentrations, mean aggregate diameters and aggregate number densities were measured for a propane-air diffusion flame using simultaneous laser light absorbtion and scattering. Fig. 5 shows the results obtained for this flame where the fuel and air streams leave the burner with a velocity of 6 cm/sec. The parameters mentioned above are plotted as a function of distance from the burner center for various height above the burner.

An inspection of Fig. 5a shows that the maximum concentration of soot occurs in a region inside the flame front. (For a precise location of the

flame front see the temperature plots later) The soot volume fraction increases with height above the burner indicating that the soot formation rate in this part of the flame exceeds the soot depletion rate by particle burn out. A slight shift of the maximum of soot volume fraction towards the burner center with height above the flame may also be observed.

Fig. 5b indicates, that the regions of maximum soot volume concentration also correspond to those in which soot aggregates of largest diameters are found. Just as the soot content, the aggregate diameters increase with height above the burner.

The aggregate number density distribution, on the other hand, shows a different trend. The maximum number of particles exist closest to the flame front with their number density decreasing in the region of maximum diameter and soot concentration. The values of number densities are less reliable than those obtained for the mean diameters and soot volume fractions since the latter are proportional to the cube root extinction coefficient and that coefficient respectively, while the number density is proportional to the square of that coefficient. This error becomes significant near the center of the burner where small "end flames" may contribute to the absorbtion signal and where the amount of light absorbed is relatively small. The number densities recorded within about 1 1/2 mm from the burner center must, therefore, be considered to be of limited use. Careful inspection of Fig. 5c indicates that there is a noticeable decrease in the number density of soot particles with height above the burner suggesting an agglomeration of soot in excess of the creation of new particles which may

be formed in this part of the flame. The agglomeration process is most pronounced in the lower part of the flame where "young soot" is smallest and most reactive. All data reported so far compare well with those obtained in other investigatiors in similar flames (Ref. 11 & 12), the latter using a different fuel.

In order to determine the degree of agglomeration of the spherical soot particles into agglomerates mentioned in the introduction soot samples were extracted at heights above the burner at which the aggregate properties had been determined. Unfortunately the spacial resolution of the sampling is not as good as that for the optical and only an average sampling per height could be obtained. These samples were viewed under a transmission electron microscope and the diameter distributions of the soot spheroids were recorded. These mean diameters are plotted versus height above burner in Fig. 6. Clearly the diameter of these elementary soot particles increases with height in the flame due to surface growth. This growth is particularly pronounced in the early part of the flame. Since the agglomerates, unlike the spheriods, are not spherical their measured diameters correspond to "equivalent diameters". Their degree of agglomeration was, therefore, estimated by comparing the mean volume of the spheroids with that obtained from using the equivalent diameter of the agglomerates determined from the light scattering technique to calculate the volume of the aggregates. The degree of agglomeration is tabulated below. Since these are "mean" degrees of agglomeration they are not integers:

Table I.

height above burner (mm)	degree of agglomeration
27	2.1
30	4.1
40	5.4
60	12.7

Thus, the number of spheroids making up the agglomerates increases with distance in the flame.

In previous studies (Ref. 13) it has been shown that soot particles formed purely by surface growth on a single nucleus follow a Gaussian distribution with standard derivation close to .2 while particles resulting from aggregation exhibit a log-normal distribution of standard deviation near .5. The standard deriations for spheroids in all parts of this flame at which soot was extracted were close to .5. Although this may, in part, be due to the coarse spacial solution compared with the thickness of the flame front an agglomeration of nuclei somewhere in the process leading to the spheroids seems, therefore, likely. This is indicative of the presence of a coagulation process very early in the flame. During coagulation small particles tend to agglomerate, the effect of which is masked by extensive surface growth.

In summary, it appears that small soot particles are formed near the hot region on the fuel side of the flame front. These grow by surface growth with some indication of the existence of coalescence of the small nuclei. The soot particle now have a velocity component in the vertical direction due to the gas flow and the effect of bouyancy of the combustion products

as well as a component towards the center of the flame due to the motion of the burnt gas away from the flame front (Ref. 12 & 14). This horizontal motion of the soot is aided by thermophorisis (Ref. 11) which is caused by the existance of a steep temperature gradient causing a greater number of molecular collisions with the particle surface on the side facing the region of higher temperature than that facing the cooler gas. As the particles move away from their position of inception, they grow by agglomeration into aggregates, which partially account for the increase in soot diameters away from the flame front and in the downstream direction. Agglomeration by itself, however, does not lead to an increase in soot volume fraction. In order to explain the increase in soot volume fraction with increasing aggregate diameter considerable surface growth must accompany aggregation process as the particles move away from the flame front and in an upward direction. Some new particles may be formed as one moves towards the region of high soot volume fraction but this generation rate must be small since the particle number density decreases in this direction indicating that aggregation process predominates. This aggregation process is most pronounced in the vicinity of new particle inception i.e., the number of particles decreases most sharply near the flame front and, to some extent, in the early part of the flame. This may be due to the higher number densities leading to more frequent collisions in the regions but also indicates a greater tendency of the small, reactive "young" soot particles to stick together because of the presence of free radicals adsorbed on the surface. The smaller particles observed near the center of the flame may have been

formed in the early part of the flame and be no longer reactive enough to agglomerate (Ref. 15) or may have arrived there since their diffusion coefficient is greater than that of the large particles.

As a next step the effect of temperature on the individual steps in soot formation process was investigated. A survey of the recent soot literature showed that a group under the direction of Prof. Glassman at Princeton investigated the effect of temperature on the sooting tendency of both premixed and diffusion flames (Ref. 16). In their studies, which relied on the concept of "sooting heights" without any measurements being carried out inside the flames itself, it was established that for premixed flames the sooting tendency decreased with increasing temperature, while in the case of diffusion flames the amount of soot produced increases with flame temperature. Prior to this investigation the principal investigator was engaged in the study of soot formation in premixed flames (Ref. 17). There it was found that an increase in flame temperature resulted in a decrease in soot volume fraction, soot aggregate diameters and spheroid diameters while the number density of soot particles was essentially unaffected by temperature. This trend fits in well with the findings of the group at Princeton.

On the other end of the scale a study of the effect of temperature on the oxygen free pyrolysis of methane and benzene (Ref. 18) showed that an increase in temperature in such a system increases the amount of soot formed but slightly decreases the diameters of the spheroids. No optical measurements were carried out in this work and no data about the aggregate

diameters are, therefore, available. A diffusion flame may be considered to consist of an internal relatively oxygen free zone surrounded by a flame front which exhibits some of the properties of a premixed flame. One of the controlling differences between premixed and diffusion flames lies in the fact that while in both cases the fuel is modified by pyrolysis prior to reaching the actual flame, this pyrolysis takes place in the former in the presence of oxygen and in an oxygen free atmosphere in the latter. This fundamental difference may be expected to influence the mechanism of soot formation.

In this study we have investigated the effect of temperature on the sooting process in a propane-air diffusion flame. In the flame front of a diffusion flame the combustion proceeds, essentially, under stoichiometric conditions. For given fuel-oxidant compositions the adiabatic flame temperature is, therefore, essentially constant. In order to be able to introduce a variation in adiabatic flame temperature for the propane-air diffusion flame, the inert nitrogen content of the oxidizer, which acts as a diluent, was varied. A decrease in nitrogen content, thus, corresponds to an increase in the adiabatic flame temperatue and a slight narrowing in the flame wedge, and vice versa. Results for flames of an oxygen to nitrogen ratio in the oxidizer flow of .27, .33 and .41 will be reported here. These flames will be referred to as T_1, T_2 and T_3. Adiabatic flame temperatures were calculated for these three cases using first a simple enthalpy balance assumming complete combustion. This method was then refined to include the effect of equilibrium concentrations within the flame as calculated using

a NASA computed code (Ref. 19). The results from these calculations are tabulated below:

Table II.

flame	predicted max temperature simple enthalpy balance	predicted max temperature including equilibrium considerations
T_1	$2394^{o}k$	$2279^{o}k$
T_2	$2670^{o}k$	$2417^{o}k$
T_3	$2930^{o}k$	$2540^{o}k$

Complete mappings of F_v, D and N are presented here in the form of constant parameter lines for cases T_1, T_2 and T_3. Fig. 7 shows a series of contour maps for the soot volume fraction throughout the flame for the three oxygen indices. In all these maps the dotted lines correspond to minimum values of the quantities being plotted. The soot volume fractions, thus, first peak and then diminish as one moves outwards from the burner center towards the flame front. Fig. 8 shows a similar trend for the agglomerate diameters at all three temperatures. Clearly the steepest gradients exist near the flame front and close to the burner center with steepness increasing as the adiabatic flame temperature goes up. The number density plot (Fig. 9), on the other hand, indicate a minimum near the center of the plots. Once again the values near the burner center are not considered to be very reliable. Close inspection of all the contour maps indicates that with an increasing adiabatic flame temperature soot formation is observed at lower distances above the burner. This reflects the

higher reaction rate for chemical processes in the presooting region with increasing temperature and will be referred to again later.

For better comparison of the physical properties of the soot agglomerates at different temperatures these data have been replotted as a function of radial distance from the burner center for different constant heights above the burner. Fig. 10 shows the soot volume fraction vs. radial distance for different heights (in mm) above the burner for the three flame temperatures. At all temperatures investigated the soot present in the flames clearly increases with height above the burner. The soot formation rate, thus, far exceeds the soot removal by, for example, burn out, even for the higher temperatures. Furthermore, the amount of soot present at any height above the burner increases with increase in flame temperature. Thus the increase in the reaction rate with temperature which increases the production of soot precursors in the lower region of the flame prior to soot formation and leads to the reduced height at which soot first appears persists in the sooting region of the flame. There the increase in temperature results in an increase in the pyrolysis reaction rate providing more large molecular weight hydrocarbons for soot growth. This increase in pyrolysis appears to be more temperature dependent than any process that may lead to soot removal such as soot burn-out and is responsible for the increase in sooting tendency with temperature observed in diffusion flames. This is in contrast with the case for premixed flames where the higher temperatures result in an increase in oxidation of pyrolysed hydrocarbon in the preheating zone thus removing possible matter for soot growth. This leads to a decrease in sooting with increasing temperature for such flames.

In Fig. 11 the soot aggregate diameters are plotted against distance from the burner center for different constant heights above the burner surface for T_1, T_2 and T_3. Clearly the mean soot aggregate diameters increase with increasing height in the flame for all temperatures investigated. Furthermore, the increase in temperature has the effect of increasing the soot agglomerate sizes found at given heights above the burner. This may be due to either an increase in the diameters of the fundamental spheriods which make up the agglomerates or to more extensive agglomeration. Samples extracted from the flames at different temperatures indicate, indeed, that there is some increase in spheriod diameters with adiabatic flame temperature, particularly in the early part of the flame (Fig. 6).

The effect of temperature on the number density of soot aggregates is shown in Fig. 12. Bearing in mind the reduced accuracy in the number density determination and neglecting results close to the burner center the changes in this parameter are far less pronounced than those discussed so far. Nevertheless, it is apparent that the number density decreases with increasing heights in the flame for all temperatures investigated. This is indicative of agglomeration taking place, particularly in the early part of the flame. Furthermore there appears to be some small decrease in number density with increasing temperature. Some of the increase in particle size with temperature may, therefore, be due to higher agglomeration particularly at higher temperatures.

Fig. 13 shows the temperature distribution for the propane-pure air diffusion flame (O/N = .21 i.e. T_1) As determined using a Pt - Pt 13% Rh thermocouple in a fashion described in the experimental section. Since the flame front of a diffusion flame is located near the region of maximum temperature, all soot appears to be present inside fuel side of the flame front. The maximum soot concentration occurs at a temperature considerably lower than that in the flame front. The temperature in the flame front is quite constant with height above the burner, which is not surprising since in this region virtually no soot is present which might lead to heat loss by radiative heat transfer. As one moves horizontally away from the flame front, the temperatue drops both in the direction towards the fuel and towards the oxidizer. Nearer the center of the flame the temperature increases with height. Heat losses by radiative heat transfer from the soot particles is, thus, more than compensated by heat addition through convection from the flame front to the center of the pyrolysis zone for this part of the flame.

The temperatures in the flame fronts for the flames with higher oxygen content in the oxidizer (T_2 & T_3) were found to be above the melting point of platinum, causing the thermocouples to break. Different thermocouple wires will, therefore, have to be used for these flames. As a check, however, a shielded thermocouple (Pt - Pt 13% Rh) was used in all three flame fronts. This probe resulted in a lower reading, because of the heat loss due to the shield, and no melting occured. It was noted that the ratios between measured "shielded" temperatures in the flame front and calculated adiabatic flame temperatues (3rd column, Table II) were the same

for all three flames to within 1%. Table III, therefore, contains the actual measured flame front temperature (without shielding) for flame T_1 and the extrapolated flame front temperatures for T_2 & T_3. The latter are, indeed, above the melting temperature of platinum (1780°C).

Table III.

flame	calcul. adiab. flame temp.	measured shielded flame temp.	measured/extrapolated flame temp.
T_1	2279°K = 2006°C	1004°C	1703°C
T_2	2417°K = 2144°C	1005°C	1790°C
T_3	2540°K = 2267°C	1133°C	1922°C

Finally it should be noted that the calculated adiabatic flame temperatures assume, as the name implies, no heat losses at all. This is clearly not the case which accounts for the lower measured values. As a matter of fact, our measured temperatures are closer to the calculated values than those obtained by other workers (eg. Ref. 16).

In summary, it has, thus, been observed that soot increases with both height above burner and with temperature. The number of soot agglomerates changes most significantly in the early part of the flame where it is reduced due to the aggregation of the "young" reactive soot particles. In this region the agglomerate diameters are further increased by a rapid increase in the size of the spherical soot particles which make up the agglomerates. The increase in the amount of soot produced may, thus, be due to both, new particle inception and surface growth, although the rate of agglomeration

seems to exceed that of new particle formation. Higher up in the flame the basic spheroid diameters grow at a reduced rate while the agglomerate number densities show relatively less change. Agglomeration continues in the upper part of the flame (see Table I) and some new particle inception may be expected near the flame front. This, along with surface growth, leads to an increase in soot present as one moves higher in the flame. The increased agglomeration leads to an increase in soot diameter in the region of high soot content but must be balanced by new soot particle formation near the flame front to account for the only slight reduction in the number of particles with increasing height. The larger agglomerates, however, seem to dominate as indicated by the larger measured mean diameters. The increased flame temperature causes an increase in spheroid diameters which leads to large agglomerates and soot volume fractions. The degree of agglomeration increases slightly with temperature (steeper gradient for aggregate diameter near the flame front in Fig. 8) while some new particles may be formed to keep the changes in number density small. Again the larger agglomerates predominate. The combined effect of soot spheroid growth and new particle inception is, thus, responsible for the increase of the soot content of the flame with height and temperature, since the agglomeration clearly has no influence on the total amount of soot present. (The above represents a small modification in the discussion presented in the last six-monthly report. It was realized that some new particle inception must be present in the higher regions of the flame in order to account for the pronounced increase in soot loadings with height and to explain the reduced decrease in number densities in the face of the continued mean

agglomeration indicated in Table I).

In order to try to quantitize the effects of both the height above the burner and the flame temperature, selected soot properties were plotted against height above the burner for the three temperatures. Since the reactions leading to soot formation may be expected to be acclerated by an increase in temperature, we have attempted to account for this. If the reactions responsible for continued soot formation in the flame are affected by temperature in a similar fashion as the reactions leading to the initial soot formation, all heights above the burner at the different temperatures must be normalized by the distance above the burner where soot is first observed for that temperature. (i.e., measured height above burner divided by first sooting height for that temperature). The soot properties selected for these plots are the total soot volume fraction at different heights above the burner (= areas under the curves) and corresponding maximum aggregate diameters. These quantities were plotted against height above burner and normalized height above burner for all three temperatures.

Fig. 14 shows the total soot volume faction across the flames as a function of height above burner (HAB) and normalized HAB for all three temperatures. The total soot increases for all three flames in the downstream direction. However, when plotted against normalized HAB the values for total soot at all temperatures fall much closer to a common line. When the lowest point for the middle temperature is neglected (it lies in a region where small particles are agglomerating; these may be susceptible to increased burn out at the high temperature) the slopes, or rates of soot formation with time, are almost equal for all three temperatures. When

maximum soot agglomerate diameters are plotted against HAB and normalized HAB (Fig. 15) the rate of diameter increase with HAB can be seen to be essentially the same for all three temperatures which is not the case for the normalized HAB. (The differences in the absolute values of the agglomerate diameters for different temperatures is at least partially due to the increase in spheroid sizes with temperature.) There is, thus, a difference in the behavior between the soot formation and agglomerate growth processess. Since HAB is essentially a time scale, soot generation is proportional to time normalized by the reaction rate in the presooting region while particle growth rate is just a function of time.

In all the above, buoyancy effects due to the different flame temperatures and the influence of the different densities of fuel and oxidizer have been neglected. Velocity measurements in similar diffusion flames have shown that the effect of buoyancy is certainly not neglegible (Ref. 11). It must, however, be pointed out that we are interested here in the differences of buoyancy between the three flames due to the differences in adiabatic flame temperatures, rather than in their absolute values. Since the temperature differences between the flames are only of the order of 10% of their absolute values the importance of the buoyancy differences is yet to be determined. These effects are currently being investigated by introducing the temperature and density differences into a Burke-Schuman type model of a diffusion flame. This may also reduce some of the scatter in the data in Figs. 14 and 15 although the correlation coefficients between the measured data and the least squares straight lines in these plots are better than .95, in some cases better than .99.

In order to predict the effect of buoyancy on the vertical velocities in the three flames a simple model has been developed. The buoyancy is due, in the first instance, to the difference in density of fuel and oxidizer. It is further increased by the relatively large horizontal temperature gradients in the diffusion flame. The differences in these effects for the three flames of different temperatures investigated must be estimated and incorporated in Figs. 14 and 15. The results of our velocity estimations using this model have been compared with results obtained in Ref. 11, where gas velocities have been measured for an ethylene-air flame on a Parker Wolfhard burner similar ot the one used in this investigation. These measurements show that buoyancy does, indeed, cause a rapid acceleration of the flow along the burner axis from 7 cm/sec at the burner mouth to about 180 cm/sec. at 110 mm above the burner.

This model is based on an analysis (Ref. 20) which deals with the investigation of the effect of the differing densities of cold fuel and oxidizer streams upon the fluid dynamic characteristics of diffusion flames. In the present model the effect of the differing temperatures of the fuel and oxidizer streams upon their densities is also taken into account. The fuel at temperature T_f and oxidizer at temperature T_o are assumed to leave the burner in parallel streams with velocity u_i at height $y = 0$ as shown in Fig. 16. The cross-sectional area of the oxidizer and fuel streams at $y = 0$ are A_{o_i} and A_{f_i} respectively. The oxidizer and fuel streams are bounded on the outside by parallel walls, but the position of the interface between the two streams (which corresponds to the reaction zone) is free to vary with height such that the cross-sectional areas of the two streams also vary with height

with $A_f + A_o = A_{tot}$ = constant. Frictional effects at the walls and the interface are neglected, and at each height the pressures in the two streams are equal. It is also assumed that T_o and T_f do not vary with height.

Applying Bernoulli's equation to each stream separately between stations o and y and using $p_f = p_o$ yields:

$$\left(\frac{u_o}{u_i}\right)^2 - \left(\frac{\rho_f}{\rho_o}\right)\left(\frac{u_f}{u_i}\right)^2 = \left[\frac{y}{(u_i^2/2g)} - 1\right]\left(\frac{\rho_f}{\rho_o} - 1\right) \tag{4}$$

Conservation of mass for the two streams gives:

$$\frac{u_o}{u_i} = \frac{(u_f/u_i)}{(1+r)\left(\frac{u_f}{u_i}\right) - r} \tag{5}$$

where the area ratio $r = A_{f_i}/A_{o_i}$. The density ratio ρ_f/ρ_o is given by

$$\rho_f/\rho_o = \left(\frac{m_f}{m_o}\right)\left(\frac{T_o}{T_f}\right) \tag{6}$$

where m_f and m_o are the molecular weights of the fuel and oxidizer and the temperatures are absolute.

Equations (4) and (5) must be solved simultaneously in order to obtain the fuel and oxidizer velocities, u_f and u_o, as functions of height above the burner, y. The parameters that must be specified are the fuel/oxidizer area ratio r, the initial velocity u_i, and the fuel and oxidizer temperatures T_f and T_o. These latter values must be obtained from temperature measurements in the flame, and are needed to obtain the density ratio ρ_f/ρ_o. In solving these

equations, it is convenient to use the dimensionless variables $U_f = u_f/u_i$, $V_o = u_o/u_i$ and $Y = y/(u_i^2/2g)$. A computer code was developed to solve Eqs. (4) and (5) numerically by an iterative technique.

In order to evaluate the model, velocities were calculated for the ethylene/air flames investigated by Kent, et al. (Ref. 11.) For their burner r = 0.05 and u_i = 7 cm/sec. The temperatures T_o and T_f were estimated from the measured temperature profiles presented in Ref. (11) for various heights. Here, temperature was a maximum in the reaction zone (interface between fuel and oxidizer streams) and decreased considerably toward the axis and toward the outer wall. Also peak temperatures decreased with increasing height above burner (1900°C to 1500°C), while the temperature near the axis was flat out to 4 mm from the axis and was nearly constant with height (about 1030°C). Thus T_f was taken to be 1030°C. The oxidizer temperature was more difficult to estimate so two cases were considered: (1) T_o = 25°C (room temperature) and (2) T_o = 528°C (mean between room temperature and T_f). The predicted fuel velocities u_f are presented in Fig. 17 along with the measured velocities at the burner axis. For heights above 30 mm the model predicts excessive vertical fuel velocities for T_o = 25°C (ρ_f/ρ_o = 0.221) and deficient fuel velocities for T_o = 528°C (ρ_f/ρ_o = 0.615). A curve fit was also obtained by matching the experimental data at 90 mm by choosing ρ_f/ρ_o = 0.368. This curve is also shown in Fig. 17 and gives excellent agreement with the experimental data down to 30 mm. The deviations of the experimental data from the theoretical curve for heights below 30 mm and at 110 mm are most likely caused by vertical temperature

gradients in the flame (see our temperature profile).

These results indicate that improvements to the model are needed in order to reliably predict vertical flow velocities in these diffusion flames without the need for curve fitting techniques.

Using the results obtained earlier for the variation of the soot agglomerate properties with temperature an attempt was made to fit the experimental data to a quantitative soot formation model. The model selected was from the work of Prado and Lahaye (Refs. 18 & 24). In this work nucleation at flame temperatures was proposed to proceed through a long sequence of chemical reactions. The soot precursors may, therefore, be considered to consist of large molecules (2000-3000 a.m.u.) or, more likely, their radicals or ions. In the high temperature region nearthe flame front this nucleation is accompanied by a reduction in particle number through coagulation. The rate of change of particle number density may thus be expressed in the form:

$$\frac{dN}{dt} = \dot{N}_u - \dot{N}_c \qquad (7)$$

Where $\dot{N}_u$= nucleation rate and $\dot{N}_c$ = the coagulation rate. As one moves away from the flame front the coagulation rate becomes dominant (cf: rapid increase in agglomerate diameters) and equation (7) may be rewritten as the Smoluchowski equation

$$\frac{dN}{dt} = - K D N^2 \qquad (8)$$

The rate constant K, which is a function of temperature, was obtained from free molecular theory assuming uncharged particles of less than 60 nm diameter, the latter being in agreement with our measured results.

Substituting for K and integrating one obtains for a large initial value of nuclei number densities:

$$N = 2.84 \times 10^{14} (T^{1/2} F_v^{1/6} t)^{-6/5} \quad (9)$$

Where T = temperature, F_v = the volume fraction of soot and t = time elapsed. See Ref. 24 for details.

Substituting the measured values of F_v and T one obtains agreement for the relative change in N with T to within the experimental accuracy of the experiment. However, the relative changes in N for the temperature difference between the three flames are small. A definitive applicability of this free-molecule coagulation model can, therefore, not be regarded as established at this point. It is proposed to rework the model to express aggregate diameters rather than number densities as a function of temperature, since the former are more sensitive to temperature changes and were measured with higher accuracy. The literature will, also, continue to be searched for other nucleation and agglomeration models, which can be compared with the results reported previously.

In a recently published report by Glassman it was pointed out that the sooting tendency of a diffusion flame can be increased by introducing traces of oxidizer into the fuel streams (Ref. 23). This can be explained in terms of the homogeneous catalytic effect of small amounts of oxidizer on pyrolysis reactions leading to an increase in large hydrocarbons available for soot formation. The above quoted report is based on overall sooting tendency measurements and has caused us to investigate the effect of the oxidizer traces on the individual steps of the soot formation process.

For this purpose 5% oxygen has been added to the fuel side of the diffusion flame with pure air as oxidizer. Optical determinations of soot volume fraction and the soot agglomerate properties have been carried out for the flames both with and without oxygen trace for fuel and air for cold burner exit velocities of 2 cm/sec. This reduced velocity results in a shorter flame which permits the measurements to be extended all the way to the flame tip. Incidentally, a comparison between flames of pure fuel and pure oxidizer at different cold gas velocities will permit the effect of reactant flow rates on soot formation to be determined.

Figs. 18, 19 and 20 show the variation of soot volume fraction aggregate diameters and number densities respectively vs distance from the burner center for different heights above the burner. Each of these figures shows plots for the flames with and without oxygen trace for easy comparison. These results have only just been obtained and have not yet been analyzed in any detail. A cursory glance, however, shows that the trends observed for the propane-air diffusion flame with 6 cm/sec reactant velocity (i.e. T_1) are still found in this smaller flame. Nearer the flame tip (above 30 mm for this flame), however, the increase in soot loading begin to diminish as does the increase in soot diameter. The soot aggregate number densities are still highest in the vicinity of the flame front and decrease towards the burner center. Some decrease in number density is observed in this flame with increasing height above the burner especially in the lower region of the flame. Nearer the flame tip the soot particle number density remains essentially constant.

The addition of 5% oxygen to the fuel side of this flame seems to have only produced minor effects. Essentially the flame has become narrower by the addition of oxygen to the fuel and has somewhat decreased in height. This is indicated by the absence of a minimum in the soot volume faction at the heighest measurement level (40 mm above the burner) for the flame with oxygen. This suggests that at 40 mm downstream the oxygenated flame is closer to its tip than the flame with pure fuel. Furthermore, the diameters near the tip begin to diminish, this effect, again, being more pronounced in the flame with oxygen in the fuel. Similarly, the effect of the oxygen on the aggregate number density is small except that at 20 mm the extensive aggregation continues in the pure fuel flame while the number density has already reached close to its final value for the oxygenated flame.

In general it would appear that the addition of oxygen causes an increase in soot loading, aggregate diameter and agglomeration in the early part of the flame but also tends to reduce the flame height. This is consistent with a "speeding up" of the combustion process by the presence of oxygen traces in the fuel. Further raw data have been obtained but, as yet, not evaluated. The processing of these data along with soot extraction for electron minoscopy and temperature measurements by thermocouples are planned for the remainder of the present budget period. Once all these results are in their final form, it will be attempted to tie in these findings with the results reported by Glassman in Ref. 23.

Tasks Remaining for the Present Budget Period.

During the remaining three months of the current budget period the probing and electronminoscopy for the flames of different temperature will be completed. The investigation of the effect of traces of oxygen introduced into the fuel side of the diffusion flame will also be continued. Local soot volume fractions, and aggregate properties will be determined from the measurements obtained to date. The spherule diameters will be obtained from the soot sampling which is still to be carried out for the flames carrying oxygen traces in their fuel.

Temperature measurements using thermocouples will be carried out for the flames of higher adiabatic flame temperatures (T_2 & T_3) as well as or those containing traces of oxygen in their fuel streams. Whenever necessary it will be attempted to use Tungsten-Tungsten/Rhenium thermocouples which are capable of withstanding higher temperatures than platinun. Some coating of these wires may be necessary since tungsten tends to turn brittle in the reactive atmosphere found near the flame front.

Since the temperature and oxygen trace measurements were carried out for flames of different cold gas velocity it will also be possible to determine the effect of the reactant flow rate on soot formation in diffusion flames. The findings for the effects of temperature, oxygen trace and flow velocity on the processes of soot formation will be continually related to soot formation models found in the literature.

On a more theoretical side, the buoyancy model described earlier will be applied to correct the relationship between the distance downstream and

time ellapsed, which is presently assumed to be linear. This should have the effect of changing the ordinates in Figs. 14 and 15 non-linearly. Whether the relative change for the three flame temperatures investigated will be significant is yet to be established. Finally, the literature will be scanned for a theory capable of relating the degree of agglomeration to the flame temperature via the aggregate diameters rather than their number densities, since the diameters seem more sensitive to changes in their environment and more accurately measurable. This search will not be restricted to papers dealing with soot, but also extended to nucleation and agglomeration theories dealing with, for example, metal particles.

A paper summarizing the effect of temperature on soot formation in diffusion flames was presented at the Fall Meeting of the Eastern Section of the Combustion Institute held at Atlantic City, N. J. last December. An extended and more up to date version of this work is presently being prepared and will be submitted for publication to a refereed journal during the present budget period.